

QUANTIFYING PACIFIC LAMPREY (*ENTOSPHEOUS TRIDENTATUS*)
AMMOCOETE HABITAT AVAILABILITY AND THE RISK ASSOCIATED WITH
THE SUMMER HYDROGRAPH RECESSION LIMB IN COASTAL NORTHERN
CALIFORNIA STREAMS

By

Katrina Clare Nystrom

A Thesis Presented to

The Faculty of Humboldt State University

In Partial Fulfillment of the Requirements for the Degree

Master of Science in Natural Resources: Environmental Science and Management

Committee Membership

Dr. Alison O'Dowd, Committee Chair

Dr. William Trush, Committee Member

Dr. Jasper Oshun, Committee Member

Dr. Erin Kelly, Graduate Coordinator

December 2020

ABSTRACT

QUANTIFYING PACIFIC LAMPREY (*ENTOSPENOUS TRIDENTATUS*) AMMOCOETE HABITAT AVAILABILITY AND THE RISK ASSOCIATED WITH THE SUMMER HYDROGRAPH RECESSION LIMB IN COASTAL NORTHERN CALIFORNIA STREAMS

Katrina Clare Nystrom

Pacific lamprey (*Entosphenus tridentatus*) are an anadromous fish that evolved before dinosaurs and are critical to the Pacific coastal stream ecosystems and Native American cultures. Pacific lamprey are threatened by past natural resource exploitation (logging, mining, dams, and streamflow diversion) and climate change (warming temperature and changing precipitation regime). The lamprey larva, known as ammocoetes, live in fine sediment deposits in coastal streams for three to seven years. The objective of this research was to predict ammocoete habitat based on channel morphology in coastal Northern California, USA and explore the impact of streamflow diversions on their habitat. I surveyed stream reaches for geomorphological features including; bed elevation longitudinal profile, river terraces, grain size distribution, and occurrence of ammocoete habitat throughout the Klamath and North Coast regions. I developed a binomial prediction model for the prevalence of ammocoete habitat and a habitat density model in reaches where ammocoete habitat was measured. I also measured streamflow in Redwood Creek, a tributary to the South Fork Eel River near Redway, CA; constructed a three-dimensional model of ammocoete habitat deposits; and

modeled impaired, with water diversions and landscape alterations, and unimpaired scenarios for the 1989-2019 dry seasons. Slope was the strongest predictor for the presence of ammocoete habitat, but was not useful for spatial modeling. Ammocoete habitat was often associated with the downstream end of an instream obstruction. Models of streamflow and ammocoete habitat indicated that an unimpaired stream might not have much risk to ammocoete habitat quality, but an impaired stream with surface water diversions can have extreme risk by dewatering ammocoete habitat annually. These results can help guide stream restoration by knowing where to focus restoration efforts, diversion management plans, and streamflow enhancement projects in coastal Northern California.

ACKNOWLEDGEMENTS

I would like to take the opportunity to thank the people that made this process possible, starting with my committee: Bill Trush, Alison O’Dowd, and Jasper Oshun. After meeting Bill in a coffee shop, he believed in me as a student and a scientist and has put up with me when I have been stubborn. Alison has guided me through this process. She has helped me make timelines, made sure all my boxes were checked off, and made seemingly never-ending edits. Jaspers has always been supportive, and his knowledge of geomorphology has been invaluable.

The California Water Resources Control Board funded the California Hydrogeomorphic Classification project; thanks to Colin Byrne, Hervé Guillon, Gregory Pasternack, and Belize Lane; and the Humboldt State University River Institute; Bill Trush and Alison O’Dowd; where I was able to measure ammocoete habitat density. Thank you to the field crew Emily Cooper, Mason London, Jesse Ritchie, Samuel Allen, Edward Davis, Alexandra Singh, Kate Stonecypher, Jacob Young, Colton Trent, Nathan Montgomery, and especially Priscilla Winters who collected ammocoete habitat data.

This project was supported by Hispanic-Serving Institution’s Education Program Grant no. 2015-38422-24058 from the USDA National Institute of Food and Agriculture, The Marine and Coastal Science Institute Graduate Student Research Award Program, and Graduate Federal Work-Study.

I would like to thank Jeremy McFarland, who was a classmate and helped me tremendously with geographic information systems spatial analysis.

I would not have been able to complete the topographic surveys without my partner Daniel Sheldon, and he is a great ‘*quaranteam*’ member. My family has believed in me when I did not, and for that, I am grateful.

TABLE OF CONTENTS

ABSTRACT.....	ii
ACKNOWLEDGEMENTS	iv
TABLE OF CONTENTS.....	vi
LIST OF TABLES	viii
LIST OF FIGURES	ix
INTRODUCTION	1
Species Description: Pacific Lamprey (<i>Entosphenus tridentatus</i>)	2
Pacific lamprey life history	5
Lamprey Importance: Ecosystem and Culture.....	7
Threats to Pacific Lamprey.....	10
Lamprey Ammocoete Habitat.....	17
Fluvial geomorphic influences on ammocoete habitat distribution	19
Research Objectives.....	27
MATERIALS AND METHODS.....	29
Site Description.....	29
Field Methods	34
Objective #1: Predict ammocoete habitat distribution for coastal watersheds in Northern California based on channel morphology (Spatial Model).....	34
Objective #2: Explore the relationship between stream channel geomorphic features and risk of ammocoete habitat loss during the summer streamflow recession limb in a northern California watershed (Redwood Creek temporal habitat loss)	40
Analytical Methods.....	42

Objective #1: Predict ammocoete distribution remotely for coastal watersheds in Northern California based on channel morphology.....	42
Objective #2: Explore the relationship between stream channel geomorphic features and risk of ammocoete habitat loss during the summer streamflow recession limb in a northern California watershed (Redwood Creek temporal habitat loss)	44
RESULTS	50
Objective #1: Predict ammocoete habitat distribution for coastal watersheds in Northern California based on channel morphology.....	50
A zero altered model for ammocoete habitat distribution	51
Geomorphic control to ammocoete habitat distribution	56
Objective #2: Explore the relationship between stream channel geomorphic features and risk of ammocoete habitat loss during the summer streamflow recession limb in a northern California watershed	61
Develop a relationship between flow, RCT, and portion of ammocoete habitat inundated.....	62
Estimate unimpaired hydrograph.....	67
Estimate current condition hydrograph.....	74
Comparison of WY 2019 unimpaired and impaired.....	78
DISCUSSION.....	81
Study assessments and improvements	81
Objective #1: Predict ammocoete habitat distribution for coastal watersheds in Northern California based on channel morphology.....	81
Objective #2: Explore the relationship between stream channel geomorphic features and risk of ammocoete habitat loss during the summer streamflow recession limb in a northern California watershed.....	85
CONCLUSION.....	92
LITERATURE CITED	93

LIST OF TABLES

Table 1. Qualitative types of deposits for Ammocoete Habitat (adapted from: Stillwater Sciences, 2013).	19
Table 2. Thresholds and controls on the discharge to stage relationship (W. Trush et al., 1988).	21
Table 3. Variables considered for selection of a comparative gage to Redwood Creek. Drainage area from gage information annual precipitation from PRISM (PRISM Climate Group & Oregon State University, 2004).	46
Table 4. Low flow risk levels and their associated conditions. Q =Flow (cfs). Q_{sec} =flow at section control (cfs). Q_0 =stage at RCT. Note: there may be risks to ammocoetes at higher flows, but they are not analyzed in this research.	49
Table 5. Model selection for Bernoulli model of the prevalence of ammocoete habitat. P-value of variable listed for the model if it was used in the model. A_c =drainage area, slope=field measured slope, bf.w.d=bankfull to depth ratio, D_{50} =median grain size, AIC =Akaike’s information criterion.	54
Table 6. Number and type of geomorphic control measured in each region.	56
Table 7. Mean slope per geomorphic control in the Klamath and North Coast regions... ..	57
Table 8. Riffle crest thalweg depths (RCTs) and hydraulic control thresholds for 10 study sites on Redwood Creek. Power function exponent (PFE) and the hydraulic threshold ratio (HTR) are dimensionless. ACT =active channel control, Q =flow, LHT= lower hydraulic transition, DOM=dominant section control, SEC =section control.....	63
Table 9. Habitat quality risk levels to ammocoetes at RC-4, condition where the risk occurs, associated flow (cfs), RCT (ft), and percent habitat inundated.	64
Table 10. Correlation between RC-4 and nearby USGS gages in 2019.	68

LIST OF FIGURES

Figure 1. Phylogenetic tree for lamprey genera and species in California. Pacific lamprey (<i>Entosphenus tridentatus</i>), are indicated by the thick border. Information from: Moyle, 2002 and Renaud, 2011.....	3
Figure 2. Side view of an adult Pacific lamprey (<i>Entosphenus tridentatus</i>). After a photograph by Brian W. Coad [prespawning male, 261.5 mm TL, NMC (= CMNFI) 1986–761, Stamp River, British Columbia, Canada] (Renaud, 2011).....	4
Figure 3. An oral disc of Pacific lamprey (<i>Entosphenus tridentatus</i>). After a drawing by Susan Laurie–Bourque [284 mm TL, NMC (= CMNFI) 1986–761, Stamp River, British Columbia, Canada] (source: Renaud, 2011).	5
Figure 4. Morphological identification for lamprey larva in California to the genus. A: <i>Entosphenous</i> caudal fin uniformly dark, caudal ridge faded to the posterior. B: <i>Lampetra</i> caudal fin speckled, caudal ridge uniformly dark (Goodman et al., 2009).....	5
Figure 5. The life history of Pacific lamprey (Streif, 2008).	6
Figure 6. Ammocoete of <i>Lampetra planeri</i> filter-feeding from their burrows (Gunther, 1960).	9
Figure 7. Estimated historic geographic distribution of Pacific lamprey (<i>Entosphenus tridentatus</i>) (Data Basin, 2011; Reid & Goodman, 2016; Renaud, 2011). Made with ArcMap version 10.6.1.	15
Figure 8. The current distribution of Pacific lamprey south of the Oregon-California border. ‘Historical’ sites have records, were surveyed, but no ammocoetes were found. ‘No records’ sites were not surveyed (Reid & Goodman, 2016).....	16
Figure 9. A generalized cross-section of a riffle crest with lines for the stage at bankfull channel control, active, dominant section, and section control stages.....	20
Figure 10. A stream channel cross-section, including white alders established between bankfull elevation (BF) and active channel elevation (ACT) (Lisle, 1988).	22
Figure 11. A longitudinal profile of channel bed elevation with multiple stage levels. The highest stage is at active channel control, the middle stage is at dominant section control, and the lowest stage is at section control. Stars mark the location of riffle crests, the highest channel bed elevation between pools.	23

Figure 12. As a meander bend becomes tighter, there is more flow separation. There is a change in the ratio of the radius of curvature (R) and the active channel width (d) as the meander bend tightens (Bagnold, 1960). 25

Figure 13. Study Area for Research Objective No. 1, including the South Fork Eel, North Coast, and Klamath Regions (South Fork Eel Region is also part of the North Coast Region). Research Objective No. 1 used a subset of geomorphic survey locations, dots, of the Hydro-Geomorphic Classification Project funded by California State Water Boards, designed by researchers at UC Davis, and field research conducted by the HSU River Institute. (Map Author: Emily Cooper). 30

Figure 14. Redwood Creek monitoring sites, labeled with stars, on a geologic base map (McLaughlin et al., 2000). Central Belt formation is in the upper right; the Coastal Belt is in the bottom left. QTw=weakly consolidated sandstone. Sp=peridotite. RC=Redwood Creek, SC=Seely Creek, MC=Miller Creek, CC=China Creek, URC=Upper Redwood Creek, and DC=Diner Creek. Made with ArcMap version 10.6.1. 32

Figure 15. Cross-sectional view of stream channel dimensions (Source: Kline et al. 2009). 35

Figure 16. Example of length and width measurements of a silty-sandy ammocoete habitat deposit during geomorphic field surveys. Deposit area was calculated by the average of at least three width measurements multiplied by the length. Modified photo from Lisle (1999). 37

Figure 17. Examples of geomorphic controls with the corresponding deposit outlined in black and arrows indicating flow direction: a willow tree acting as an obstruction (A), debris dam holding sediment on the upstream side (B), off-channel alcove from side-channel (C), small radius of curvature (D), erosion from the bank, and edge deposit (E), and a pool tail out (F). 39

Figure 18. Streamflow monitoring sites in Redwood Creek. RC=Redwood Creek, SC=Seely Creek, MC=Miller Creek, CC=China Creek, URC=Upper Redwood Creek, and DC=Diner Creek. Made with ArcMap version 10.6.1. 41

Figure 19. Sites surveyed for ammocoete habitat deposits. Sites categorized by ammocoete habitat density (m^2/m) (darker shade=higher density) and streams categorized by slope (darker shade=higher slope). Klamath and North Coast Region in different shades. Made with ArcMap version 10.6.1. 51

Figure 20. Box plots of variables explored for correlation with ammocoete habitat, only where ammocoete habitat was present. Ac=drainage area, slope=in stream slope, bf.d=bankfull depth, bf.w=bankfull width, bf.w.d= bankfull width to depth ratio, D50= median

grain size, ammo.area=total area (m²) in reach of habitat, and hab.dens= density of ammocoete habitat in reach (m²/m). 53

Figure 21. Bernoulli model for the presence of ammocoete habitat as it related to drainage area and slope. The most informative variables were drainage area and slope. Models are shown in the response scale, which takes the median value of the other variable to show the impact it would have on prevalence. Ac=Drainage area. 54

Figure 22. The best fit model displayed in the linear predictor (function of slope) and response scale for the Gamma model: ammocoete habitat density for when habitat is present. 55

Figure 23. Klamath Region mean slope and sample size by geomorphic control: dams, edge, obstruction (OBS), pool tail out (PTO), and radius of curvature ratio (RC). *The survey slope associated with dams was significantly different compared to the other variables: edge v. dam p-value=3x10⁻⁴, obstruction v. dam p-value=0.05, pool tail out v. dam p-value=3x10⁻³, radius of curvature ratio p-value=2x10⁻³. 58

Figure 24. North Coast region mean survey slope and sample size by geomorphic control of dams, edge, obstruction (OBS), pool tail out (PTO), and radius of curvature ratio (RC). *The survey slope of dams was significantly different from the other variables, except pool tail out: edge v. dam p-value=8x10⁻⁵, obstruction v. dam p-value=1x10⁻⁴, pool tail out v. dam p-value 0.05, radius of curvature ratio p-value 1x10⁻⁵. 59

Figure 25. Mean area of ammocoete deposits (m²) and sample size per geomorphic control of dams, edge, obstruction (OBS), pool tail out (PTO), and radius of curvature ratio (RC) in both the Klamath and North Coast regions (combined). *The mean habitat deposit area (m²) associated with pool tail outs were significantly larger than other deposits (PTO v. dam p-value = 2x10⁻⁵, PTO v. edge p-value=2x10⁻³, PTO v. obstruction p-value=2x10⁻⁵, PTO v. radius of curvature p-value=2x10⁻⁵). 60

Figure 26. Unit runoff per geologic belt of the monitoring sites in Redwood Creek. Most sites were entirely within the Coastal Belt (DC, CC, URC, MC, RC-1.5, and RC-1.8), one site was located in peridotite (RC-2.5), one site drained a completely Central Belt watershed (SC), and two were located in the Central Belt but also had discharge from the Coastal Belt (mix)(RC-3 and RC-4). 62

Figure 27. Binomial logit function to predict the portion of habitat surface area inundated based on the RCT at Redwood Creek site RC-4. Portion Inundated=e⁻(-3.5+4.6RCT)/(1+e⁻(-3.5+4.6RCT)). Deviance explained= 98.8%. 64

Figure 28. Redwood Creek site RC-4 riffle crest thalweg depth (ft) and flow (cfs) rating curve with power curve function (RCT=0.3728Q^{0.2857}, R²= 0.9667). Note: this curve does not include an estimate for active channel flow..... 65

Figure 29. Redwood Creek RC-4 riffle crest thalweg depth (ft) and flow (cfs) rating curve, the x-axis and y-axis are adjusted to show the lowest flows, with a power curve trendline ($RCT=0.3728Q^{0.2857}$, $R^2= 0.9667$) and a linear trendline that goes through (0,0) for the lower flow values ($RCT=1.4415Q$, $R^2=0.806$). 66

Figure 30. Exceedance plots of May 1st flow (cfs) at the Elder Creek gage (USGS #11475560). Each line has a different range; 50, 30, 20, and 10 years. The top inset graph has the full range of cfs values; the bottom larger graph shows a smaller range of flows. 67

Figure 31. Redwood Creek WY 2019 RC-4 - Elder Creek gage (USGS #11475560) correlation. Linear function $y=1.403x-1.9674$, $R^2=0.9945$ 68

Figure 32. WY 2018 unit runoff for Elder Creek (USGS #11475560), Bull Creek (USGS gage #11476600), and measurements at Redwood Creek RC-4. Bull Creek stopped operation November 1st, 2018..... 69

Figure 33. WY 2019 unit runoff for Elder Creek (USGS #11475560) and field measurements of Redwood Creek RC-4..... 69

Figure 34. Comparison of the actual flow estimated from the water level logger in Redwood Creek site RC-4 (ends 9/21/2019), the flow estimated from the 2019 correlation with Elder Creek gage (USGS #11475560), and the measurements taken in the field. The full range of data is inset; the larger graph has a smaller range of cfs values to better display the lowest flows..... 71

Figure 35. Percent rank of Redwood Creek RC-4 estimated May 1st flow from 1989-2019 using the watershed scaling equation to estimate unimpaired flow. The Upper dashed line is 100% inundation of fine sediment deposits; the lower dashed line is section control when risk increases for ammocoetes. Darker shades of lines represent higher flows on May 1st of that year. 72

Figure 36. Percent habitat surface area inundated at Redwood Creek site RC-4; unimpaired, 20% diverted from unimpaired, 50% diverted from unimpaired, and 90% diverted from unimpaired. Dashed line = section control. Darker shades of lines represent higher flows on May 1st of that year. 73

Figure 37. Number of days above section control with a diversion from the unimpaired flow between May 1st and December 31st, 1989-2019 at Redwood Creek site RC-4. Darker shades of lines represent higher flows on May 1st of that year..... 74

Figure 38. Redwood Creek site RC-4 water level and ammocoete deposits exposed at different streamflow thresholds in the recession limb. Hollow arrows point to the highest elevation of the deposits. Solid arrows point in the direction of the flow. 75

Figure 39. RCT (ft) for Redwood Creek RC-4 from 1989 to 2019 May 1st to December 31st current condition. Top dashed line is when the habitat surface area is completely inundated. Next lower line is section control. Flow stops when RCT=0.0. The habitat surface area is completely dewatered at the lowest dashed line. Darker shades of lines represent higher flows on May 1st of that year. 77

Figure 40. Exceedence of the count of days below section control at site RC-4 in Redwood Creek in each year (1989-2019) given the current condition based off 2019 correlation with Elder Creek (USGS #11475560). 78

Figure 41. Redwood Creek site RC-4 unimpaired flow based on the watershed scaling equation with Elder Creek (USGS gage #11475560) and the flow estimated from the water level logger at the site for WY 2019, water level logger data ends September 21st. 79

Figure 42. Redwood Creek site RC-4 WY 2019 daily average flow estimated from the logger (actual), the daily average flow of the unimpaired estimate, and the measured flows. The scale ranges from zero to ten cfs, water level logger data end on September 21st. 80

INTRODUCTION

Pacific lamprey (*Entosphenus tridentatus*) are jawless fish native to the North Coast of California that are ecologically and culturally important, generally understudied and misunderstood. Pacific lamprey populations face a myriad of threats. Pacific lamprey adults supply fatty, ocean-derived nutrients in the dead of winter to the riverine ecosystem (Parker, 2018). Native American tribes around the Pacific Rim have relied on Pacific lamprey as a food resource for centuries (Petersen, 2006). The larva, ammocoetes, are important for nutrient cycling in the stream not only because of the sheer amount of biomass they contribute, but also because they provide bioturbation to the stream bed with their burrowing behavior (Shirakawa et al., 2013). The fossil records of lamprey in North America date them back 280-310 MYA, before the dinosaurs (Renaud, 2011). For lamprey species, there is a plethora of research on the invasive Great Lakes Sea lamprey (*Petromyzon marinus*) because of eradication efforts, but less on the west coast's Pacific lamprey (Docker, 2015). Pacific lamprey populations have dwindled since the 1960s when those in power didn't recognize their value to the ecosystem or the consequences of their actions in landscape manipulation (Petersen, 2006; Reid & Goodman, 2016; Simpson, 2019). Among threats to Pacific lamprey are dams, logging, effects from human population growth including water use, and climate change (Goodman & Reid, 2012). Although Pacific lamprey are understudied and misunderstood, research into ammocoete habitat distribution and seasonality can help inform restoration practitioners on how to restore ammocoete habitat while benefitting the larger ecosystem. Pacific

lamprey will recolonize streams if adequate passage and suitable habitat are available (Reid & Goodman, 2020). Ammocoetes live in rivers for many years, where there is ample opportunity for habitat restoration (Formosa & Kelly, 2020).

Species Description: Pacific Lamprey (*Entosphenus tridentatus*)

Lamprey are in the phylum Chordata and the Order Petromyzontiformes (Renaud, 2011). The only other Order in the phylum Chordata is Mixiniformes, the Hagfish (Figure 1). “Petro” comes from the Greek word for rocks and is part of the Order name Petromyzontiformes because of how lamprey move rocks from the stream bottom during spawning (Renaud, 2011). There are three Families in the Order Petromyzontiformes, two of which are restricted to the Southern Hemisphere: Geotriidae (one species) and Moraciidae (two species) (Renaud, 2011). The Family in Petromyzontiformes found in the Northern Hemisphere is Petromyzontidae (35 species) (Renaud, 2011). The Northern and Southern Hemisphere Families are split by the tropics where there are no lamprey because the larvae have a maximum thermal tolerance of 31.4 °C (Renaud, 2011). In California, there are two lamprey genera, *Lampetra* and *Entosphenus* (Moyle, 2002). Pacific lamprey (*Entosphenus tridentatus*) were previously classified in the genus *Lampetra*, but mitochondrial DNA analyses indicate that Pacific lamprey is actually in the genus *Entosphenus* (Moyle, 2002; Renaud, 2011).

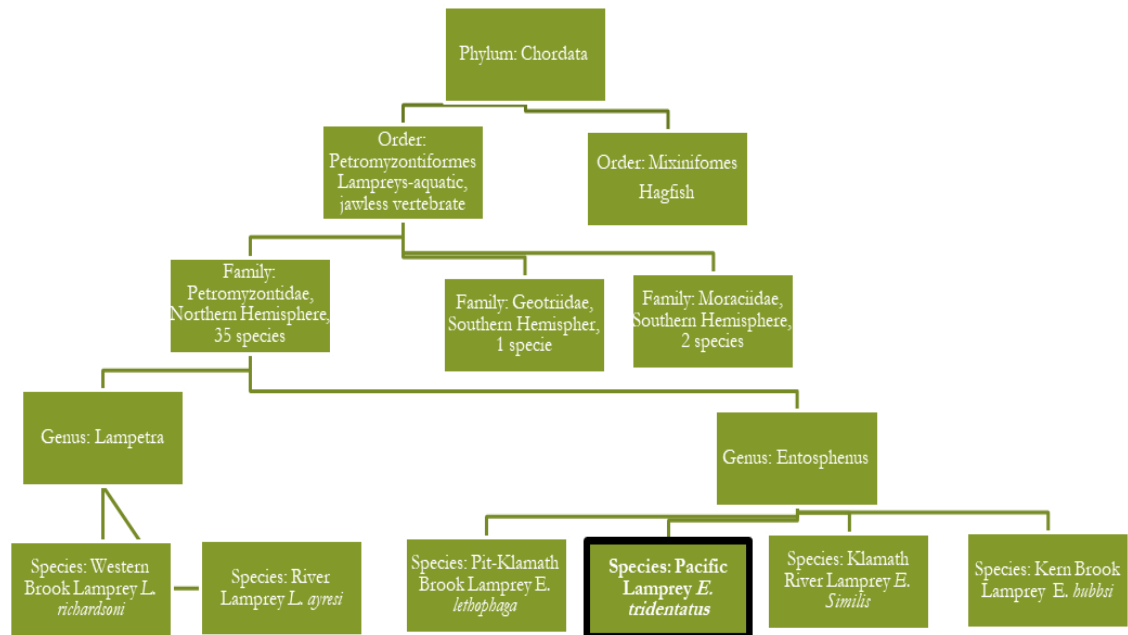


Figure 1. Phylogenetic tree for lamprey genera and species in California. Pacific lamprey (*Entosphenus tridentatus*), are indicated by the thick border. Information from: Moyle, 2002 and Renaud, 2011.

Lampreys have unique physical features and a compelling life history. Lampreys have a skeleton of cartilage, keratin teeth, notochord axial support, a pineal eye, incomplete cranium, and do not have paired fins as compared to other fish taxa (Renaud, 2011). The juvenile life-stage of all lamprey species, called ammocoetes, live in freshwater streams. The lamprey adult life-history varies among species and includes: (1) anadromous and parasitic in the ocean, (2) parasitic in freshwater only, and (3) nonparasitic in freshwater (Renaud, 2011). California has lamprey species that exhibit each of these three life-history strategies (Moyle, 2002).

In California, the anadromous Pacific lamprey are the largest lamprey species (>40 cm total length) and are parasitic in the ocean only (Figure 2). The main identifying feature for the adults is their sucking disc with the crescent-shaped supraoral lamina with three sharp cusps, the middle cusp smaller than the other two (Figure 3) (Moyle, 2002). The larva in California cannot be visually identified to species, but can be visually identified to genus. *Entosphenus* have a dark caudal fin, and the caudal ridge fades towards the posterior. In contrast, *Lampetra* has a speckled caudal fin, and the caudal ridge is uniformly dark (Figure 4) (Goodman et al., 2009).

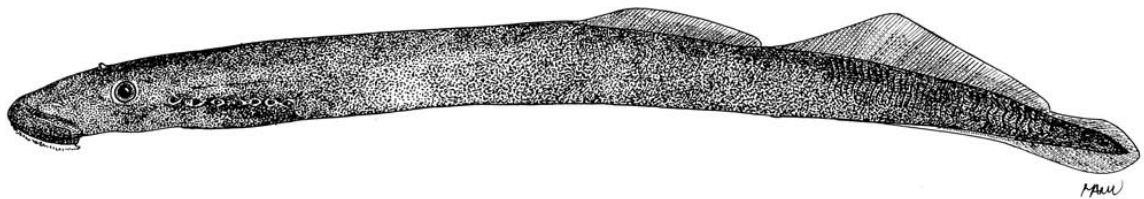


Figure 2. Side view of an adult Pacific lamprey (*Entosphenus tridentatus*). After a photograph by Brian W. Coad [prespawning male, 261.5 mm TL, NMC (= CMNFI) 1986-761, Stamp River, British Columbia, Canada] (Renaud, 2011).

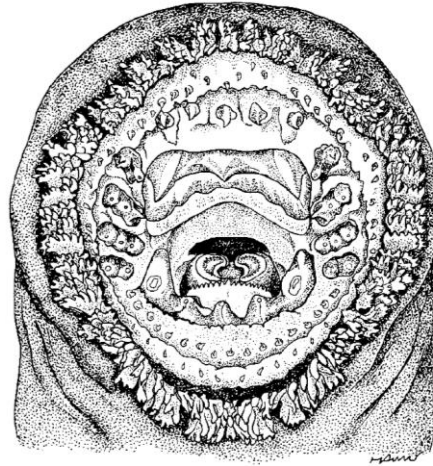


Figure 3. An oral disc of Pacific lamprey (*Entosphenus tridentatus*). After a drawing by Susan Laurie-Bourque [284 mm TL, NMC (= CMNFI) 1986–761, Stamp River, British Columbia, Canada] (source: Renaud, 2011).

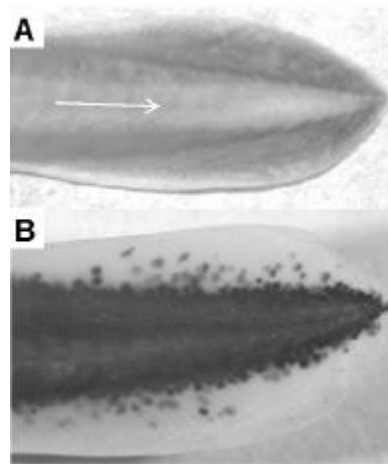


Figure 4. Morphological identification for lamprey larva in California to the genus. A: *Entosphenous* caudal fin uniformly dark, caudal ridge faded to the posterior. B: *Lampetra* caudal fin speckled, caudal ridge uniformly dark (Goodman et al., 2009).

Pacific lamprey life history

The lifespan of Pacific lamprey can range from 6-15 years (Moyle, 2002) (Figure 5). The eggs of Pacific lamprey take about 20 days to hatch in 15 °C water (Moyle,

2002). The newly hatched ammocoetes (larvae) spend some time in the nest gravel before they emerge and are washed downstream to an area of soft sand and silt (Moyle, 2002). The word “ammocoete” comes from Greek for sleeping in the sand (Renaud, 2011) because they burrow in fine substrate and do not have eyes. Ammocoetes of Pacific lamprey do not spend their whole larval life stage in one deposit but are active all year (Moyle, 2002). The duration of the ammocoete life stage can range from 3-7 years (Moyle, 2002; Streif, 2008). Ammocoetes have a net downstream movement in the river during this life stage (Docker, 2015) and reach 14-16 cm before metamorphosis (Moyle, 2002).

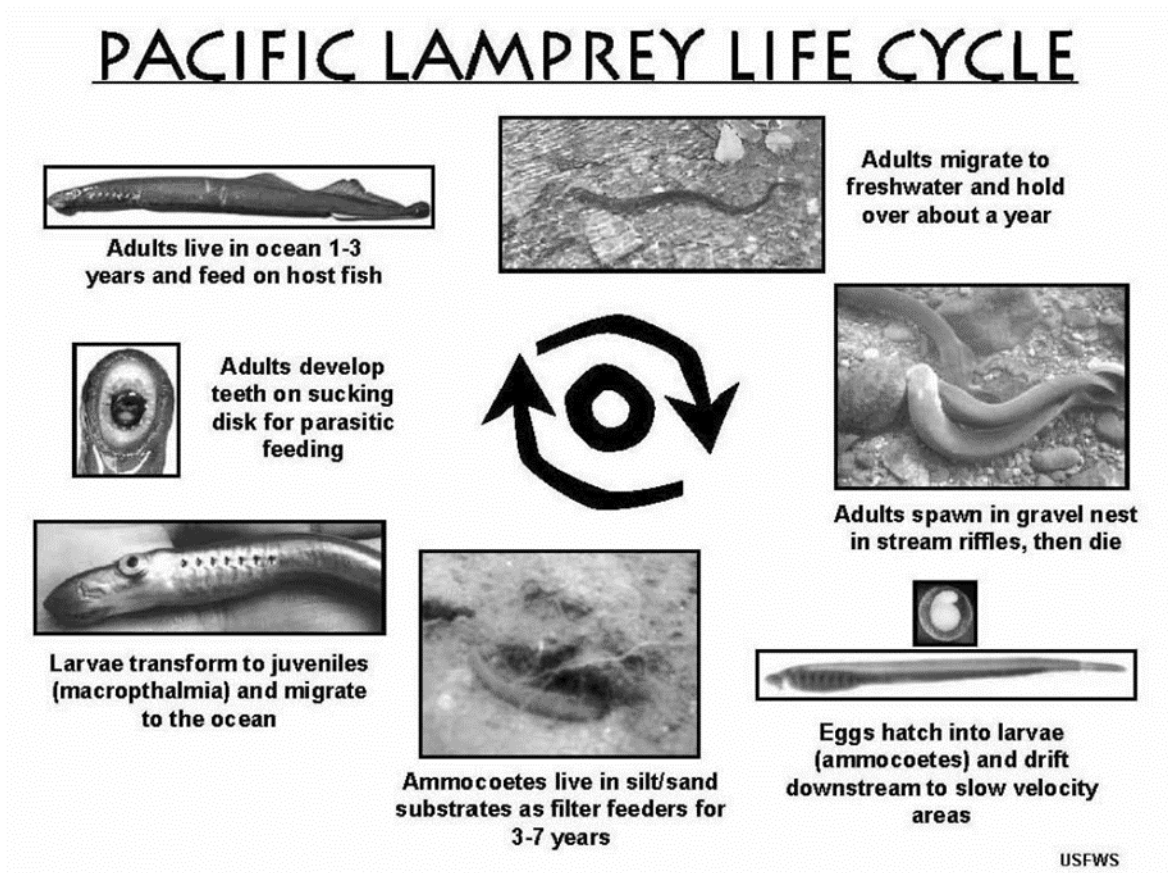


Figure 5. The life history of Pacific lamprey (Streif, 2008).

The life stage in which Pacific lamprey change from detritus-feeding juveniles to predatory adults ready to emigrate toward the ocean is called macrophthalmia (Goodman et al., 2015; Moser et al., 2015). Many body changes must occur, including growing eyes and suckorial disks (McGree et al., 2008).

Adult Pacific lamprey are parasitic in the ocean and attach to a variety of fishes, including salmon (Renaud, 2011). They inhabit the mesopelagic zone and have been found up to 117 km deep off the coast of Oregon (Renaud, 2011). The adult ocean phase of Pacific lamprey can last 1.5-4 years (Moyle, 2002; Renaud, 2011).

Most adult Pacific lamprey re-enter the river in the winter, but can return to freshwater at all times of the year (Parker, 2018). Spawning Pacific lamprey adults migrate upstream in river systems. They can use their suckorial disc to climb vertical surfaces (Renaud, 2011). Both sexes work together to construct a redd in the stream, the females lay 20,000-200,000 eggs in a single redd, and the fertilized eggs attach to the rocks at the downstream end of the redd where the spawners cover them with loose gravel (Moyle, 2002).

Lamprey Importance: Ecosystem and Culture

Throughout their range, Pacific lamprey are an essential element of the aquatic food web. Because Pacific lamprey are anadromous, they bring nutrients into freshwater systems from the ocean. Pacific lamprey have a much higher lipid content than

salmonids, which makes them more appealing to predators (Close, 2002). Ammocoetes can provide a majority of the biomass of all fishes in the stream (Leach, 1940).

Ammocoetes cycle nutrients in the system via bioturbation, which is the act of burrowing and coming up to the surface. Ammocoetes create loose burrows, less defined in sand than in silt (Applegate, 1950) (Figure 6). Ammocoetes come to the surface to feed with their oral hood, which catches microorganisms and detritus in the drift (Applegate, 1950). Water is pumped in and out with the respiratory system, some of the organisms in the water are consumed, and detritus builds-up on the oral hood, periodically the detritus built-up is blown out in a 'coughing motion' (Applegate, 1950) (Figure 6). Studies by Shirakawa, Yanai, and Goto (2013) found that the Japanese lamprey, *Lethenteron camtshaticum* and *Lethenteron* sp. N (formally the Northern form of *L. reissneri*), kept the surface of the benthic substrate softer, more oxygenated, and with higher levels of fine particulate organic matter via bioturbation compared to areas without ammocoetes over 21 days.

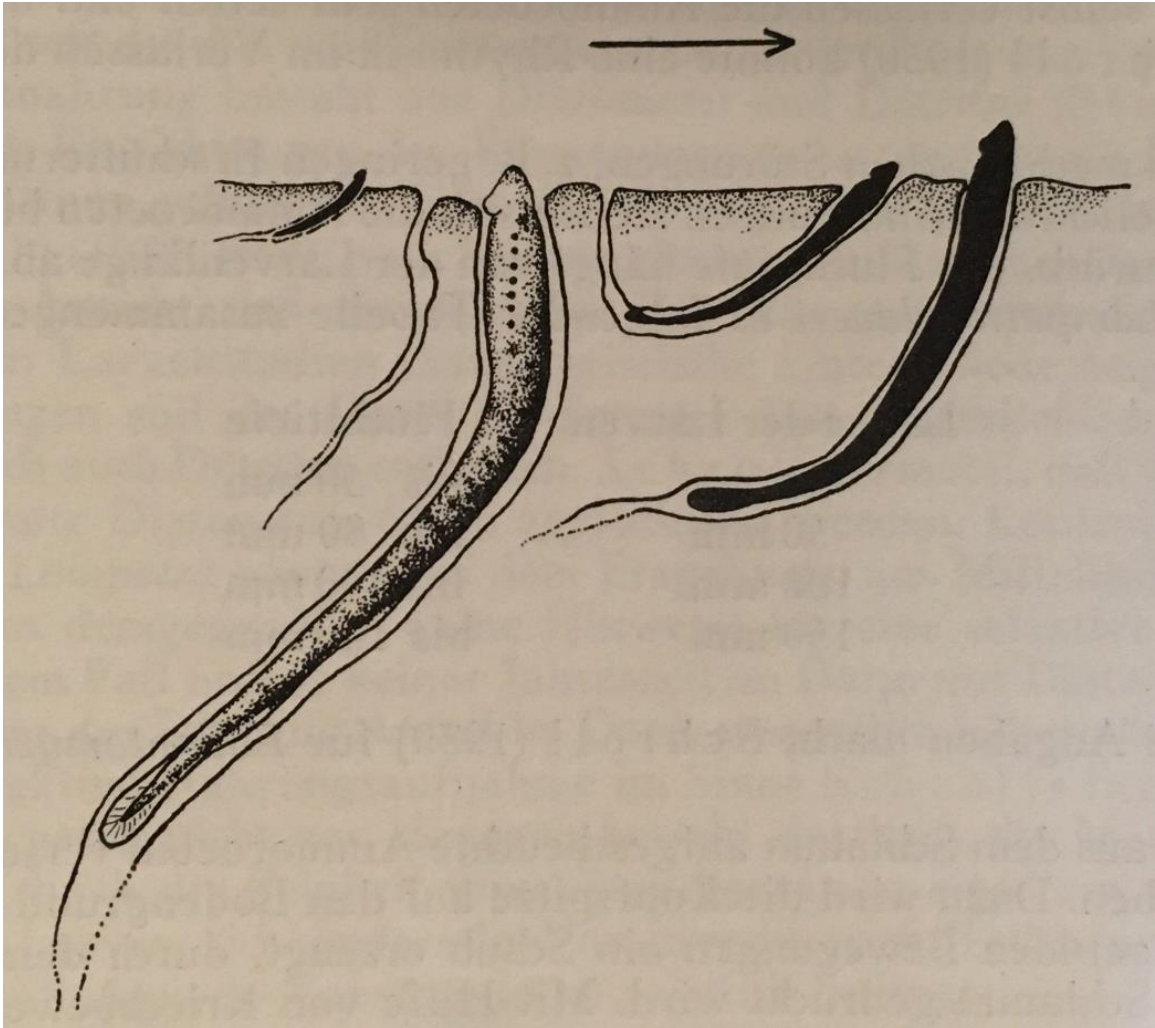


Figure 6. Ammocoete of *Lampetra planeri* filter-feeding from their burrows (Gunther, 1960).

Native American tribes use Pacific lamprey for subsistence fishing and cultural purposes (Petersen, 2006). Since lamprey return to the freshwater environment at a time of year when it is cold, and there is a lull in salmon runs, Pacific lamprey provide an essential source of food high in fat for Native American tribes in the winter (Petersen, 2006). Pacific lamprey are often referred to as ‘eels’ in California because of their shape, and ‘eeling’ is the term used by Native Americans for fishing for lamprey. There are

three common ways of eeling; (1) hooking lamprey at the mouth of a river, (2) catching lamprey with a net left out over-night near the bank of the river, and (3) picking off individual lamprey at waterfalls (Petersen, 2006) and, in more recent years, off the face of dams (Simpson, 2019).

Eeling is a way for tribal members to be in rhythm with natural processes and cycles. For example, eeling at the mouth of the river requires knowledge of tidal cycles, river morphology, and the other species present (Petersen, 2006). After eeling, the Pacific lamprey are distributed among the other tribal members starting with the Elders in exchange for stories and cookies (Petersen, 2006; Simpson, 2019).

Threats to Pacific Lamprey

Pacific lamprey populations have historically not been monitored (Reid & Goodman, 2016; Wang & Schaller, 2015) because of their status as “trash fish,” but through traditional ecological knowledge we know that populations have declined over the past century (Petersen, 2006; Simpson, 2019).

Low streamflow threatens Pacific lamprey in many stages of their life cycle. Northern California has a Mediterranean Climate; 90% of rainfall occurs between October and April (Lisle et al., 1990). During the warm, dry summer, streamflow naturally recedes, the temperature rises steadily, and reaches can become dewatered. Streamflow declines below the natural baseflow throughout the California North Coast region are a result of many factors, including land management, dams, diversions, and climate change (Klein et al., 2016). Some adults over-summer by burrowing into the

cobble of the streambed. Burrowed adults may not get the cue to emerge from the cobble until the water level has already receded, limiting their ability to migrate to a more suitable location (pers. comm. D. Goodman, 2020). Pacific lamprey eggs in a redd can die from desiccation, high temperatures, or lack of oxygenated water (Stillwater Sciences, 2014).

Low flow is a threat to the ammocoete life stage as well. When the stage of a river is dropping, ammocoetes do not receive the cue to leave their burrows until the surface is already dewatered, because they do not respond to changes in head pressure (Liedtke et al., 2015). Once they emerge from their burrow, they wiggle along the surface or swim to a more suitable location (Liedtke et al., 2015). The risk of ammocoete mortality 48 hours after a deposit is dewatered depends on the length of ammocoete. If the ammocoete is 20 mm or less, the mortality risk is estimated to be 100%; at 60 mm, the risk is 80-100%; and at 120 mm, this risk reduces to 15-40% (Liedtke et al., 2015). During the trials in Liedtke et al. (2015), if an ammocoete came to the surface, it was four times as likely to perish compared to the ammocoetes that stayed burrowed. The smaller ammocoetes were 60% more likely to come to the surface and, once emerged, struggled more to find water compared to larger ammocoetes (Liedtke et al., 2015).

Increased temperature is another water quality threat to Pacific lamprey who are temperature-dependent for maturation and ammocoete development (Clemens et al. 2009; Holmes 1990). Instream temperatures increase in the summer due to an increase in solar radiation and decreased streamflow. Pacific lamprey migration ceases as the water temperature reaches and exceeds 20 °C (Stillwater Sciences, 2014). Moreover,

temperatures above 18-22 °C during spawning and egg development reduce Pacific lamprey egg survival (Stillwater Sciences, 2014). Thermal refugia determine where lamprey juveniles reside in an estuary (Goertler et al., 2019). Temperature increases from year to year have been documented in the Eel River Basin of northern California since 1977 (Higgins, 2013; Kubicek, 1977).

Poor water quality also threatens lampreys. Ammocoetes live in fine sediments, where pollution tends to accumulate (Nilsen et al., 2015). Lamprey ammocoetes accumulate toxins by filter-feeding; in the Trinity River (northern California), they can accumulate 25 times more mercury than mussels, another filter feeder, from effects of the historic gold and mercury mining in the watershed (Bettaso & Goodman, 2010). When ammocoetes were tested in a lab for the effects of toxins in the substrate, the ammocoetes were slower to burrow into contaminated sediment and came up to the water column to ‘cough,’ which leaves them vulnerable to predation (Unrein et al., 2016). Traditional ecological knowledge from the Klamath Basin suggests that herbicides from the logging industry and direct poisoning from dam operators and California Department of Fish and Game (i.e., because lamprey would clog the turbines), caused a significant decrease in lamprey populations in the 1960s and 1970s (Petersen, 2006). The Oregon Fish Commission had a practice from 1940 to 1980s to remove non-game fish from rivers across the state using rotenone, a piscicide, resulting in the decimation of many age classes of lamprey (Close et al., 1995).

Migrational barriers are a threat to lamprey because they are anadromous. Barriers to migration can prevent adults from spawning in suitable freshwater habitat and

macrophthalmia from reaching the ocean. Pacific lamprey have evolved the ability to climb up vertical waterfalls, but unlike salmon, they cannot leap. Traditionally, if there is a migration barrier, fisheries restoration professionals have made passage available to jumping anadromous fish (i.e., fish ladder), but this does not necessarily allow lamprey passage (Stillwater Sciences, 2014). Migration barriers for adult Pacific lamprey include culverts and fish ladders with 90° angles at the top (Goodman & Reid, 2017).

There are also migration barriers for juvenile lamprey. Ammocoetes are not strong swimmers; they drift downstream and settle in low-velocity water with fine sediment (Docker, 2015). Newly hatched ammocoetes are found in drift nets during the low summer flows and macrophthalmia can be found in driftnets in spring flows (White & Harvey, 2003). Fish screens are installed at stream diversions to protect downstream migrating salmonids but pose a barrier to downstream migrating lamprey because they impinge on screens, which can result in mortality (Moser et al., 2015)

Dams and diversions also pose a threat to lamprey by altering the natural flow. Sudden decreases in flow can dewater deposits suddenly stranding ammocoetes, as seen by members of the Karuk Tribe in the Klamath Basin (Petersen, 2006). Reductions of streamflow due to diversions can dewater lamprey redds, leaving the eggs to die (Petersen, 2006). If too much water is diverted from a river, the lamprey cannot migrate to smaller tributaries where the redds would be protected from larger, scouring flows (Petersen, 2006).

Pacific lamprey populations are in decline throughout their range (Reid & Goodman, 2015), but there are efforts to protect them. Historically, the range of Pacific

lamprey was coastal streams along the Pacific Ocean as far south as Japan on the west side of the Pacific Ocean and Baja California on the east side of the Pacific Ocean (Figure 7). The current southern extent of Pacific lamprey in California is the Big Sur River (Reid & Goodman, 2016) (Figure 8). In 2003, the United States Fish and Wildlife Service received a petition by conservation groups to list Pacific lamprey along with river lamprey (*Lampetra ayresi*), western brook lamprey (*Lampetra richardsoni*), and Kern brook lamprey (*Entosphenus hubbsi*) as threatened or endangered and designate critical habitat under the Endangered Species Act (Vaile et al., 2003). The petition did not provide information describing how the portion of the species' petitioned range is appropriate for listing under the Endangered Species Act, so the lamprey were not granted listing (Reid & Goodman, 2015). The USFWS created the Pacific Lamprey Conservation Initiative (PLCI) to facilitate addressing threats, restore habitat, increase the knowledge of Pacific lamprey, and expand the range in the U.S. of Pacific lamprey (Reid & Goodman, 2015).

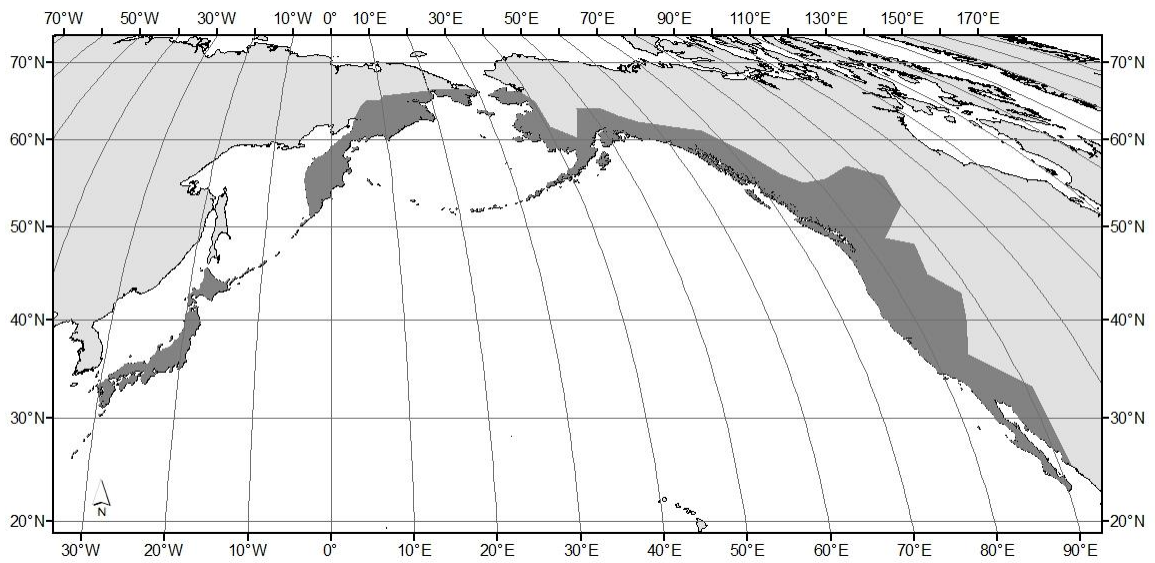


Figure 7. Estimated historic geographic distribution of Pacific lamprey (*Entosphenus tridentatus*) (Data Basin, 2011; Reid & Goodman, 2016; Renaud, 2011). Made with ArcMap version 10.6.1.

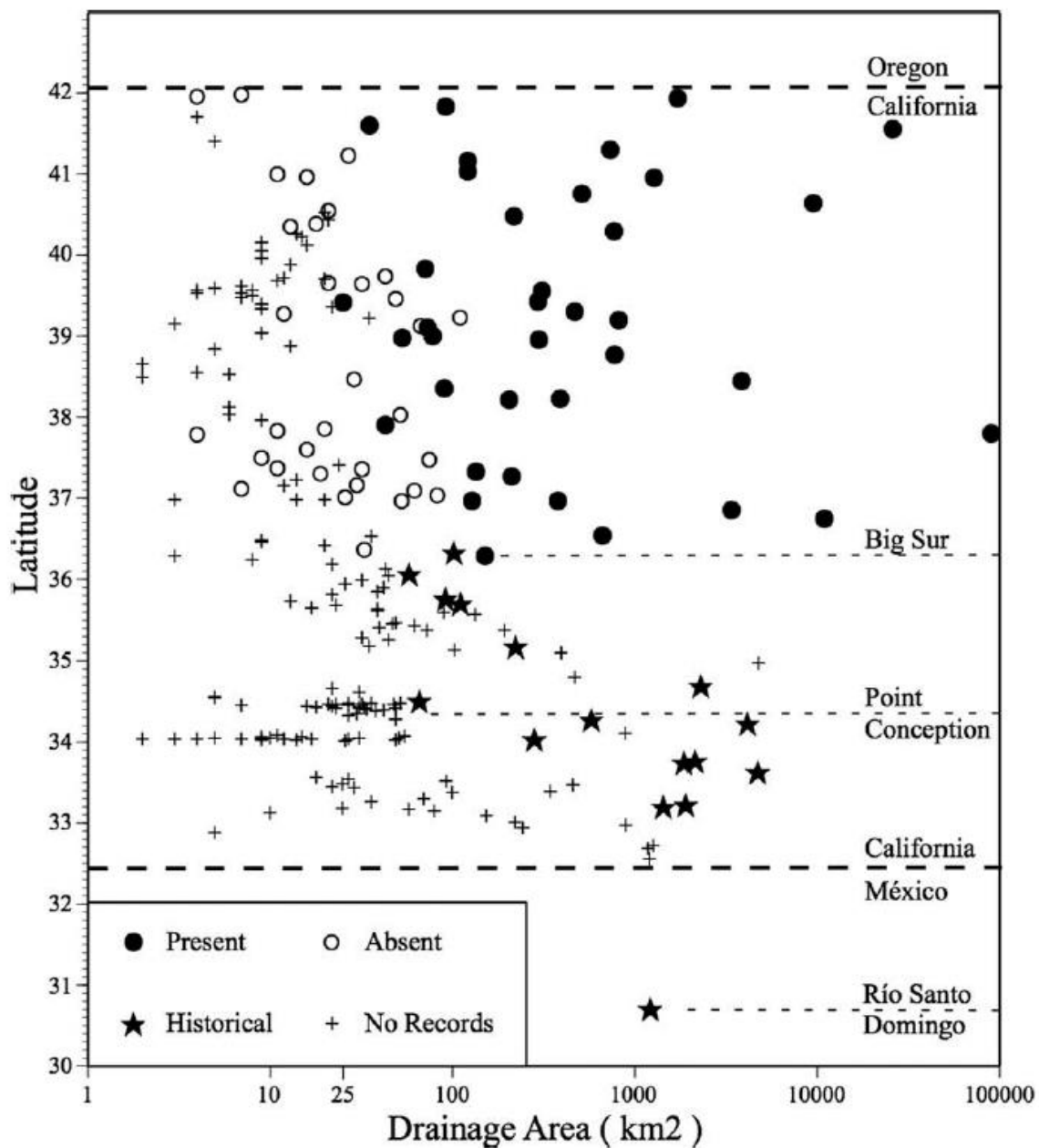


Figure 8. The current distribution of Pacific lamprey south of the Oregon-California border. ‘Historical’ sites have records, were surveyed, but no ammocoetes were found. ‘No records’ sites were not surveyed (Reid & Goodman, 2016).

Lamprey Ammocoete Habitat

Lamprey ammocoetes of all orders utilize a similar habitat; in California, the majority of ammocoetes are Pacific lamprey. Ammocoetes filter feed on the organic matter within fine sediments (Dawson et al., 2015; Gunther, 1960). Ammocoetes are found in fine substrate with organic material at the surface (Dawson et al., 2015). The presence of leaf litter may not be as significant in suitable habitat selection by ammocoetes as the presence of fine sediment because ammocoetes create a buildup of detritus on the surface (Sugiyama & Goto, 2002). Ammocoetes live in fine sand because it can be moved by ammocoetes and burrows held together by mucus, whereas finer sediment could block the gill lamellae and heavier sediment would be too difficult to move (Dawson et al., 2015).

Burrowing protects ammocoetes from predation (Dawson et al., 2015). The depth to which the lamprey burrows may depend on species and size (Dawson et al., 2015). Sea lampreys burrow only to a depth equal to their length, up to six inches (Applegate, 1950). Pacific lamprey ammocoetes were found to burrow 0-7.6 cm primarily, and no deeper than 15.2 cm in trials with substrate of $D_{50}=0.378$ mm with no organic matter; in this experiment, there was not a difference in ammocoete size and corresponding burrow depth (Liedtke et al., 2015). For the Far Eastern brook lamprey (*Lethenteron reissneri*) larger ammocoetes are more likely found in deep substrate, but smaller ammocoetes are

more likely found in substrate over 2 cm and at higher densities (Sugiyama & Goto, 2002).

Ammocoetes can be found at high densities. Pacific lamprey ammocoetes have been found at densities greater than 100/m² in the Middle Fork John Day River, OR, USA (Torgersen & Close, 2004) but there hasn't been an upper limit of density found on the west coast (pers. comm., D. Goodman, 2020). In British Columbia, over large scales, ammocoete densities average 27/m² (Beamish & Youson, 1987). Sea Lamprey ammocoetes survive at a higher rate with a density of 25/m² than at a density of 75/m² (Morman, 1987).

Lamprey densities are greater in fine substrate with higher amounts of organic matter. Ammocoete habitat quality is often categorized into three qualitative types (Type I, Type II, and Type II) first described by Applegate (1950) and further described by Stillwater (2013) (Table 1). Type I is comprised of silt and fine-to-medium sand and contains organic matter, which is the easiest substrate for an ammocoete to burrow into (Applegate, 1950). Type II is comprised of medium to coarse sand combined with little silt or organic matter and fine gravel combined with fine sand, silt, or organic matter (Applegate, 1950). Type III is considered not suitable for ammocoetes; Type III is small to large cobble or clay and bedrock, which the ammocoetes cannot burrow into (Applegate, 1950).

Table 1. Qualitative types of deposits for Ammocoete Habitat (adapted from: Stillwater Sciences, 2013).

Ammocoete Habitat Type	Ammocoete Use	Dominant Substrate	Particle Size Range (mm)	Needed Additions
Type I	preferred	silt	0.004-0.062	with or without organic matter
Type I	preferred	fine to medium sand	0.063-0.50	organic matter
Type II	suitable	medium to coarse sand	0.25-2.0	organic matter or silt
Type II	suitable	fine gravel	2.0-8.0	silt, fine sand, or organic matter
Type III	not suitable	clay	<0.004	
Type III	not suitable	medium to coarse gravel	8.0-64	
Type III	not suitable	small cobble to bedrock	>64	

In addition to fine sediment, ammocoetes require slowly flowing water to feed. Optimal Pacific lamprey ammocoete habitat has 0-0.1 m/s water velocity (Stone & Barndt, 2005). Ammocoetes need some water velocity to provide a food supply because they are filter feeders (Torgersen & Close, 2004). Ammocoetes are less likely to be in backwater areas that are not flowing, likely because of a lack of oxygen (pers. comm. D. Goodman, 2020). Although ammocoetes can handle oxygen levels lower than most teleost fishes; they can survive for at least four days of oxygen levels of 7-10 mmHg at 5 °C, 12-16 mmHg at 15.5 °C, and 13-21 mmHg at 22.5 °C (Dawson et al., 2015).

Fluvial geomorphic influences on ammocoete habitat distribution

The relationship between flow, water depth, velocity, and channel width change with the hydraulic geometry of the cross-section (Leopold et al., 1964). The two main

hydraulic controls on the discharge-to-stage relationship are the shape of the channel and the shape of the riffle crest cross-section (Rantz, 1982). Typically, in natural rivers, the riffle crest is the hydraulic control in base flows, and the shape of the channel is the hydraulic control in higher flows (Rantz, 1982). This is because once the stage (water surface) rises above its banks (bankfull), the width of the cross-section expands more than when the stage is below bankfull (Leopold & Maddock, 1953) (Figure 9). The controls to the stage-discharge relationship can be broken up further into four controls: channel, active, lower hydraulic transition, dominant section, and section control (Table 2).

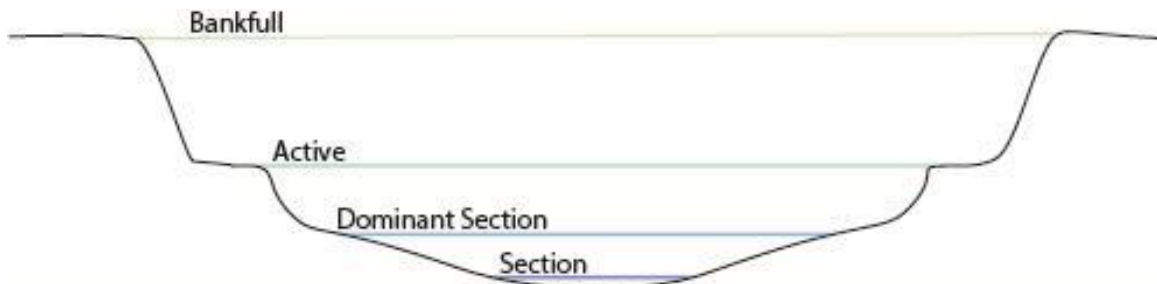


Figure 9. A generalized cross-section of a riffle crest with lines for the stage at bankfull channel control, active, dominant section, and section control stages.

Table 2. Thresholds and controls on the discharge to stage relationship (W. Trush et al., 1988).

Threshold	Flow	Description	Field Indicators
Channel Control	Q_{BF}	The shape of the valley and the floodplain affect the stage; the friction from the riffle crest is too small to affect flow.	Stage is above bankfull.
Active Channel	Q_{ACT}	The flow is high enough for the velocity to mobilize fine sediment.	Stage is near base of riparian trees. Water is turbid.
Lower Hydraulic Transition	Q_{LHT}	Sectional and active channel control is balanced.	Leaves at the bottom of pools are mobilized.
Dominant Section Control	Q_{DOM}	Riffle crests controls the stage upstream, with velocity through the pools.	The sides of riffle crests are inundated.
Section Control	Q_{SEC}	The riffle crest controls stage upstream. There is only velocity at the entrance to the pool. Water quality drops.	Leaves build up at riffle crest and sink.

The active channel is a smaller channel within bankfull that is altered by common storm events (Figure 9)(W. Trush et al., 1988). The annual exceedance probability of the active streamflow can range from 8% to 11% (W. Trush et al., 1988). The riparian zone is bounded by an upper bankfull stage and lower active channel stage (Figure 10). The most common way to locate the active channel stage is a bench where the base of alders/willows are located (W. Trush et al., 1988). Riparian vegetation is established at the edge of the active channel so that the vegetation can access water from the stream via groundwater throughout the dry season (Lisle, 1988).

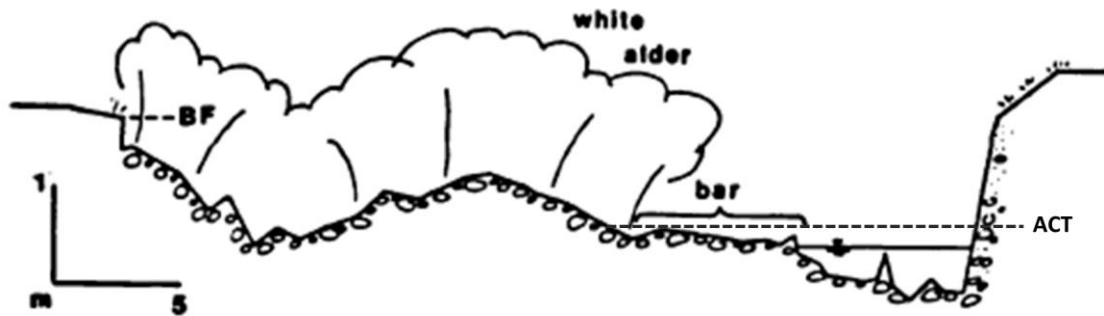


Figure 10. A stream channel cross-section, including white alders established between bankfull elevation (BF) and active channel elevation (ACT) (Lisle, 1988).

The riffle crest hydraulically controls the upstream stage (Richards, 1976), and therefore, the extent of ammocoete habitat deposit inundation. The riffle crest thalweg (RCT) is the lowest channel bed elevation along the riffle crest cross-section, which also is the highest bed elevation longitudinally between two pools. Therefore, when the streamflow recedes to zero, the riffle crest cross-section is the first portion of the thalweg dewatered (Lisle, 1987) (Figure 11). Pools are tempting places to monitor water depth and elevation from year to year, but they fill and scour of sediment regularly, so you cannot compare slope from year to year. Whereas, riffle crests are a generic location to measure depth, making them a reliable location to measure depth and elevation. Riffle crest thalweg depths are similar from pool to pool as well.

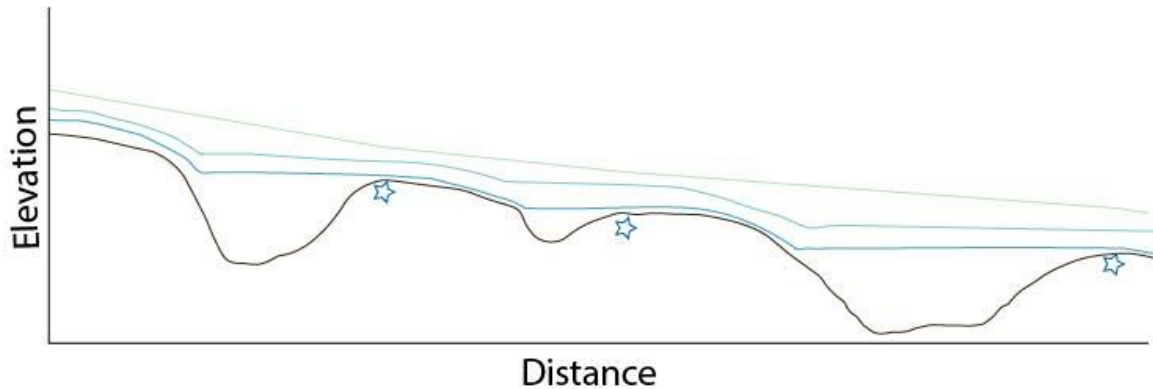


Figure 11. A longitudinal profile of channel bed elevation with multiple stage levels. The highest stage is at active channel control, the middle stage is at dominant section control, and the lowest stage is at section control. Stars mark the location of riffle crests, the highest channel bed elevation between pools.

The RCT depth is an important metric because of its functional relationship to stream ecological process and life history requirements. For example, defining a minimum RCT depth for salmonid passage can guide analysis for adult salmonids upstream migration (W. J. Trush, 1989) and juvenile salmonids downstream migration (Kastl et al., 2019). If a portion of the flow is diverted because of human use, a 5% change in the RCT depth from diversions could keep habitat conditions and processes unharmed (Mierau et al., 2018).

A riffle crest to flow rating curve can also be used to assess lamprey rearing habitat water quality. Once the RCT has reached section control, the water quality drops because the velocity in the pool drops to near zero. Fallen leaves start to build-up by the riffle crest, where they become waterlogged. When the waterlogged leaves sink to the bottom of the pools, they begin decomposing, a process that uses oxygen (Willoughby, 1974). Below section control, there are fewer bubbles forming when water travels over

riffles, so there is less dissolved oxygen in the water (Chanson, 1995). Between more oxygen being used from leaves decomposing and less oxygen being added in riffles, dissolved oxygen availability for ammocoetes plummets as the stage drops below section control. Without water movement over the deposit, ammocoetes are unable to filter feed, thus risking growth and possibly survival.

For ammocoete habitat deposits to form, fine sediment must be entrained upstream. Silt and sand are eroded when shear stress reaches the critical shear stress, as described by Shields (Shields, 1936). The Shields parameter, τ_c^* , is a dimensionless number that predicts the threshold of motion of sediment on a riverbed. The equation,

$$\tau_c^* = \tau / (\rho_s - \rho) g D_{50}$$

accounts for gravitational acceleration, g , the fluid density ρ , the density of sediment ρ_s , and the median grain diameter D_{50} . The shear stress the fluid imparts on sediment resting on the bed, τ , is defined as ρghS , where ρ is the density of the fluid, g is the constant of gravitational acceleration, h is the depth of the flow, and S is the slope of the fluid in the downstream direction (often estimated by the downstream slope of the river bed). (Miller et al., 1977). Miller et al. (1977) were able to expand on the equation by referencing experiments in lower and higher ranges. The typical Shields parameter, τ_c^* , for incipient motion in sand is ~ 0.03 .

Reach level geomorphic controls on ammocoete habitat

At the reach scale, stream geomorphic variables that affect ammocoete habitat availability include stream slope, sinuosity, bankfull width, and grain size distribution.

The slope is rise over run, or the change in elevation per length of stream channel. Lower slope reaches tend to deposit finer sediment (Ferguson et al., 1996). Sinuosity describes how many meander bends there are in the river. The equation for sinuosity is:

$$\text{Sinuosity} = \text{Reach length} / \text{valley length}$$

With each meander bend exists an opportunity for flow separation and an overflow channel. Flow separation is caused in a bend when there is excess pressure on the outside of the bend and a lack of pressure on the inside of the bend; there will be a backward flow of water to fill the gap and eddying results (Bagnold, 1960) (Figure 12).

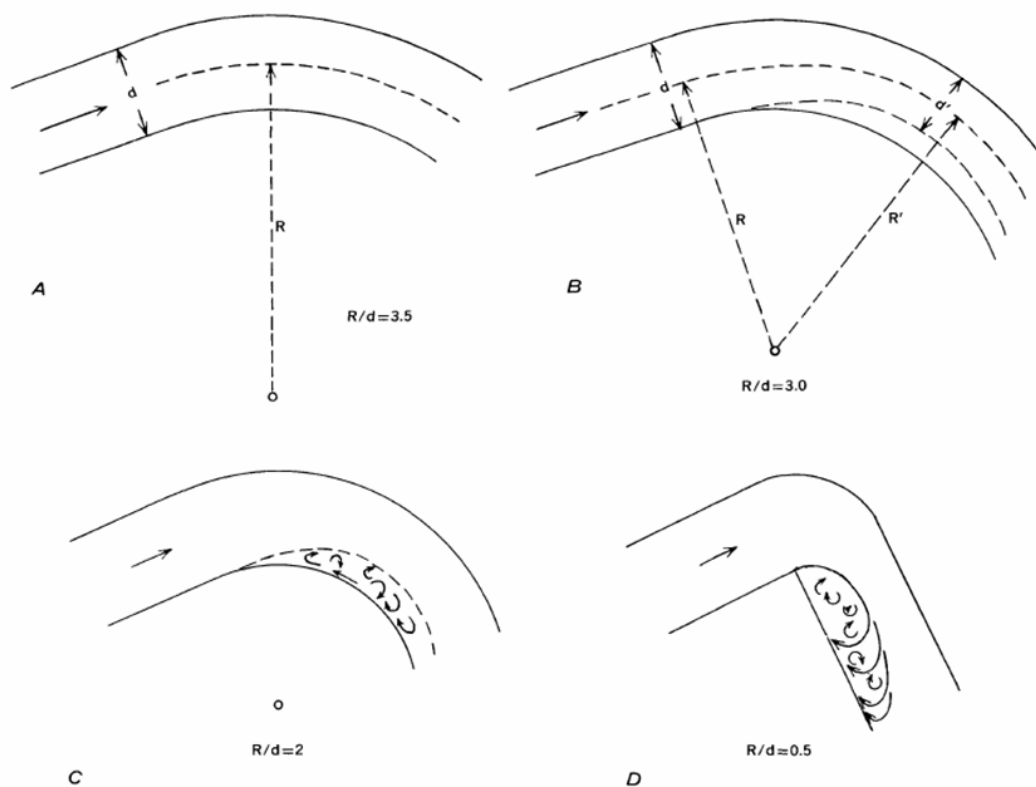


Figure 12. As a meander bend becomes tighter, there is more flow separation. There is a change in the ratio of the radius of curvature (R) and the active channel width (d) as the meander bend tightens (Bagnold, 1960).

The R/d is the ratio of the radius of curvature (R) to active channel width (d) and determines whether a flow separation occurs along the inside edge of the meander bend (Bagnold, 1960). The flow along this outside edge of a meander bend continues with high velocity, but the inside of the curve has a wild eddying effect (Bagnold, 1960). A tighter meander bend in a river has a smaller R/d ratio. The smallest R/d is 0.05; a right angle; anything smaller is an obstruction. When a river of any size creates its own meanders, it will have R/d ratios between two and three (Bagnold, 1960), therefore to have an R/d ratio lower than 2.0, the bend must be forced.

An overflow channel is created when flows exceed bankfull depth in a sinuous channel (Amoros et al., 1987). The overflow channel has alcoves at the entrance and outlet that are filled with fines (Amoros et al., 1987). The alcoves filled with fines are connected to the main channel after the stage drops, and the majority of the overflow channel is dewatered (Amoros et al., 1987).

Bankfull width, flow, and drainage area tend to trend together (Legleiter, 2014). Either bankfull width or drainage area can be used to describe channel size.

The source and supply of sediment can be a control of the size of the sediment in the stream. Softer bedrocks will erode easier providing more fines to the river sediment (Lisle & Hilton, 1999). The local sediment supply can be a control of bedload transport (Yager et al., 2012).

Deposit level controls on ammocoete habitat availability

Besides reach level controls on fine sediment, there are also controls on fine sediment at a smaller scale. Discrete habitat of varying quality can be found in diverse

geometric settings within a single stream. Schultz et al. (2014) analyzed different types of habitat by ammocoete catch per unit effort (CPUE) (Schultz et al., 2014). Off channel habitat had four times the densities as pools and 32 times the densities as riffles (Schultz et al., 2014). Small-scale ammocoete habitat was associated with patchy fluvial features like backwaters, eddies, insides of bends, and downstream ends of sand bars (Schultz et al., 2014). In the Willamette River watershed, other than habitat type, nearby anthropogenic disturbance and percentage area of fines were significant predictors for ammocoete presence (Schultz et al., 2014). Schultz et al. (2014) used the anthropogenic disturbance index from the National Fish Habitat Partnership Data System that uses 15 disturbance variables ranked on their influence to fish; top variables in order of weight were: urbanization, point-source pollution, pasture lands, and dam densities (Esselman et al., 2011). Ammocoete density was similar throughout most of the Willamette River watershed, but more ammocoetes were found lower in the watershed, where more fine sediment habitat was available (Schultz et al., 2014).

Research Objectives

Pacific lamprey population numbers are drastically lower than they once were. Pacific lamprey ammocoetes represent a vulnerable, relatively immobile life stage. They are unable to swim upstream, yet live in highly mobile deposits up to ten years (Stillwater Sciences, 2013). Abundant, high-quality habitats are required for Pacific lamprey recovery (Reid & Goodman, 2020). My specific research objectives were to 1) predict

ammocoete habitat distribution in coastal watersheds in northern California based on channel morphology (Spatial Model), and 2) explore the relationship between stream channel geomorphic features and ammocoete habitat loss during the summer streamflow recession limb in a northern California watershed (Redwood Creek temporal habitat loss).

MATERIALS AND METHODS

Site Description

Study sites for Research Objective No. 1 (Spatial Model) included a variety of northern California watersheds, including the Klamath, Eel, Smith, and Mad rivers, as well as smaller drainages along the coast and watersheds surrounding Humboldt Bay (Figure 13). Research Objective No. 1 used a subset of geomorphic survey locations of the Hydro-Geomorphic Classification Project funded by the California State Water Resources Control Board, designed by UC Davis researchers, and field research conducted by the HSU River Institute. The study area is home to many Native American groups, including the Yurok, Wiyot, and Hoopa tribes, who actively monitor lamprey (Stillwater Sciences, 2010). Most of the region is rural with industries in forestry and agriculture (including cannabis) (Bauer et al., 2015; Formosa & Kelly, 2020). The urban areas include Weaverville, the Humboldt Bay area, Crescent City, and Willits, California.

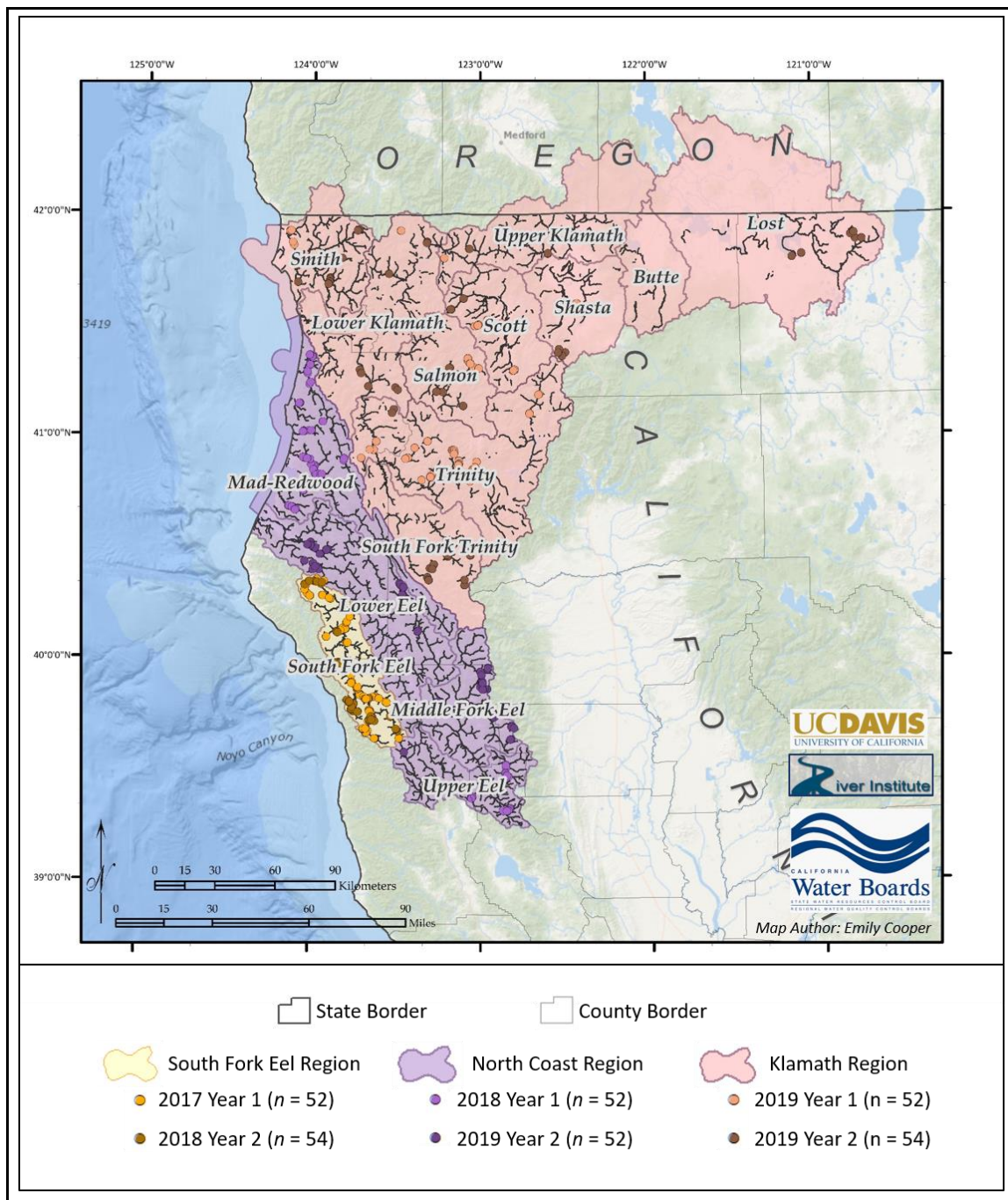


Figure 13. Study Area for Research Objective No. 1, including the South Fork Eel, North Coast, and Klamath Regions (South Fork Eel Region is also part of the North Coast Region). Research Objective No. 1 used a subset of geomorphic survey locations, dots, of the Hydro-Geomorphic Classification Project funded by California State Water Boards, designed by researchers at UC Davis, and field research conducted by the HSU River Institute. (Map Author: Emily Cooper).

The study area for Research Objective No. 1 (Spatial Model) is located within two California geomorphic provinces: the Klamath Mountains and the Coast Ranges (California Geological Survey, 2002). The Klamath Mountains have peak elevations of ~2,000 m asl and an uplifted plateau with successive benches with canyons (California Geological Survey, 2002). The Coast Ranges have mountains that trend in the northwest direction with peaks of 600-1000 m composed of thick sedimentary strata; the study area is in the northern section of the Coast Ranges, dominated by the Franciscan Complex (California Geological Survey, 2002).

For Research Objective No. 2 (Redwood Creek temporal habitat loss), I chose ten study sites within the Redwood Creek watershed, a 25 mi² tributary to the South Fork Eel River (Figure 14). The Redwood Creek watershed is 63.5% forest cover, and only 2.2% developed land (USGS, 2019). The only town within the Redwood Creek watershed is Briceland, and residents live on small parcels dispersed throughout the watershed. The longest flow path along Redwood Creek is 11 mi, and the mean annual precipitation is 65 inches (PRISM Climate Group & Oregon State University, 2004). The major industries in the Redwood Creek watershed are forestry, ranching, and agriculture, including cannabis cultivation.

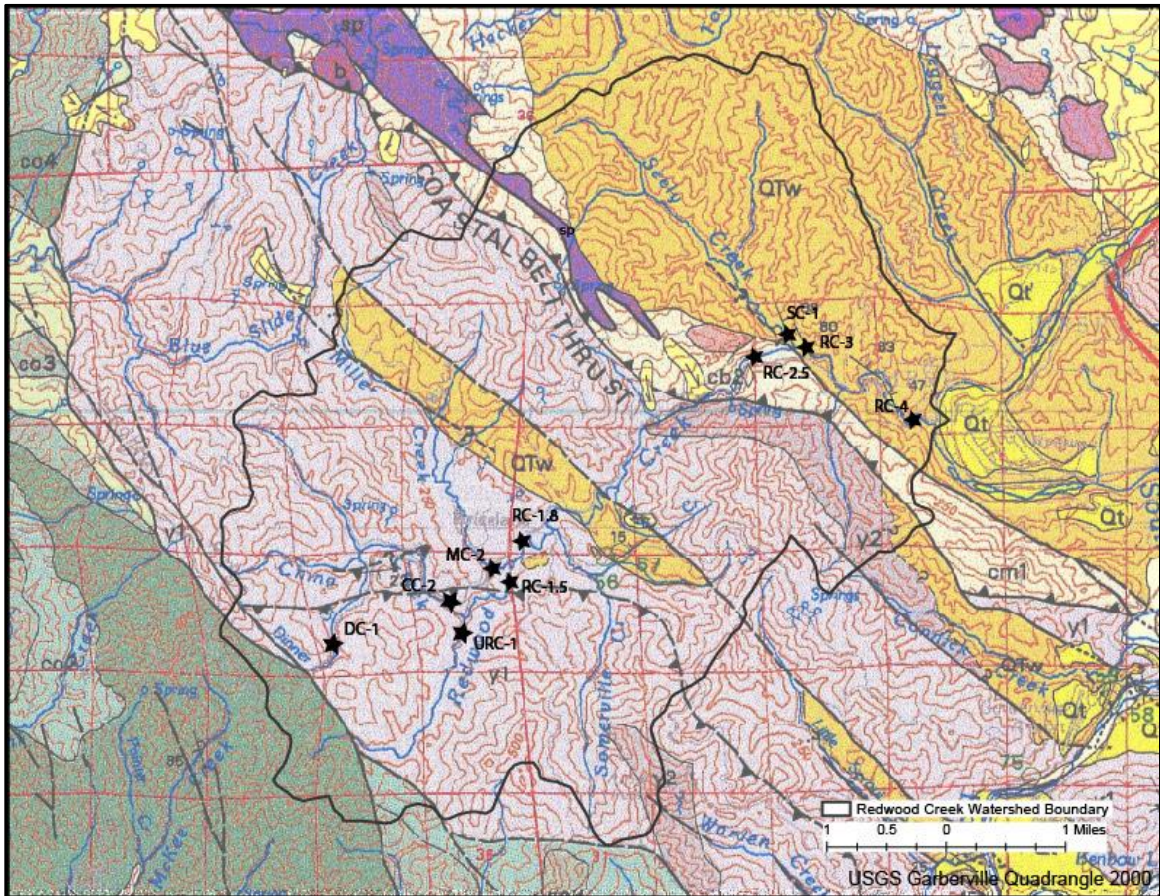


Figure 14. Redwood Creek monitoring sites, labeled with stars, on a geologic base map (McLaughlin et al., 2000). Central Belt formation is in the upper right; the Coastal Belt is in the bottom left. QTw=weakly consolidated sandstone. Sp=peridotite. RC=Redwood Creek, SC=Seely Creek, MC=Miller Creek, CC=China Creek, URC=Upper Redwood Creek, and DC=Diner Creek. Made with ArcMap version 10.6.1.

Redwood Creek is partially in the Coastal and Central Belts with a peridotite wedge in the middle (Figure 14). An eastward dipping thrust fault forms the boundary between the older Central Belt and the younger Coastal Belt (Figure 14). The Coastal Belt is composed primarily of argillite and sandstones with some conglomerate facies. The thickly weathered material of the Coastal Belt stores vast volumes of water that

sustain perennial streams (Lovill et al., 2018). The Central Belt is composed of a highly sheared argillite matrix and a wide range of more competent units such as greywacke sandstone, basalt/greenstone, chert, and blueschist. A comparatively thin weathered zone results in limited subsurface water storage and ephemeral streams in the Central Belt (Lovill et al., 2018). Between the Coastal and Central Belts in the Redwood Creek watershed is a strip of peridotite and a broken formation of greywacke, both water storing units.

Low flow problems were apparent to Redwood Creek watershed residents beginning in the early 2010s. The Salmonid Restoration Federation (SRF) was called to action and responded in a manner that mirrored the monitoring program of Sanctuary Forest, who monitored the headwaters of the Mattole watershed just west of Redwood Creek (Klein, 2018). SRF measured Redwood Creek streamflow between 2013-2019 during the low flow season, roughly June to November (Klein, 2018). Eleven sites were measured in 2013 and 2014. In 2015 and 2016, another site was added, and SRF used three continuous pressure transducer data loggers on three mainstem sites to measure the river stage. In 2018 and 2019, the monitoring sites were streamlined to ten sites.

Recent low flows on Redwood Creek have been attributed to climate change, change in vegetation species and age, land disturbance, stream bed sedimentation exacerbating sub-surface streamflow, and water withdrawal for human use (Klein, 2018). Precipitation has gradually decreased in September across northwest California and southwest Oregon (Asarian & Walker, 2016). Young Doug fir trees in coastal northern California use more water per basal area than older trees (Stubblefield et al., 2012). The

area was clear cut in the 1950s and 1960s, so much of the area has young trees and high water demand (Stubblefield et al., 2012). Flow diversions for cannabis in the early 2010s accounted for an estimated 80% of the seven-day low flow of Redwood Creek at the confluence with the South Fork Eel (Bauer et al., 2015).

Field Methods

Objective #1: Predict ammocoete habitat distribution for coastal watersheds in Northern California based on channel morphology (Spatial Model)

I used the California hydrogeomorphic classification system to sample a broad representation of channel types throughout the Klamath and North Coast regions. This classification integrates geomorphic, geospatial, and statistical methods with nested hydrologic and geomorphic classifications (Lane et al., 2016). For site selection, the classification project separates stream reaches into 15 ‘bin types’ depending on the upstream watershed area and channel slope; there are three categories of drainage area and five categories of slope. The study was designed to sample an equal number of reaches from each bin in each region. For the purposes of my research, selected reaches were not randomly sampled because of constraints on site access and frequency of bin types in each region (Cooper et al., 2017). Reach lengths were 15 times the mean bankfull width of the channel. I measured a total of 37 reaches for ammocoete habitat in the summer of 2018 in the North Coast Region. In the summer of 2019, with the field crew, I measured 115 reaches in the North Coast and Klamath regions.

The field crew and I measured traditional geomorphic diagnostics from Rosgen (1994) in each reach, including channel slope, bankfull width, bankfull depth, sinuosity, bed surface sediment composition, and entrenchment ratio as well as floodplain elevation and undulations (Lane et al., 2016). We measured channel slope using standard surveying equipment (tripod, level, stadia rod) and a laser range finder or measuring tape for measuring reach length. I calculated channel slope by dividing the change in elevation by reach length (i.e., distance from the riffle crest at the beginning of the reach to a riffle crest at the end of the reach via the thalweg). Bankfull width is the wetted width of the channel when the water surface reaches the top of the banks and typically has a recurrence interval of every ~1.5 years (Leopold et al., 1964) (Figure 15). Bankfull depth is the maximum depth measured from the thalweg to the estimated water surface at bankfull. The grain size distribution of the bed was measured using a gravelometer; eight particles of bed substrate were measured along ten transects and placed in a size class, for 80 particles measured in the reach. The minimum number of particles needed for reproducible results is sixty (Brush, 1961).

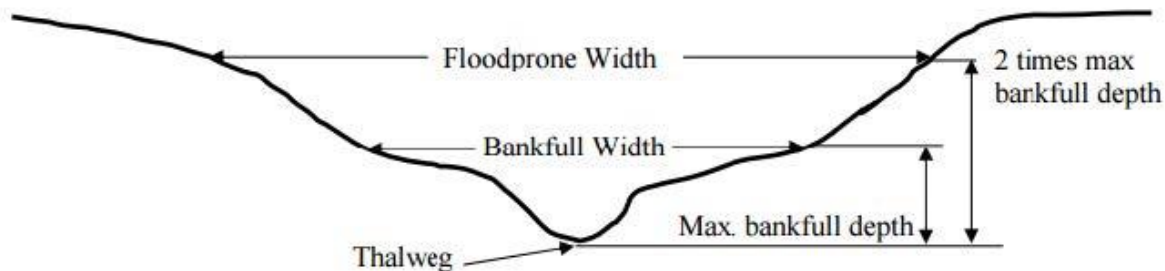


Figure 15. Cross-sectional view of stream channel dimensions (Source: Kline et al. 2009).

During each geomorphic survey, I identified silty-sandy deposits suitable for ammocoetes inundated within the active channel. At each suitable silty-sandy deposit, deposit area was measured and the associated categorical geomorphic controls recorded. I visually assessed the substrate size to determine ammocoete habitat quality type (Table 1) as Type I or Type II substrates. The minimum size of a deposit inventoried was five centimeters deep and one meter wide (in any direction). To estimate the deposit area, three to five representative widths and at least one length (more if needed to characterize area) of the deposit was measured (Figure 16) using a stadia rod, laser range finder (model: TruPulse 200x), or marked walking stick for deposit width and length measurements. I checked the minimum depth requirement of the silty-sandy deposits with an instrument about one centimeter in diameter that can penetrate the substrate, such as a pencil with five centimeters depth marked. Substrate can appear as a deep bed of silt, but after investigation with a finger or a pencil, be only a thin silt layer overlaying a cobble or impenetrable substrate.



Figure 16. Example of length and width measurements of a silty-sandy ammocoete habitat deposit during geomorphic field surveys. Deposit area was calculated by the average of at least three width measurements multiplied by the length. Modified photo from Lisle (1999).

I recorded categorical geomorphic depositional controls for each measured deposit, including obstructions, the radius of curvature ratio, overflow channel type,

debris dams, overflow channels, pool tail outs, bank erosion, and confluence (Figure 17). Types of obstructions included large woody debris, live riparian vegetation, and boulders (Figure 17 A). Natural large wood dams in the North Coast typically occur from a buildup of large woody debris (Bilby & Likens, 1980; Keller & Swanson, 1979); they can hold back sediment on the upstream end (Figure 17 B). Types of deposits from overflow channels include side channels, alcoves, and inlets (Figure 17 C). Tight curves in the river can have deposits on the inside bend (Figure 17 D). Bank erosion leads to ammocoete habitat when fines are deposited directly below an actively eroding bank (Figure 17 E). Pool-tail outs are when the water velocity drops enough so that fines drop out of the water column before the riffle crest, usually in long pools (Figure 17 F). Confluence is when there is a buildup of fine sediment where two creeks meet (Best, 1987; Mazgareanu et al., 2020).

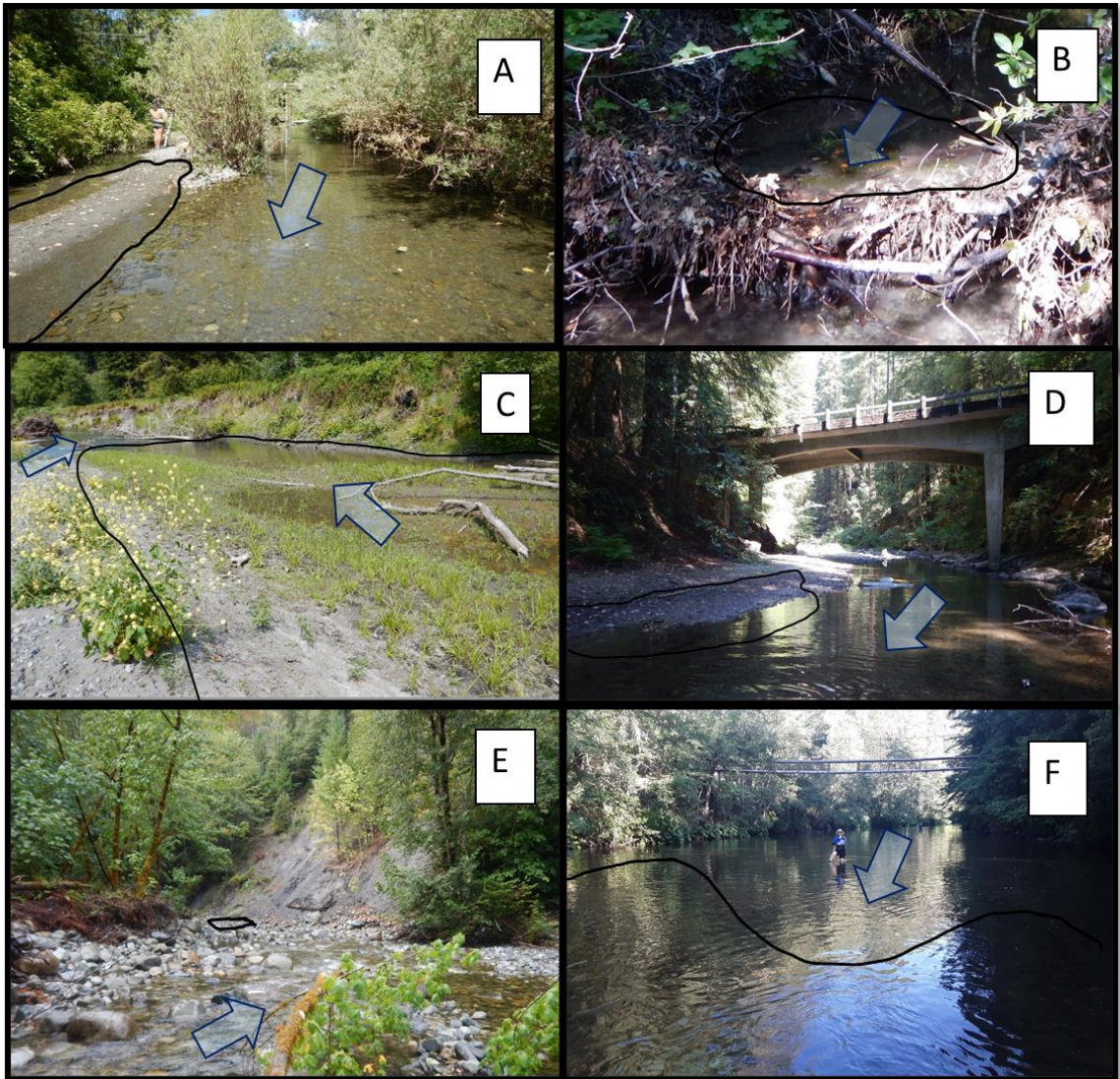


Figure 17. Examples of geomorphic controls with the corresponding deposit outlined in black and arrows indicating flow direction: a willow tree acting as an obstruction (A), debris dam holding sediment on the upstream side (B), off-channel alcove from side-channel (C), small radius of curvature (D), erosion from the bank, and edge deposit (E), and a pool tail out (F).

Ammocoete habitat density was defined as the ratio of available habitat area (m^2) divided by reach length (m).

$$\text{Habitat density} = \frac{m^2 \text{ available habitat}}{m \text{ reach length}}$$

Objective #2: Explore the relationship between stream channel geomorphic features and risk of ammocoete habitat loss during the summer streamflow recession limb in a northern California watershed (Redwood Creek temporal habitat loss)

I measured streamflow (cfs) on Redwood Creek, a tributary to the South Fork Eel River at ten sites biweekly from May 11 to November 29, 2019 (Figure 18). I measured streamflow in the field with a velocity meter (Marsh-McBirney 2000) or the volumetric method as outlined in the Quality Assurance Project Plan (QAPP) for the Redwood Creek, South Fork Eel River, Water Conservation, Monitoring, Planning and Assessment, and Education Project (Stolzman et al., 2015). With a velocity meter, I used a minimum of six cells that were a minimum of 0.6 ft deep, 0.1 ft wide, and had a minimum of 0.05 ft/s current velocity. If I could not locate a cross-section that had ten cells meeting those criteria, I found an alternate location using the volumetric method. The volumetric method requires a drop in elevation of a streambed to capture all the flow in a container. I measured the time (sec) the container filled, and the volume of water (L) filled in that time to calculate flow. I made sure that not more than 5% of the flow escaped the sides of the container and filled the container for more than one second. I repeated measurements at least four times and until there were three measurements within 10% of each other. The final flow was the average of these three measurements.

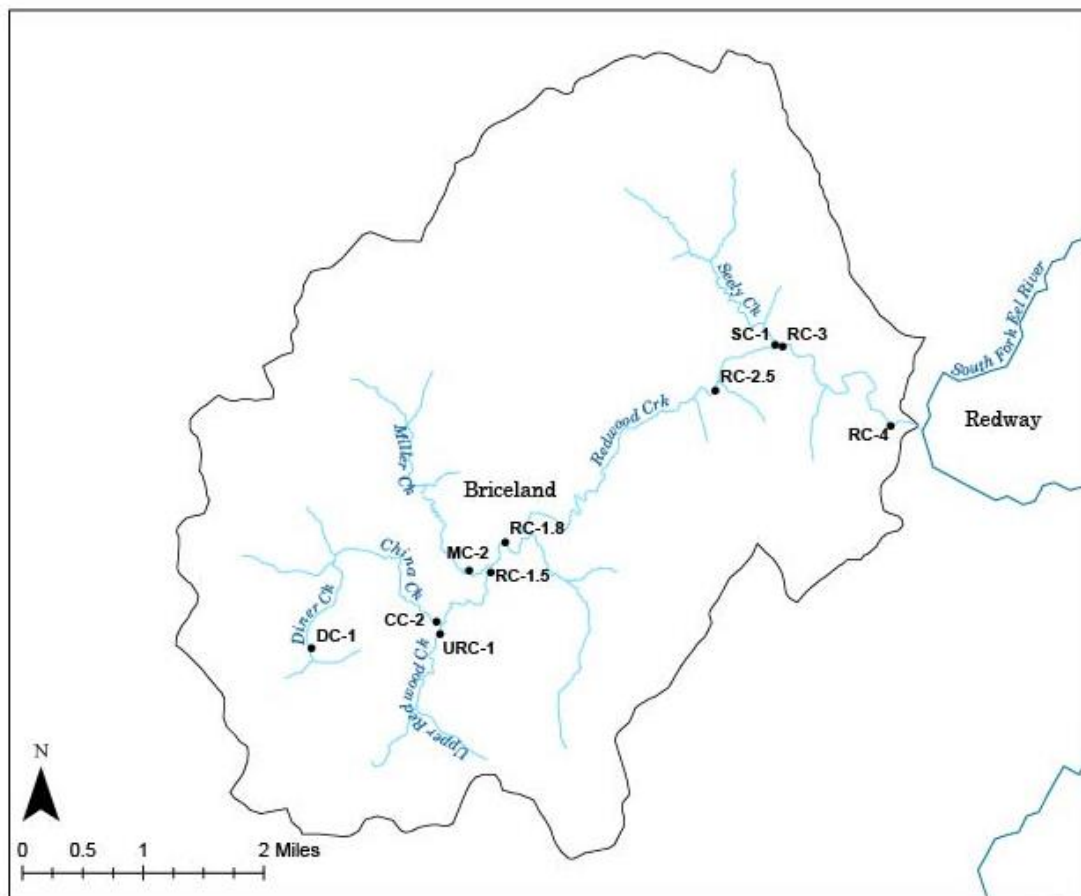


Figure 18. Streamflow monitoring sites in Redwood Creek. RC=Redwood Creek, SC=Seely Creek, MC=Miller Creek, CC=China Creek, URC=Upper Redwood Creek, and DC=Diner Creek. Made with ArcMap version 10.6.1.

Each time I measured streamflow, I measured the vertical distance from a reference point to the water surface. The reference point was typically a nail in a root or a tree that overhung a pool. This acted as a stage reference in place of a staff plate to avoid theft or vandalism. I installed water level loggers (HOBO U20L) at seven sites to record stage every 15 minutes for measurement in-between monitoring at increments of 0.001 ft (0.003×10^{-1} m). I had one pressure transducer in the air that recorded barometric pressure to correct for atmospheric fluctuations.

I used a total station (Leica TCP12013 and RX1220T) to survey a detailed topographic map of nine sites (some sites have multiple individual deposits in one pool) in the Redwood Creek watershed. The only site where I did not survey a deposit was the Seely Creek Site (SC-1, Figure 18), where there was no suitable deposit in the gage pool. At each site, I set up at least two temporary benchmarks, one for the total station and one as a backsight. To characterize the deposit, I surveyed points around the edges, at any inflections, and at least 0.15 m apart. I only surveyed deposits in the pools with a reference stage, the RCT, and reference points. I did not survey-in the whole stream channel.

Analytical Methods

Objective #1: Predict ammocoete distribution remotely for coastal watersheds in Northern California based on channel morphology.

A zero altered model for ammocoete habitat

The hydrogeomorphic team at UC Davis calculated stream slope, drainage area, confinement, average bankfull width, and average bankfull depth from the data the field crew and I collected (Byrne et al., 2020; Guillon et al., 2020). I determined the underlying lithology of bedrock from published USGS maps (Ludington et al., 2005). I used the Mohs scale to create a hardness attribute associated with bedrock type (Chesterman, 1978).

Ammocoete habitat density was defined as the total area of inventoried ammocoete deposits (m^2) per length of stream channel (m). Density is often a unitless variable, one area compared to another area, or a count per area. Because m^2/m is a rare variable to use, I explored the idea of using a density of an area per area of stream reach by multiplying the reach length by the bankfull length. There was no difference in variability between habitat area per length and habitat area per bankfull area. Because I measured ammocoete habitat deposits within the active channel, not the bankfull channel, I kept my original metric (m^2/m).

Variables examined included drainage area, slope, bankfull depth, bankfull width, bankfull depth to width ratio, the median grain size (D_{50}), and prevalence of ammocoete habitat (0=absent and 1=present). I used the variance inflation factor (VIF) to eliminate excess variables.

With many reaches without deposits, I created a zero altered model. The zero altered model has two parts, a presence/absence model to compute the frequency of occurrence and a Gamma distribution for the positive values only. I used (1) a Bernoulli distribution to model the prevalence of ammocoete habitat and (2) a Gamma distribution to model the habitat density because the response was continuous and had no negative values. For both models, I used backward selection, AIC, and R^2 to pick the best model for ammocoete habitat prevalence and density. I started with the full model, which included all the variables selected using VIF and interactions between them. A variable that was not significant was dropped and its associated interactions.

I used the ArcMap 10.6.1 spatial join feature to attach the slope, area, confinement from the stream layer, and rock hardness information from the geology layer to the individual sites where I collected ammocoete habitat data. The spatial join took the information from the closest stream reach segment to the GPS point for transect 1 of the reach within 100m. Transect 1 was the upstream end of the stream survey reach. I exported the attribute table to Excel to perform QAQC, which included removing extra rows, columns, and edited site names for consistency. I performed model selection using different distributions for prevalence and habitat density where present.

Geomorphic control to ammocoete habitat

I explored the difference in average slope among geomorphic controls. I started by comparing differences in average slope between the North Coast and Klamath region sites surveyed using an analysis of variance (ANOVA). I used graphical diagnostics to ensure that the ANOVA assumptions of normality and homogeneity of variance were met. Tukey's Honestly Significant Difference identified which geomorphic controls had a statistically significant difference in slope and size.

Objective #2: Explore the relationship between stream channel geomorphic features and risk of ammocoete habitat loss during the summer streamflow recession limb in a northern California watershed (Redwood Creek temporal habitat loss)

I chose to focus my analysis of exploring the relationship between stream channel geomorphology and diversion risks to ammocoete habitat availability during the summer streamflow recession limb at site RC-4 because it best represents the Redwood Creek

watershed. RC-4 is the lowest site in the watershed and receives streamflow inputs from both the Central Belt and the Coastal Belts. RC-4 also exhibits cumulative impacts from the upstream watershed, including landscape alterations and water diversions.

Estimate unimpaired hydrograph

In 2016, the California Department of Fisheries and Wildlife (CDFW) studied Redwood Creek as part of its California Water Action Plan (CWAP) (Cowen, 2018b). Their study objectives were to estimate unimpaired streamflow time series for Redwood Creek by scaling Bull Creek's (USGS gage #11476600) record, develop a hydrograph for Redwood Creek and its tributaries using 2016 monitoring data, and compare Redwood and Bull Creek 2016 hydrographs. The method CDFW used was watershed scaling recommended by the California Water Board Division of Water Rights for estimating flow in an ungaged watershed (California Water Resources Control Board, 2014). The method uses mean daily discharge (MDD) in cubic feet per second (cfs), drainage area (DA) in square miles, and mean annual precipitation (MAP) in inches.

$$MDD(ungaged) = MDD(gaged) \left(\frac{DA(ungaged)}{DA(gaged)} \right) \left(\frac{MAP(ungaged)}{MAP(gaged)} \right)$$

CDFW chose Bull Creek as the gaged stream for watershed scaling because it has a similar drainage area, precipitation, flow path length, and close proximity to Redwood Creek. The Bull Creek gage stopped operating November 1, 2018, before my research started. I wanted to estimate unimpaired flow using the flows I measured in 2019. To find another gage to compare with Redwood Creek, I considered the drainage area, distance from Redwood Creek, annual precipitation, the years gaged, and the R^2 of their

correlation. I selected three gages in the vicinity of Redwood Creek for comparison (Table 3): Elder Creek (USGS gage #11475560), South Fork Eel at Leggett (USGS gage #11475800), and Mattole River at Ettersburg (USGS gage #11468900). Elder Creek has the largest difference in annual precipitation from the Redwood Creek watershed. Leggett has the largest difference in drainage area from the Redwood Creek watershed. Ettersburg has the most similar drainage area, the shortest distance from Redwood Creek, the most similar precipitation, but has the shortest period gaged and is the most disturbed (PRISM Climate Group & Oregon State University, 2004).

Table 3. Variables considered for selection of a comparative gage to Redwood Creek. Drainage area from gage information annual precipitation from PRISM (PRISM Climate Group & Oregon State University, 2004).

Gage Name	Gage Number	Drainage ₂ Area (mi ²)	Distance from Redwood Creek (mi)	Annual Precipitation (inch)	Begin Date	Years gaged in 2019
Redwood Creek		26		64.92		
Elder	11475560	6.5	29	88.98	1967	52
Leggett	11475800	248	18	77.78	1956	63
Ettersburg	11468900	70.9	8	84.09	2001	18

The USGS gages in Table 3 have been in operation for 18-63 years. I wanted to determine if fewer years retain the same flow variability to streamline the analysis. Once I found a gage to use, I ranked water years on their May 1st flow for the past 50, 30, 20, and 10 years, then plotted their exceedance curves. I chose to start the time range on May 1st because it is the beginning of the summer streamflow recession and Pacific lamprey

ammocoete emergence. Pacific lamprey spawning begins around early April and larvae emerge early May (Brumo, 2006)

Estimate current condition hydrograph

I correlated flow measurements in Redwood Creek sites with the recorded flow measurements on the Elder Creek USGS gage (#11475560) to be used as current condition flow using Microsoft Excel. I constructed a rating curve between flow at Redwood Creek site RC-4 and riffle crest thalweg depth using Microsoft Excel.

Develop a relationship between flow, RCT, and portion habitat inundated

I used the data collected by the total station survey to create a raster surface in ArcGIS. I used the Multi-Volumes for ArcGIS 10 tool to measure the area inundated at every 0.001m in elevation of the complete range of elevation of the deposit (Gabrisch, 2013). I converted water elevation to RCT. I used RStudio, R version 3.5.1, to create a binomial logit function to predict the percent habitat surface area inundated based on the RCT. I chose a binomial logit function because the maximum inundated would be one, and the minimum would be zero, compared to a generalized linear model that would extrapolate past one and under zero. The RCT may increase past the highest elevation of the deposit, but the portion of the area inundated will not increase; similarly, when the stage drops below the deposit's lowest elevation, the portion inundated is not negative.

Evaluate hydrographs against criteria

To calculate the water quality threshold of section control, I needed the drainage area (mi^2) of the watershed upstream of the site, the RCT depth when the flow is at active stage (RCT_{ACT}), the power function exponent (PFE), and the hydraulic threshold ratio

(HTR) (Mierau et al., 2018). I found the drainage area for each monitoring site at Redwood Creek using USGS online application StreamStats (USGS, 2019). I measured depth of the active channel at the riffle crest in the field, RCT_{ACT} . The active channel unit discharge is $10 \text{ cfs}/\text{mi}^2$, I estimated the flow, cfs, of the active channel, Q_{ACT} (cfs), by multiplying the drainage area by $10 \text{ cfs}/\text{mi}^2$ (pers. comm., W. Trush, 2019). I found the power function exponent by fitting a power curve between the RCT and flow that ranges from near zero to the active channel stage. The HTR uses the PFE.

$$HTR = 0.3997PFE^{-0.678}$$

I found the lower hydraulic transition flow by multiplying the HTR by the active flow.

$$Q_{LHT} = HTR * Q_{ACT}$$

I found the threshold flow for dominant section control by multiplying the HTR by the flow at the lower hydraulic transition.

$$Q_{DOM} = HTR * Q_{LHT}$$

I found the threshold flow at section control, the flow I am using as a risk threshold for ammocoete habitat quality, by multiplying the HTR by the flow at dominant section control.

$$Q_{SEC} = HTR * Q_{DOM}$$

I found the RCT at section control by using the RCT-Q WY 2019 rating curve.

I used section control as a threshold for risk to ammocoete habitat because once the flow is below section control habitat quality declines (Table 4). Once the riffle crest stops flowing, there is no movement of detritus from pool to pool, resulting in a loss of nutrients for the ammocoetes to consume. Ammocoetes may survive with the deposit

dewatered (Liedtke et al., 2015; Rodríguez-Lozano et al., 2019), but it is most likely detrimental because of lack of feeding capabilities and poor water quality.

Table 4. Low flow risk levels and their associated conditions. Q =Flow (cfs). Q_{sec} =flow at section control (cfs). Q_0 =stage at RCT. Note: there may be risks to ammocoetes at higher flows, but they are not analyzed in this research.

Risk	Condition	Description
Low	$Q > Q_{sec}$	Flow is above section control.
Moderate	$Q_{sec} > Q > Q_0$	Flow is below section control, but water is still flowing over the riffle crest.
High	$Q_0 > Q > \text{deposit dewatered}$	Water has stopped flowing over the riffle crest, but there may still be water in the pool and over the ammocoete habitat.
Extreme	$Q < \text{deposit dewatered}$	The ammocoete habitat does not have any water inundation, although there may still be water in the pool.

Establish baseline condition ammocoete habitat using criteria

I counted the number of days under section control for each year for impaired flow for the deposits at site RC-4 in the Redwood Creek watershed, a tributary to the South Fork Eel River. I counted unimpaired days for each year and the number of days under different diversion rate scenarios. Impaired and unimpaired calibrated from Elder Creek (USGS gage # 11475560).

RESULTS

Objective #1: Predict ammocoete habitat distribution for coastal watersheds in Northern California based on channel morphology.

I surveyed 151 channel reaches for Type I and Type II ammocoete habitat deposits in the Klamath and North Coast Regions in summers 2018 and 2019 (Figure 19). Sites with larger drainage areas and lower slopes near the coast have a higher ammocoete habitat density. The lower ammocoete habitat density sites were predominantly to the east in smaller drainage areas and steeper slopes. Overall mean ammocoete habitat density for the 151 channel reaches surveyed was 0.4 m²/m: 29% of the reaches had zero ammocoete habitat deposits.

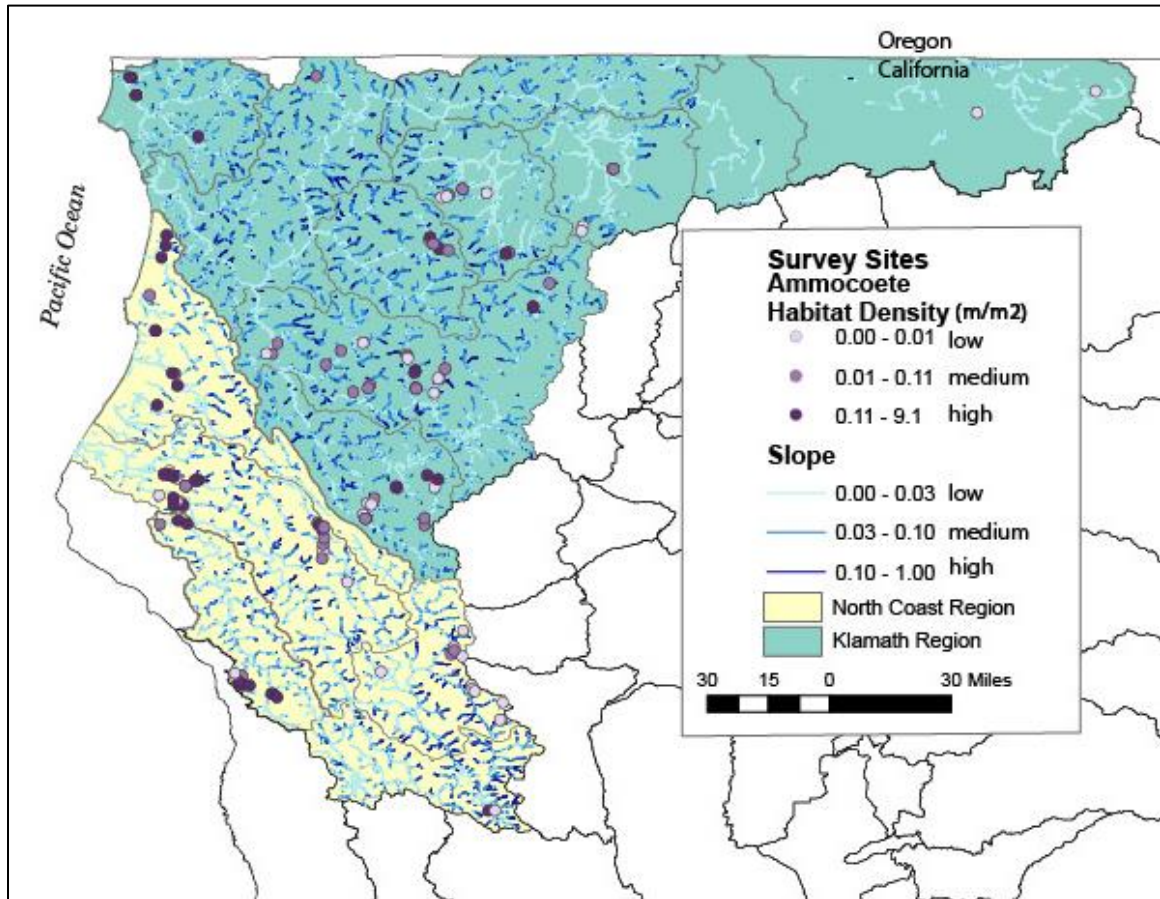


Figure 19. Sites surveyed for ammocoete habitat deposits. Sites categorized by ammocoete habitat density (m^2/m) (darker shade=higher density) and streams categorized by slope (darker shade=higher slope). Klamath and North Coast Region in different shades. Made with ArcMap version 10.6.1.

A zero altered model for ammocoete habitat distribution

Before creating a zero altered model, I started with data exploration. I explored the explanatory and response variables drainage area, slope, bankfull depth, bankfull width, the bankfull to width ratio, median grain size, ammocoete habitat area, and ammocoete habitat density with boxplots. Data exploration using boxplots revealed that there were many data points that were relatively large compared to the majority of the

observations; 50% of the data are within the box, 95% of the data is within the whiskers, the dots represent observations outside the 95% (Figure 20). I investigated the observations that were outside the 95% to determine if they were outliers. The longest reach was 2100 m on the lower Smith River. The largest drainage areas were on the South Fork Eel River and the lower Smith River, both over 1700 km². The highest slope was in the Trinity River drainage (30%); field notes confirmed that it was very steep with boulders. The largest bankfull depths were categorized as unconfined low slope for the site selection process. The highest D₅₀ was a bedrock reach, and the next two highest were boulder reaches confirmed with site pictures. The highest ammocoete habitat area (m²) was in a reach in the lower Smith River. The largest ammocoete habitat density (m/m²) was an unconfined channel in the Smith River, downstream of timberland. After investigation, I found that the large values in each variable were not outliers and I could not delete them from the analysis. Because of this wide variation in variables, I chose to use a Gamma distribution for modeling ammocoete habitat density.

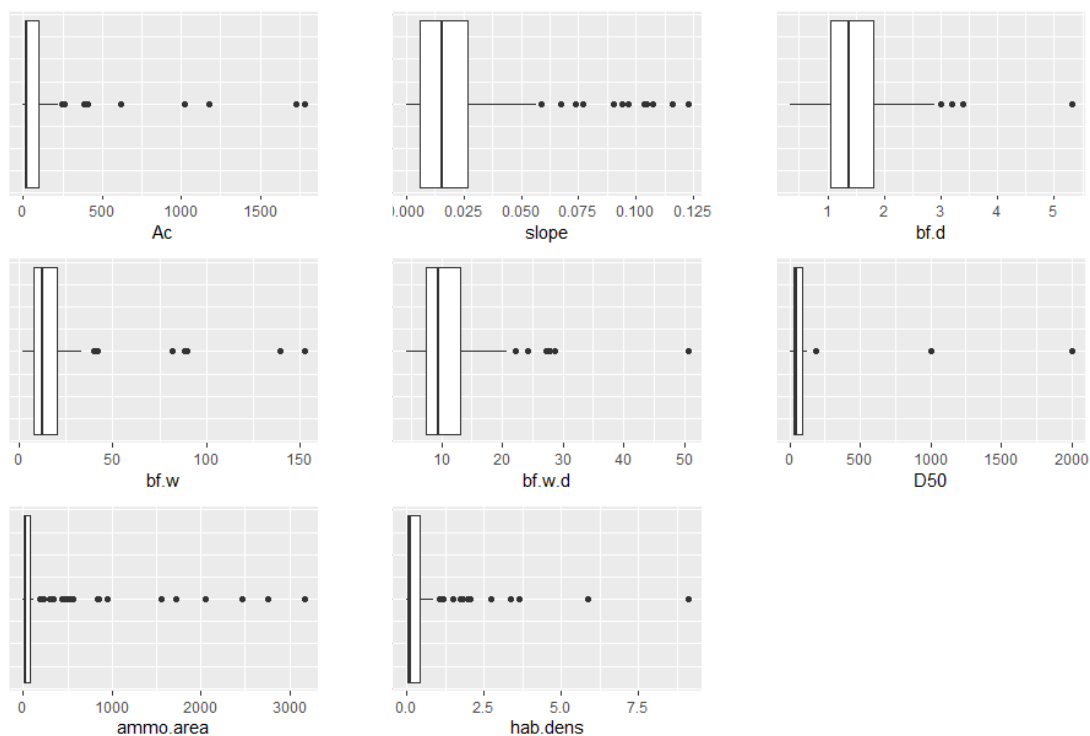


Figure 20. Box plots of variables explored for correlation with ammocoete habitat, only where ammocoete habitat was present. Ac=drainage area, slope=in stream slope, bf.d= bankfull depth, bf.w=bankfull width, bf.w.d= bankfull width to depth ratio, D50= median grain size, ammo.area=total area (m^2) in reach of habitat, and hab.dens= density of ammocoete habitat in reach (m^2/m).

I modeled prevalence, present and absence of ammocoete habitat with the explanatory variables that were not correlated with each other: drainage area, surveyed slope, bankfull width to depth ratio, and median grain size. The only significant variable for the presence of ammocoete habitat was slope, but drainage area explained more of the variability in the data, as indicated with a lower AIC (Table 5). The confidence interval for drainage area was large on the response scale (Figure 21).

Table 5. Model selection for Bernoulli model of the prevalence of ammocoete habitat. P-value of variable listed for the model if it was used in the model. Ac=drainage area, slope=field measured slope, bf.w.d=bankfull to depth ratio, D₅₀=median grain size, AIC =Akaike's information criterion.

model	intercept	Ac	slope	bf.w.d	D ₅₀	AIC
full	0.00654	0.14484	0.00441	0.54186	0.80576	168.03
1	0.00664	0.13942	0.0028	0.55011		166.09
2	0.000291	0.158541	0.002596			164.44
3	1.68E-09		0.000178			166.59

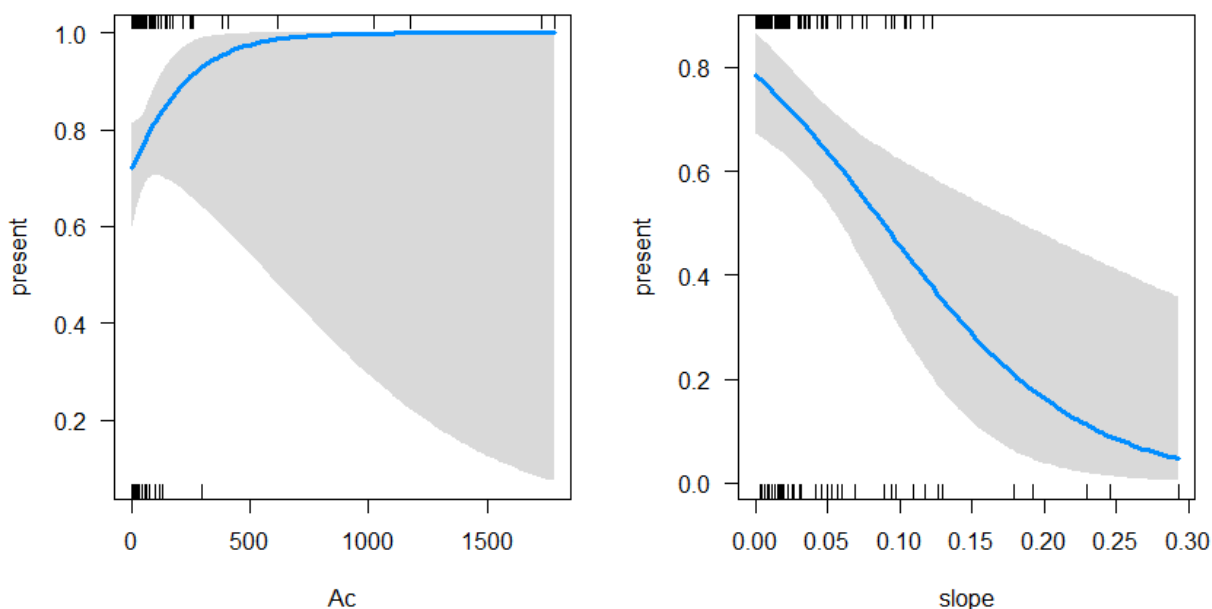


Figure 21. Bernoulli model for the presence of ammocoete habitat as it related to drainage area and slope. The most informative variables were drainage area and slope. Models are shown in the response scale, which takes the median value of the other variable to show the impact it would have on prevalence. Ac=Drainage area.

I modeled ammocoete habitat density in the reaches where ammocoete habitat was present and excluded reaches with no habitat observed. I used the explanatory variables that were not highly correlated with each other; drainage area, surveyed slope, bankfull width to depth ratio, and median grain size in the model. The only significant

variable in the Gamma model of habitat density was slope (habitat density~slope, R^2 adj = 0.251, deviance explained = 41.3%). The points fit around the line well in the linear predictor scale graph, but uncertainty increased with slope (Figure 22). There was almost exponentially lower ammocoete habitat density as slope increased.

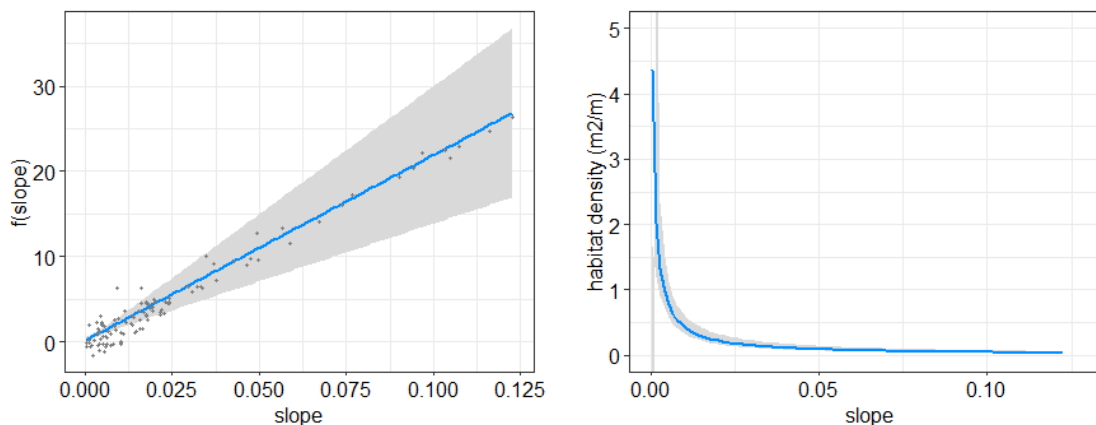


Figure 22. The best fit model displayed in the linear predictor (function of slope) and response scale for the Gamma model: ammocoete habitat density for when habitat is present.

The UC Davis hydrogeomorphic team created a spatial stream layer with desktop calculated slope from a 10 m DEM in 100 m sections of stream to use for survey site selection (Byrne et al., 2020). Of the reaches where I measured ammocoete habitat, 74% of the reaches were over 100 m long, and median reach length was 162 meters. I categorized the bedrock by the Mohs hardness scale to use as a predictor variable. I performed model selection with the variables of drainage area, confinement, and bedrock hardness. None of the variables were significant in explaining the location of the ammocoete habitat. Without slope as a predictor, the spatial models could not explain the variation in ammocoete habitat density or prevalence.

Geomorphic control to ammocoete habitat distribution

Given slope was the most prevalent predictor of ammocoete habitat, I tested the hypothesis of a difference in geomorphic controls of ammocoete habitat in slope. I started with testing to determine if the slope was similar in the Klamath and North Coast regions. I used an analysis of variance and found that the slopes were not similar between regions (p-value=0.007). The average slope of the measured reaches in the Klamath region was 0.03, in the North Coast region it was 0.01. I decided to examine slope separately for each region. The geomorphic controls fit into seven categories; many reaches had no deposits (Table 6). The greatest number of deposits was associated with obstructions followed by radius of curvature in both regions. I decided to compare only categories that had ten or more measurements in each region, which included dam, edge, obstruction, pool tail out, and radius of curvature. I dropped confluence and overflow channel from the analysis because they had less than ten measurements in each region.

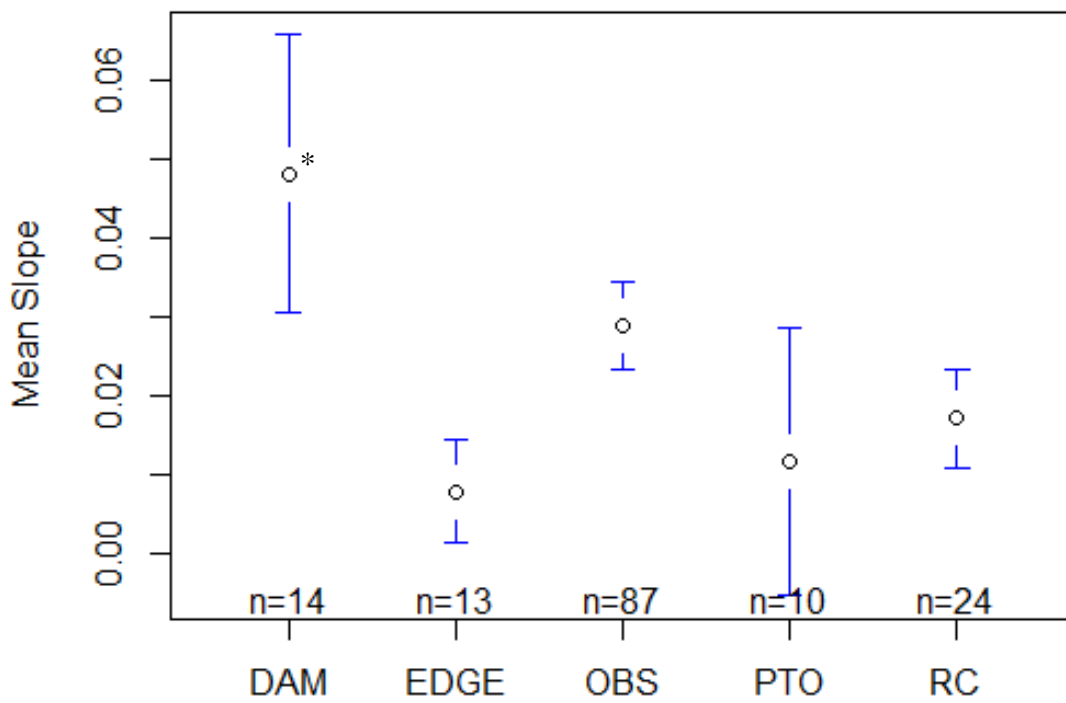
Table 6. Number and type of geomorphic control measured in each region.

Geomorphic Control	Klamath Region	North Coast Region
No deposit found in reach	18	27
Confluence	0	2
Dam	14	13
Edge	13	18
Obstruction	87	133
Overflow Channel	4	10
Pool Tail Out	10	10
Radius of Curvature Ratio	24	74

I used analysis of variance to test the null hypothesis that there was no difference in mean slope between the geomorphic controls for both regions. Both regions had at least one mean slope for a geomorphic control significantly different from the others (Klamath p-value= 4.9×10^{-5} , North Coast p-value= 7.1×10^{-6}) (Table 7). For the Klamath region, the slope at dams was significantly different from the slope of other geomorphic controls (edge v. dam p-value= 3×10^{-4} , obstruction v. dam p-value=0.05, pool tail out v. dam p-value= 3×10^{-3} , radius of curvature v. dam p-value= 2×10^{-3}) and the mean slope where obstructions were found was significantly different than the mean slope for where edge deposits were found (p-value=0.03) (Figure 23). The slopes of other geomorphic controls were not significantly different. In the North Coast Region, the slopes of dams were significantly different from edges (p-value= 8×10^{-5}), obstructions (p-value= 1×10^{-4}), and radius of curvatures (p-value= 1×10^{-5}) (Figure 24). The mean slope of dam locations was not significantly different in the North Coast region from pool tail outs (p-value=0.5). The mean slope of the other geomorphic controls was not significantly different.

Table 7. Mean slope per geomorphic control in the Klamath and North Coast regions.

Geomorphic Control	Klamath Region Slope	North Coast Region Slope
Dam	0.045	0.048
Edge	0.007	0.008
Obstruction	0.029	0.016
Pool Tail Out	0.011	0.028
Radius of Curvature Ratio	0.017	0.012



Geomorphic Control, Klamath Region

Figure 23. Klamath Region mean slope and sample size by geomorphic control: dams, edge, obstruction (OBS), pool tail out (PTO), and radius of curvature ratio (RC).
 *The survey slope associated with dams was significantly different compared to the other variables: edge v. dam p-value= 3×10^{-4} , obstruction v. dam p-value=0.05, pool tail out v. dam p-value= 3×10^{-3} , radius of curvature ratio p-value= 2×10^{-3} .

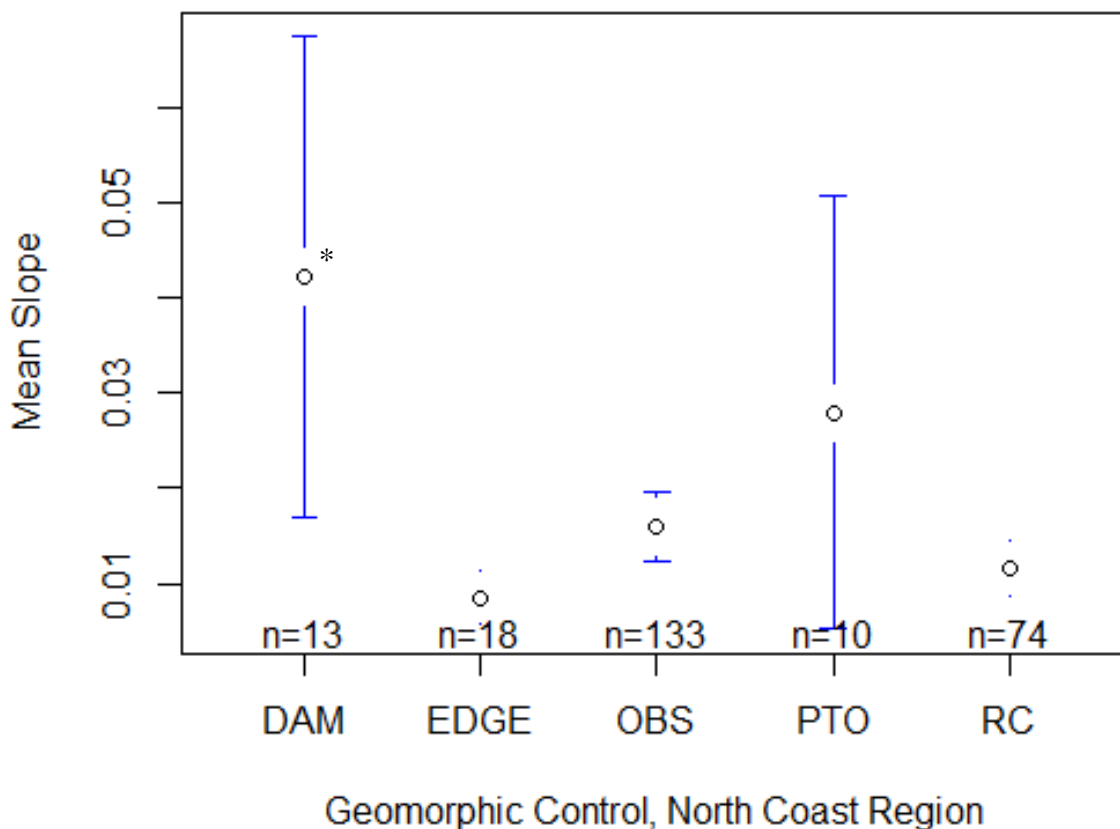


Figure 24. North Coast region mean survey slope and sample size by geomorphic control of dams, edge, obstruction (OBS), pool tail out (PTO), and radius of curvature ratio (RC). *The survey slope of dams was significantly different from the other variables, except pool tail out: edge v. dam p-value= 8×10^{-5} , obstruction v. dam p-value= 1×10^{-4} , pool tail out v. dam p-value 0.05, radius of curvature ratio p-value 1×10^{-5} .

The area (m^2) of the ammocoete habitat deposits was similar in both regions when tested with an ANOVA (p-value=0.99). Deposits located in pool tail outs were significantly larger than other deposits (PTO v. dam p-value = 2×10^{-5} , PTO v. edge p-value= 2×10^{-3} , PTO v. obstruction p-value= 2×10^{-5} , PTO v. radius of curvature p-value= 2×10^{-5}) and the mean deposit area of dams was smallest, but not significantly

different than the others except pool tail outs (Figure 25). The most common geomorphic control in the Klamath and North Coast regions was obstructions (n=220, 48%), followed by radius of curvature (n=98, 21%).

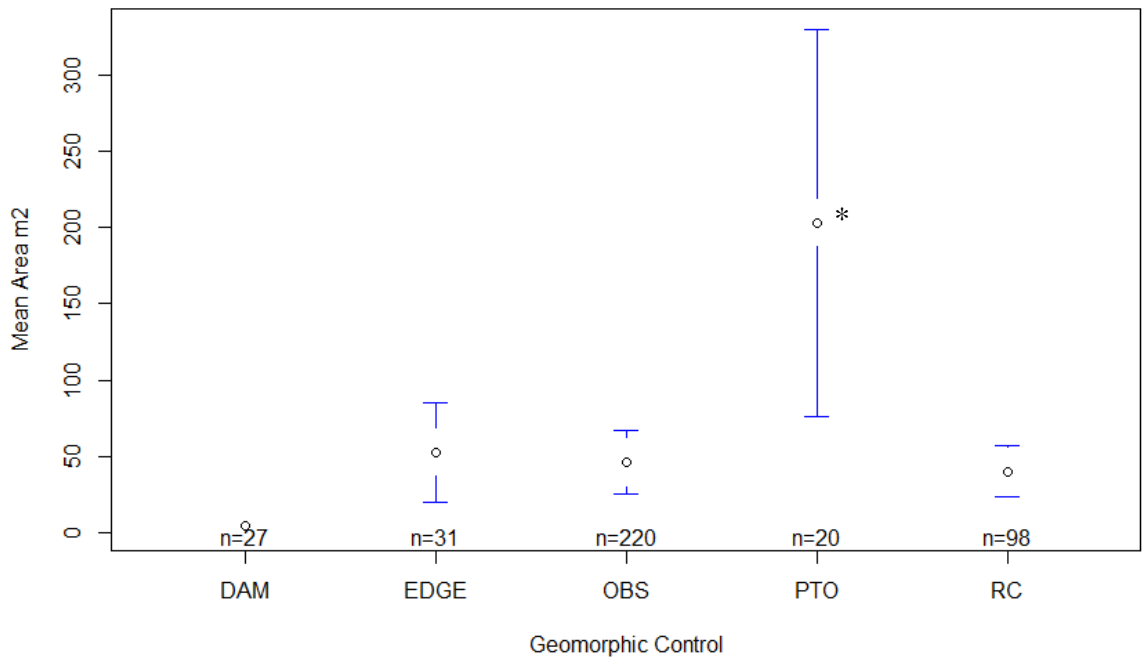


Figure 25. Mean area of ammocoete deposits (m^2) and sample size per geomorphic control of dams, edge, obstruction (OBS), pool tail out (PTO), and radius of curvature ratio (RC) in both the Klamath and North Coast regions (combined). *The mean habitat deposit area (m^2) associated with pool tail outs were significantly larger than other deposits (PTO v. dam p-value = 2×10^{-5} , PTO v. edge p-value = 2×10^{-3} , PTO v. obstruction p-value = 2×10^{-5} , PTO v. radius of curvature p-value = 2×10^{-5}).

Objective #2: Explore the relationship between stream channel geomorphic features and risk of ammocoete habitat loss during the summer streamflow recession limb in a northern California watershed

Redwood Creek did not have a consistent unit runoff between monitoring sites (Figure 26). The site in the peridotite gorge had the highest unit runoff throughout the dry summer. The only site that was solely in the Central Belt had the lowest unit runoff throughout the dry summer. The Coastal Belt and the mix sites had runoff levels between the peridotite and Central Belt.

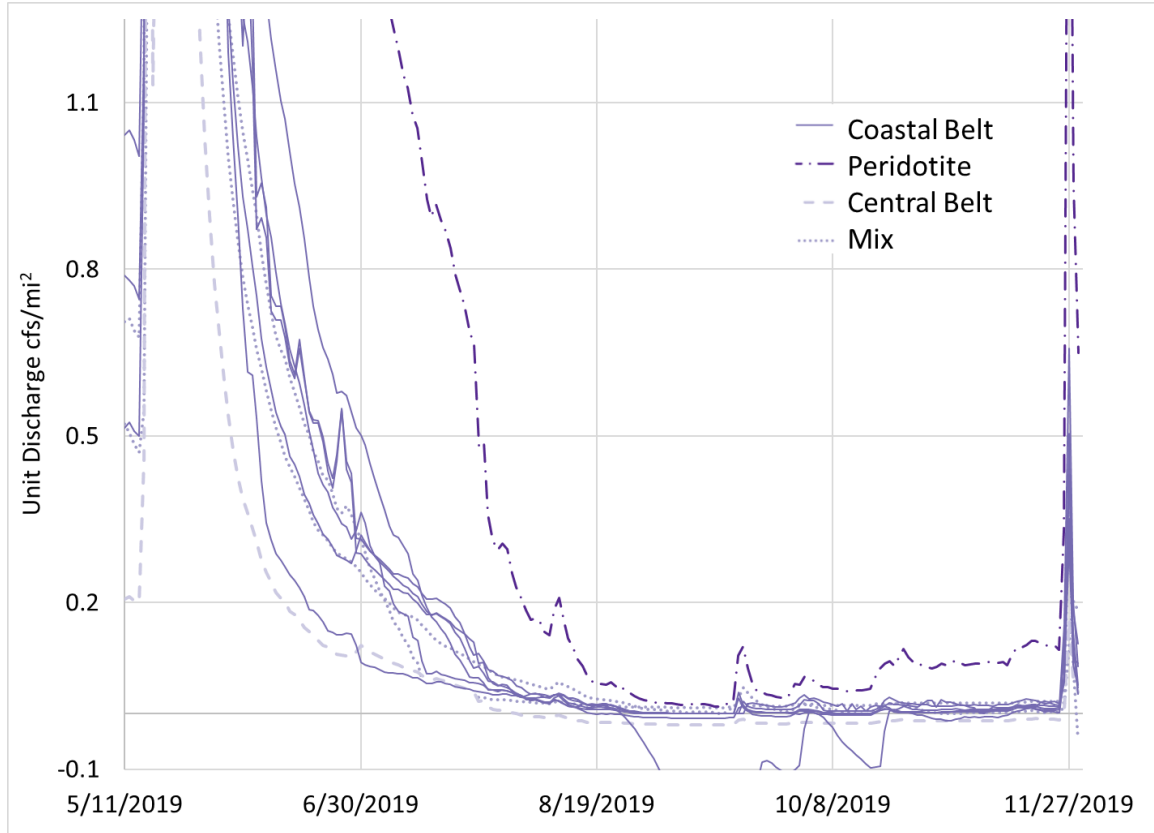


Figure 26. Unit runoff per geologic belt of the monitoring sites in Redwood Creek. Most sites were entirely within the Coastal Belt (DC, CC, URC, MC, RC-1.5, and RC-1.8), one site was located in peridotite (RC-2.5), one site drained a completely Central Belt watershed (SC), and two were located in the Central Belt but also had discharge from the Coastal Belt (mix)(RC-3 and RC-4).

Develop a relationship between flow, RCT, and portion of ammocoete habitat inundated

I estimated the RCT depth at section control, RCT_{sec} (ft), at all ten monitoring sites on Redwood Creek (Table 8). I calculated the flow at the active channel control, Q_{ACT} (cfs); the power function exponent, PFE; the hydraulic threshold ratio, HTR; the flow at the lower hydraulic transition, Q_{LHT} (cfs); the flow at dominant section control, Q_{dom} (cfs); and the flow at section control, Q_{sec} (cfs). The flow at section control at the Redwood Creek monitoring sites ranged from 0.04 cfs at the site with the smallest

drainage area and confined channel (DC-1) to 1.9 cfs at the site with the second-largest drainage area with a broad riffle crest (RC-3).

Table 8. Riffle crest thalweg depths (RCTs) and hydraulic control thresholds for 10 study sites on Redwood Creek. Power function exponent (PFE) and the hydraulic threshold ratio (HTR) are dimensionless. ACT =active channel control, Q=flow, LHT= lower hydraulic transition, DOM=dominant section control, SEC =section control.

Site code	Drainage Area (mi ²)	RCT _{ACT} (ft)	Q _{ACT} (cfs)	PFE	HTR	Q _{LHT} (cfs)	Q _{dom} (cfs)	Q _{sec} (cfs)	RCT _{sec} (ft)
RC-4	25.8	1.85	258	4.36	0.15	38.0	5.59	0.823	0.51
RC-3	23.5	2.3	235	2.76	0.20	47.2	9.46	1.90	0.45
RC-2.5	17.1	1.7	171	4.94	0.14	23.1	3.13	0.42	0.63
SC-1	5.8	1.25	58	2.69	0.20	11.9	2.42	0.49	0.25
MC-2	3.6	1.2	36	3.42	0.17	6.25	1.09	0.19	0.73
DC-1	1	0.75	10	3.74	0.16	1.63	0.27	0.04	0.15
CC-2	3.9	1.62	39	4.48	0.14	5.64	0.82	0.12	0.32
URC-1	2.7	1.13	27	5.00	0.13	3.63	0.49	0.07	0.30
RC-1.8	10.8	1.40	108	4.11	0.15	16.6	2.54	0.39	0.28
RC-1.5	6.9	2.04	69	3.88	0.16	11.0	1.75	0.28	0.35

To predict the proportion of ammocoete habitat inundated from an RCT, I constructed a binomial model. The 3D survey at site RC-4 included five separate deposits with a total area of 177 ft² and an elevation range of 1.84 ft. I used the information from the total station survey and the Multi-Volumes Tool for ArcGIS 10 to model the portion of total habitat inundated. I used a binomial logit function:

$$portion\ inundated = \frac{e^{-3.5+4.6RCT}}{1 + e^{-3.5+4.6RCT}}$$

to predict the percentage of habitat surface area inundated based on the RCT, the binomial model had a deviance explained of 98.8% (Figure 27). If stage rose above the top of the habitat, the model did not predict over a hundred percent inundated, and if the

stage lowered below the lowest elevation of the deposit the model does not predict negative portions dewatered.

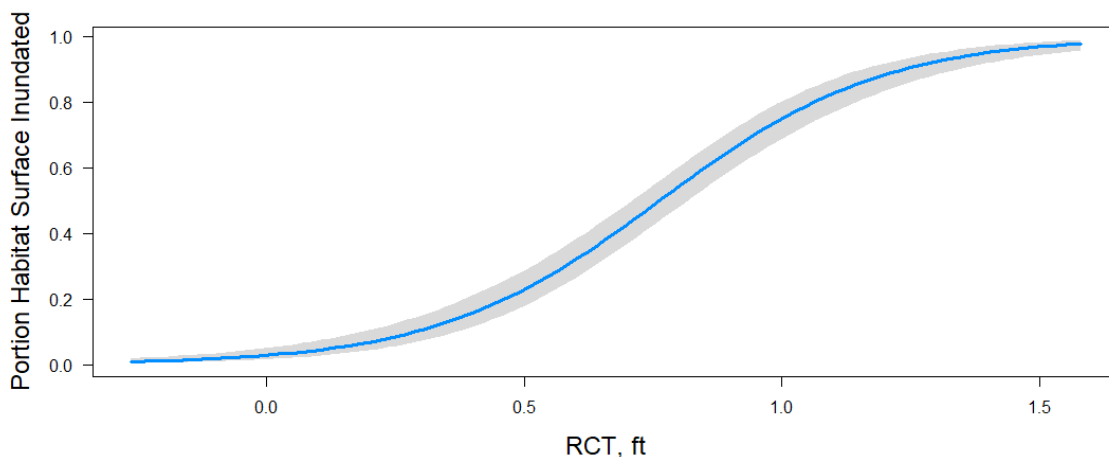


Figure 27. Binomial logit function to predict the portion of habitat surface area inundated based on the RCT at Redwood Creek site RC-4. $\text{Portion Inundated} = \frac{e^{(-3.5+4.6\text{RCT})}}{1+e^{(-3.5+4.6\text{RCT})}}$. Deviance explained= 98.8%.

I used the RCT-Q rating curves and the binomial logit function for the portion of habitat inundated to estimate the flow (cfs), RCT (ft), and percent inundated for each level of risk for ammocoetes at the RC-4 gaging pool (Table 9).

Table 9. Habitat quality risk levels to ammocoetes at RC-4, condition where the risk occurs, associated flow (cfs), RCT (ft), and percent habitat inundated.

Risk	Condition	Flow, cfs	RCT, ft	% habitat inundated
Low	Completely inundated	47	1.59	100
Moderate	Section control	0.82	0.51	24
High	Point of zero flow	0.0	0.0	2.8
Extreme	Deposit not inundated	n/a	-0.09	0

To predict RCT from any flow, I constructed a rating curve with a power function for the relationship between RC-4 flow (cfs) and the RCT (ft) with the measurements from 2019 ($RCT=0.3728Q^{0.2857}$, $R^2= 0.9667$) (Figure 28). I needed a linear function forced through the intercept (0,0) for the lowest flows to predict low and theoretical negative flows to then predict when habitat deposits were completely dewatered. The low flow rating curve was $RCT= 1.4415Q$, $R^2= 0.806$ (Figure 29). The 50-year and the 30-year exceedance lines plotted similarly; thus, the past 30 years should retain a similar variability in flows than if I used the last 50 years (Figure 30).

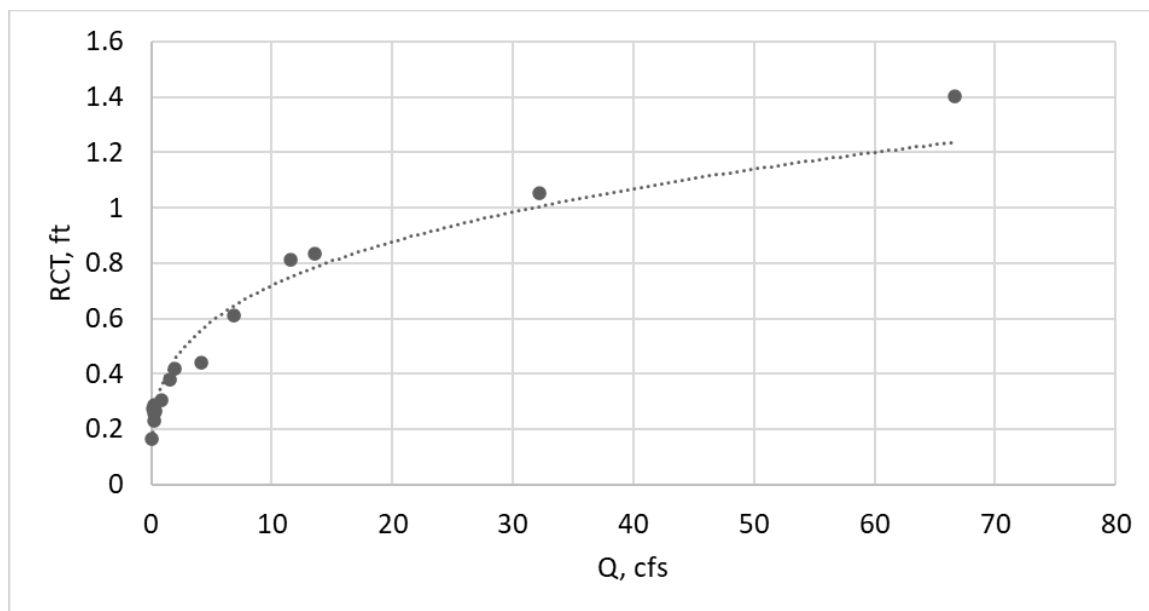


Figure 28. Redwood Creek site RC-4 riffle crest thalweg depth (ft) and flow (cfs) rating curve with power curve function ($RCT=0.3728Q^{0.2857}$, $R^2= 0.9667$). Note: this curve does not include an estimate for active channel flow.

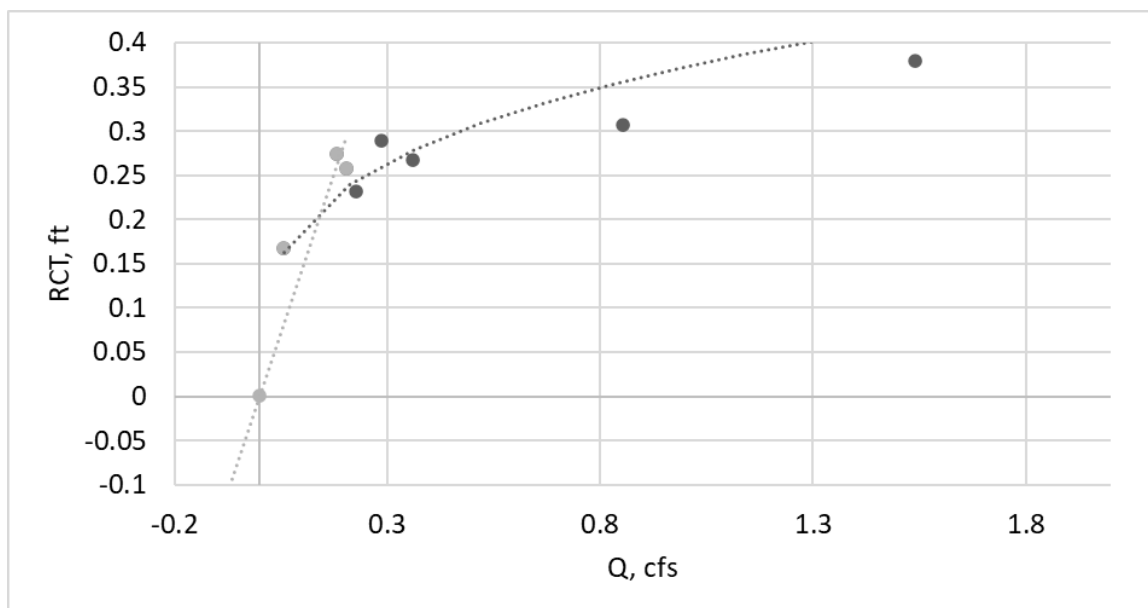


Figure 29. Redwood Creek RC-4 riffle crest thalweg depth (ft) and flow (cfs) rating curve, the x-axis and y-axis are adjusted to show the lowest flows, with a power curve trendline ($RCT=0.3728Q^{0.2857}$, $R^2=0.9667$) and a linear trendline that goes through (0,0) for the lower flow values ($RCT=1.4415Q$, $R^2=0.806$).

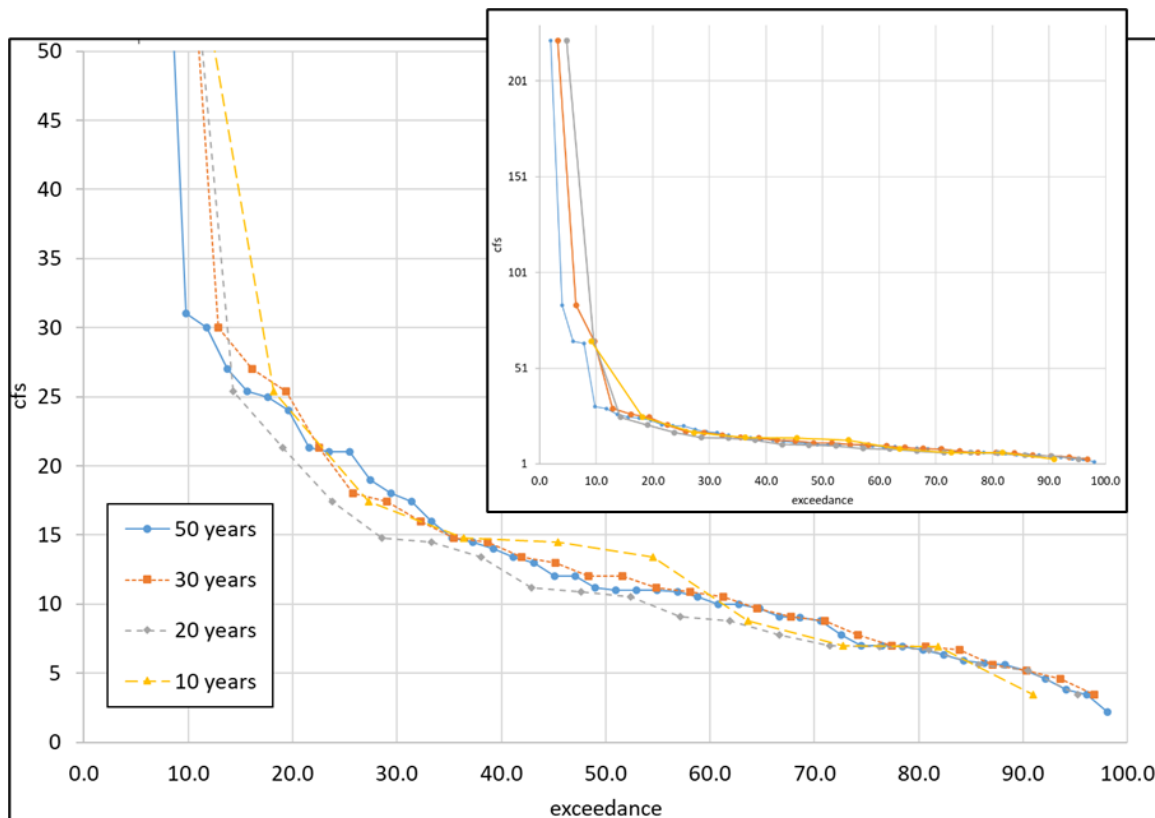


Figure 30. Exceedance plots of May 1st flow (cfs) at the Elder Creek gage (USGS #11475560). Each line has a different range; 50, 30, 20, and 10 years. The top inset graph has the full range of cfs values; the bottom larger graph shows a smaller range of flows.

Estimate unimpaired hydrograph

I correlated flows between RC-4 and three nearby USGS gages: Leggett (USGS gage # 11475800), Ettersburg (USGS gage #11468900), and Elder Creek (USGS gage # 11475560). I examined the fit visually (Figure 31) and compared their R^2 . Leggett and Ettersburg had the same $R^2=0.975$, and Elder Creek had the highest $R^2=0.9945$ (Table 10).

Table 10. Correlation between RC-4 and nearby USGS gages in 2019.

Gage name	USGS gage number	Equation	R ²
Leggett	11475800	RC-4=0.481*Leg-0.1786	0.975
Ettersburg	11468900	RC-4=0.1492*Ett-0.6335	0.975
Elder	11475560	RC-4=1.4803*Eld-1.9674	0.9945

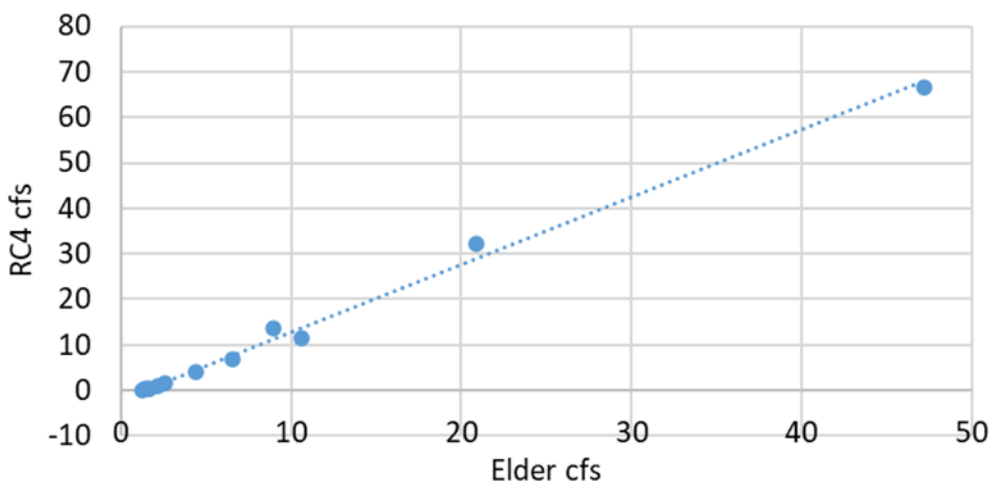


Figure 31. Redwood Creek WY 2019 RC-4 - Elder Creek gage (USGS #11475560) correlation. Linear function $y=1.403x-1.9674$, $R^2=0.9945$.

I compared unit runoff (cfs/mi²) of Bull Creek (USGS gage #11476600), Elder Creek (USGS #11475560), and RC-4 for 2018 (Figure 32) and 2019 (Figure 33). In 2018, SRF measured streamflow at RC-4 between the end of June and mid-November, when Redwood Creek flows are the most impaired. Bull Creek (USGS gage #11476600) stopped operating November 1, 2018. In 2019, I started measuring streamflow at RC-4 earlier in the season to encompass a wider range of flows than in 2018 (May 11th to November 29th). RC-4 unit runoff was similar to Elder Creek (USGS #11475560) unit runoff above 0.5 cfs/mi².

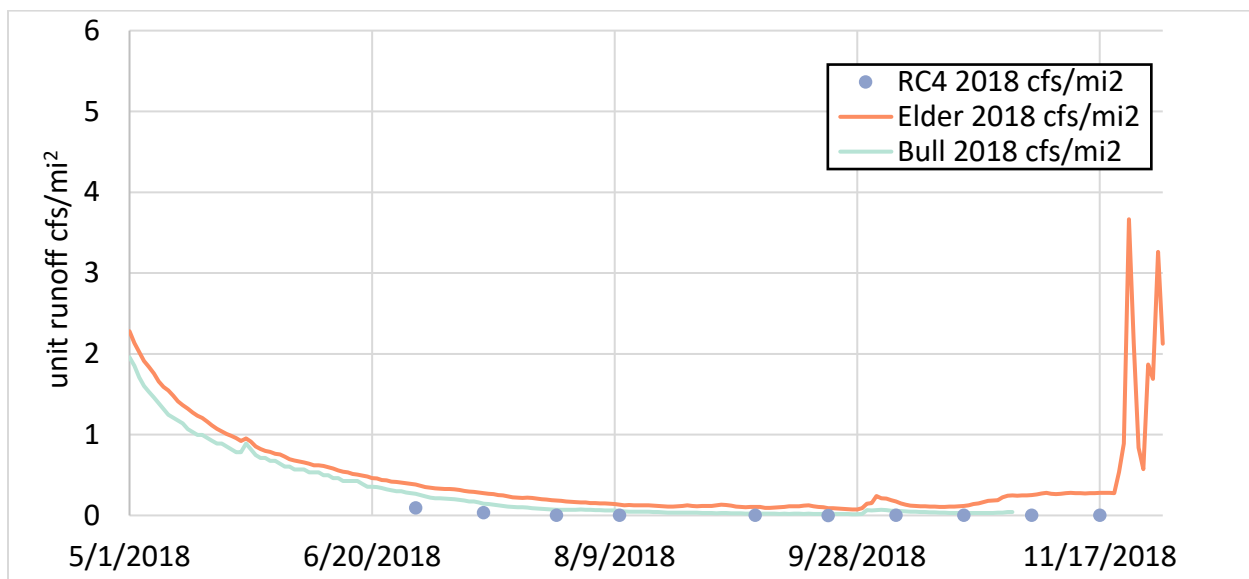


Figure 32. WY 2018 unit runoff for Elder Creek (USGS #11475560), Bull Creek (USGS gage #11476600), and measurements at Redwood Creek RC-4. Bull Creek stopped operation November 1st, 2018.

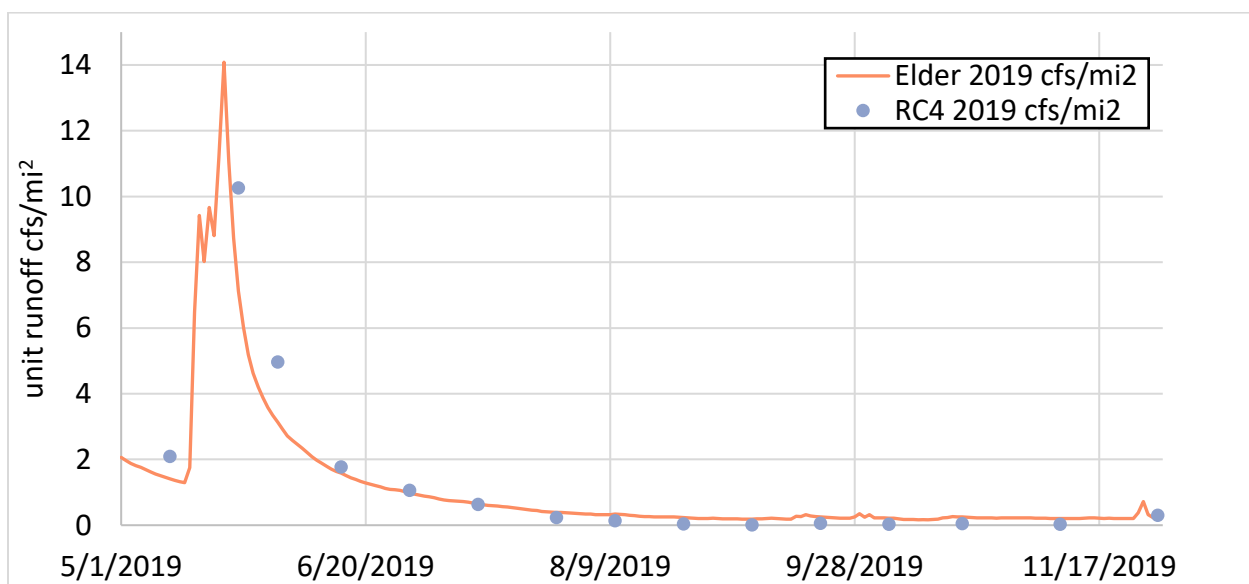


Figure 33. WY 2019 unit runoff for Elder Creek (USGS #11475560) and field measurements of Redwood Creek RC-4.

To estimate unimpaired stream flows in Redwood Creek, I chose the Elder Creek gage (USGS #11475560) because it is unimpaired, has a strong R^2 value in a correlation

between RC-4, and the unit runoff is similar above 0.5 cfs/mi^2 when the Redwood Creek would be less impaired by diversions. I decided not to use Bull Creek as the unimpaired watershed for two reasons: (1) the headwaters of Bull Creek are disturbed from past land-use practices and (2) the flow gage (USGS gage #11476600) was not running the years I collected data (2019). The data logger at RC-4 was lost in a high-water event before I could download the last portion of data (last download 9/21/2019, logger lost between 11/9/2019 and 11/29/2019). I compared the 2019 data logger average daily flow to the 2019 correlation with Elder Creek's daily average flow to the measurements that I took in the field (Figure 34), and both lines tracked the measurements well.

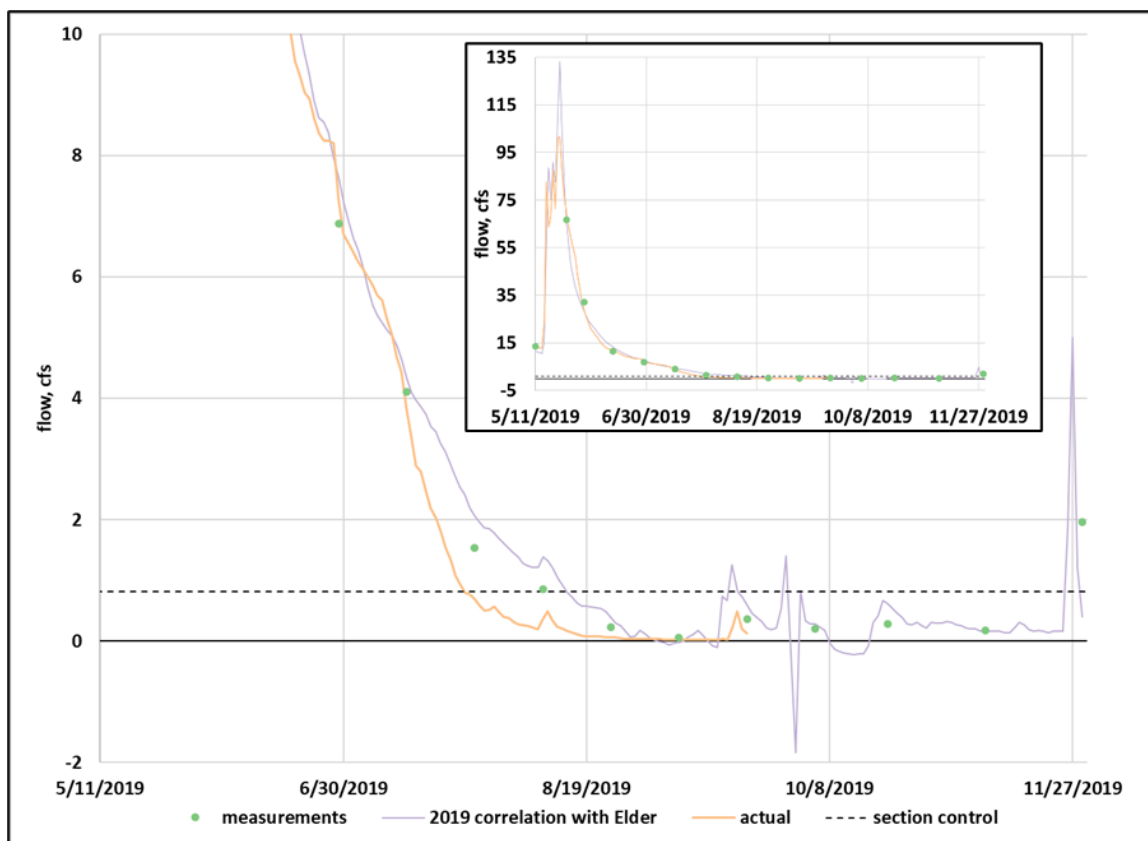


Figure 34. Comparison of the actual flow estimated from the water level logger in Redwood Creek site RC-4 (ends 9/21/2019), the flow estimated from the 2019 correlation with Elder Creek gage (USGS #11475560), and the measurements taken in the field. The full range of data is inset; the larger graph has a smaller range of cfs values to better display the lowest flows.

I used the watershed scaling equation to estimate unimpaired flows from 1989 to 2019. I ranked the May 1st unimpaired flow at RC-4, then graphed the flow against the rank (Figure 35). I added dashed lines for 100% inundated and section control. Mostly the high flow years have the whole deposit inundated on May 1st of the unimpaired scenario. None of the years were below section control on May 1st in the unimpaired scenario.

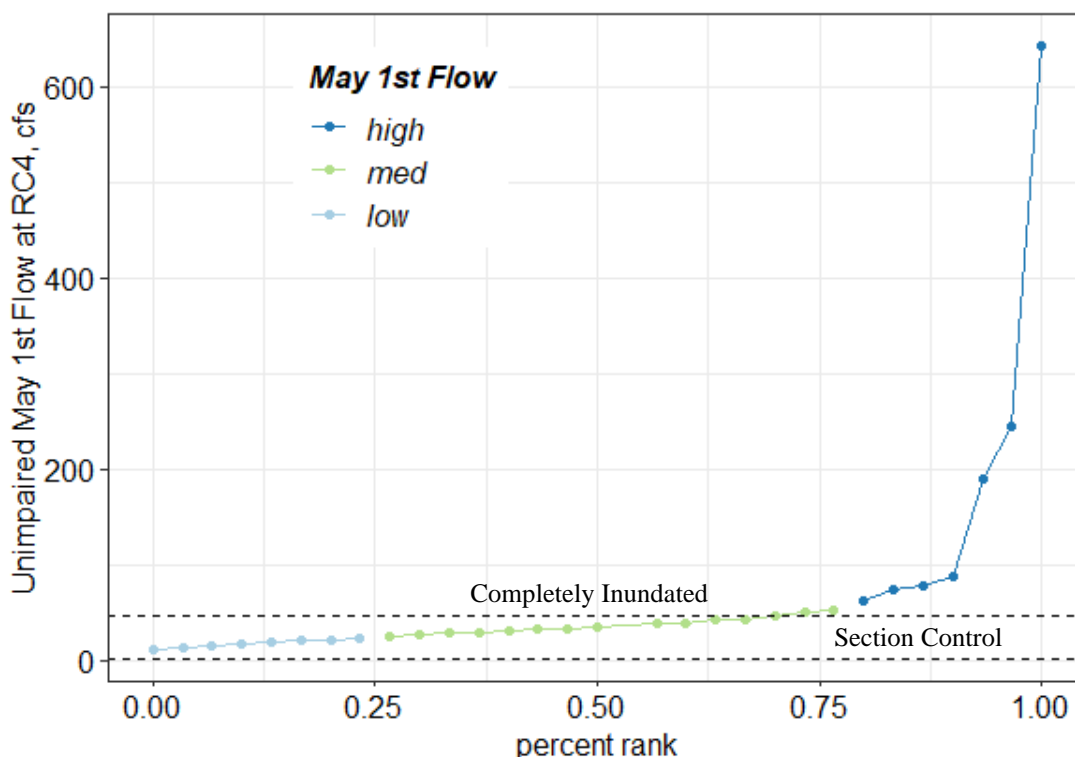


Figure 35. Percent rank of Redwood Creek RC-4 estimated May 1st flow from 1989-2019 using the watershed scaling equation to estimate unimpaired flow. The Upper dashed line is 100% inundation of fine sediment deposits; the lower dashed line is section control when risk increases for ammocoetes. Darker shades of lines represent higher flows on May 1st of that year.

Evaluate unimpaired hydrograph against risk criteria

Daily average unimpaired streamflows, based off of the watershed scaling equation between Redwood Creek site RC-4 and Elder Creek (USGS gage # 11475560) watershed scaling equation for 1989-2019, never dropped below the section control threshold (Figure 36). Only by applying a diversion rate of 20% or greater to the daily unimpaired streamflow were any days below section control ($Q = 0.823\text{cfs}$). I subtracted 20% from the flow to illustrate the scenario of Redwood Creek having 20% of ambient streamflow diverted daily. At 50% diversion, some years went below the section control

threshold. For a maximum of two months starting in August and ending in November, when 90% of the flow is diverted, every year the flow fell below the section control threshold, starting at the end of May, and there were days below section control even through December.

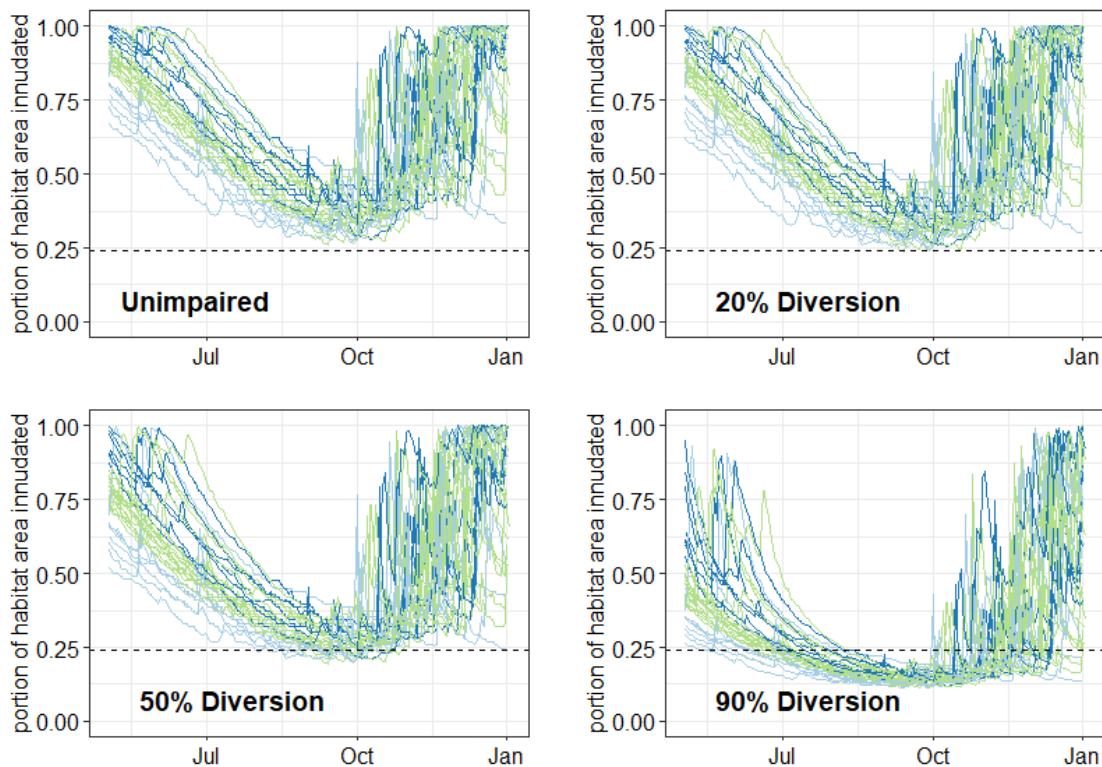


Figure 36. Percent habitat surface area inundated at Redwood Creek site RC-4; unimpaired, 20% diverted from unimpaired, 50% diverted from unimpaired, and 90% diverted from unimpaired. Dashed line = section control. Darker shades of lines represent higher flows on May 1st of that year.

I evaluated habitat quality as a function of diversion rate. I quantified the difference in the number of days the deposit would be at high risk (below section control) as a function of diversion rate (Figure 37). For the unimpaired flow at RC-4, the flow did not go below section control between May 1st and December 31st. Diversions did not

affect the number of days ammocoete habitat was below section control until 20% of the unimpaired flow was diverted. Wetter years took a larger diversion rate than dryer years.

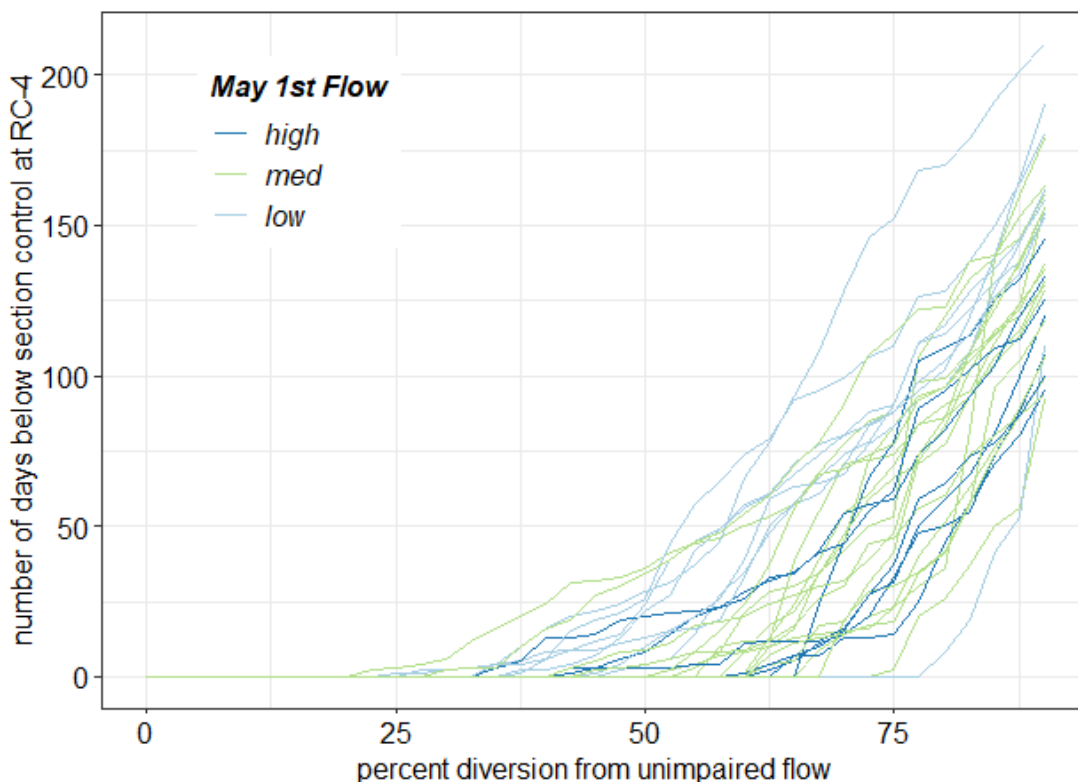


Figure 37. Number of days above section control with a diversion from the unimpaired flow between May 1st and December 31st, 1989-2019 at Redwood Creek site RC-4. Darker shades of lines represent higher flows on May 1st of that year.

Estimate current condition hydrograph

I documented with photographs the stage at RC-4 at different thresholds and controls to the discharge to stage relationship (Figure 38). At the lower hydraulic transition, the stage was up the side of the bank and only a small area of the ammocoete deposit was exposed. At dominant section control, the stage was lower on the bank, the riffle crest was visible, and there was more ammocoete deposit exposed. At section

control, the water surface had retracted from the bank, most of the riffle crest was exposed, and only 4% of the deposit was inundated. Below section control, leaves had accumulated upstream of the riffle crest, the water was brown from the tannins in the leaves, and there were multiple deposits at the Redwood Creek site RC-4 dewatered.



Figure 38. Redwood Creek site RC-4 water level and ammocoete deposits exposed at different streamflow thresholds in the recession limb. Hollow arrows point to the highest elevation of the deposits. Solid arrows point in the direction of the flow.

Evaluate current condition against risks

I examined the amount of time the habitat deposits at Redwood Creek site RC-4 were under section control in the current condition for 1989-2019. I modeled the date range from May 1st to December 31st to ensure each year emerged from section control in early winter. I created a graph of the estimated RCT at RC-4 for the 1989-2019 dry season based on the WY 2019 RC-4-Elder Creek correlation (Figure 39). To visually

compare water years, I separated the water years by the flow (cfs) on May 1st of each year between 1989 and 2019. I ranked the May 1st flows at the Elder Creek gage (USGS #11475560) from 1989 to 2019 and plotted the percent rank against the flow. I located natural breaks between high, medium, and low flows on May 1st. In almost every year, the stage dropped below the elevation that completely dewatered the ammocoete habitat deposits. I used the logit function for the portion inundated from the RCT. When the RCT is dewatered, there is still 3% of the habitat deposit inundated. For almost every year, the model predicted the deposit dewatered, which is an extreme risk to ammocoete habitat quality.

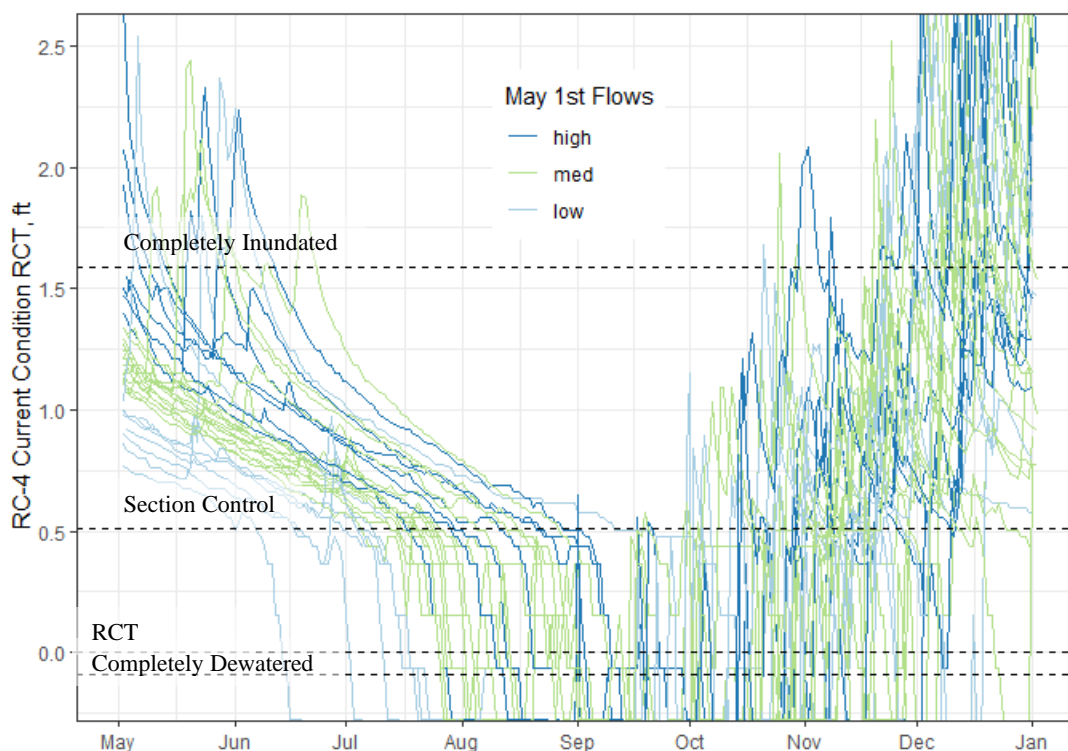


Figure 39. RCT (ft) for Redwood Creek RC-4 from 1989 to 2019 May 1st to December 31st current condition. Top dashed line is when the habitat surface area is completely inundated. Next lower line is section control. Flow stops when RCT=0.0. The habitat surface area is completely dewatered at the lowest dashed line. Darker shades of lines represent higher flows on May 1st of that year.

I counted the days that the deposit was under section control for the current condition (Figure 40). The lowest number of days below section control was 41 in 1990; the highest was 191 days below section control in 2014; the median number of days below section control was 113, which occurred in 2004. The year this research was completed, 2019, had 96 days under section control with 67% exceedance (67% of years had more days below section control than 2019).

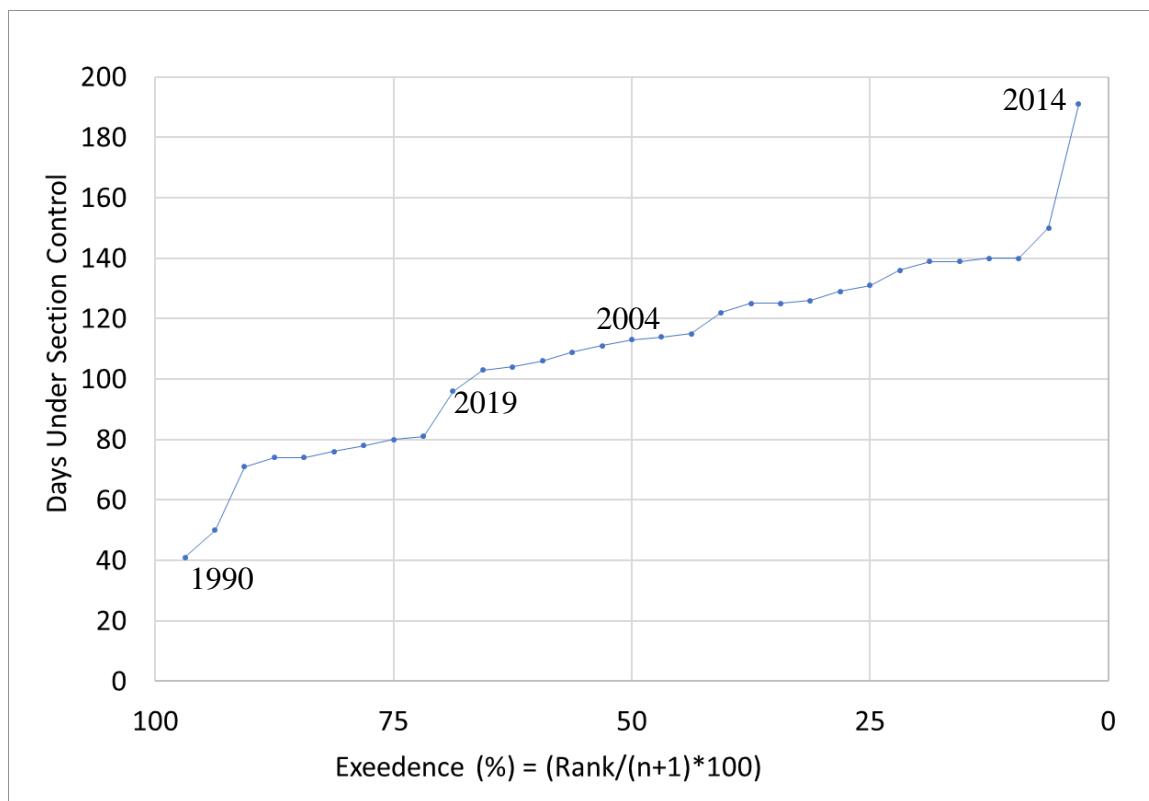


Figure 40. Exceedence of the count of days below section control at site RC-4 in Redwood Creek in each year (1989-2019) given the current condition based off 2019 correlation with Elder Creek (USGS #11475560).

Comparison of WY 2019 unimpaired and impaired

I examined the difference between the measured 2019 flow and the estimated unimpaired flow (Figure 41). I used the average daily flow estimated from the data logger placed in the gage pool. The data logger flow was close to the measurements, but the logger was not recovered at the end of the season (Figure 42). The logger may have been stolen or washed away in high water. The period recorded was May 11th to September

21st, 2019, the last download. On average, the actual flow was 24% of the unimpaired flow. In late September, the actual flow was 1% of the estimated unimpaired flow.

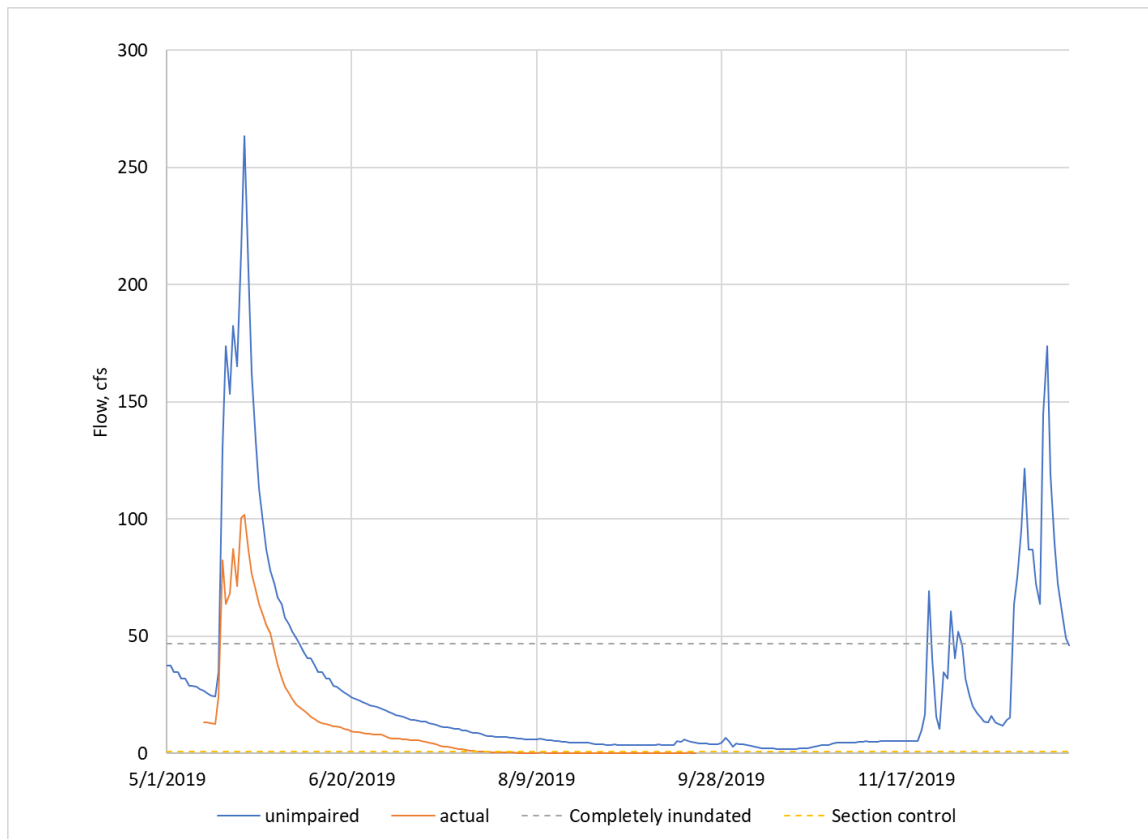


Figure 41. Redwood Creek site RC-4 unimpaired flow based on the watershed scaling equation with Elder Creek (USGS gage #11475560) and the flow estimated from the water level logger at the site for WY 2019, water level logger data ends September 21st.

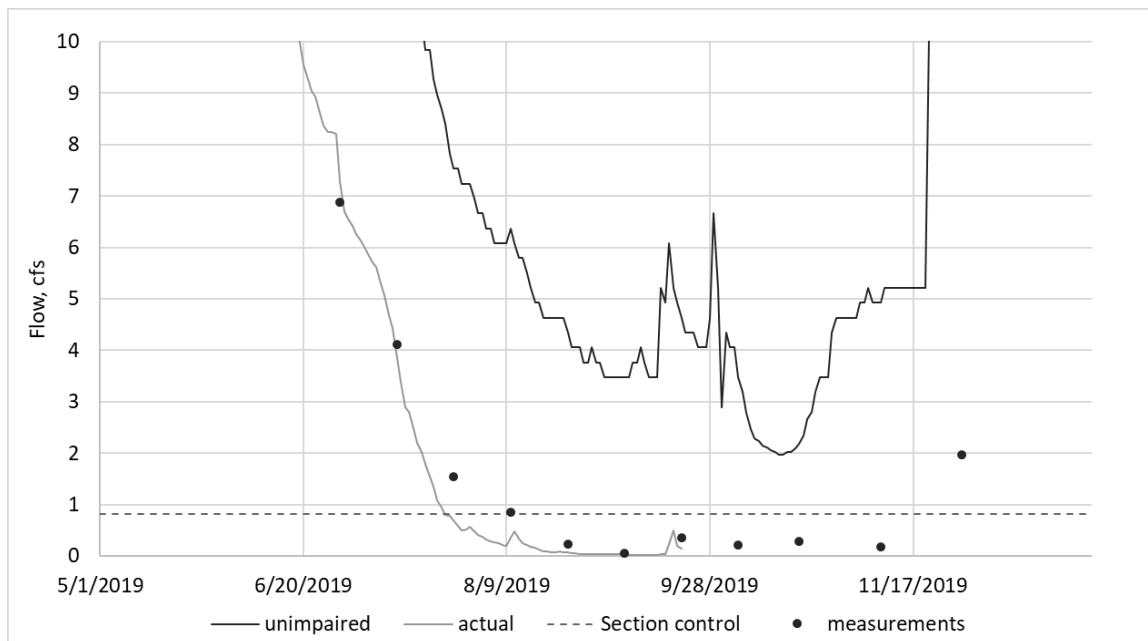


Figure 42. Redwood Creek site RC-4 WY 2019 daily average flow estimated from the logger (actual), the daily average flow of the unimpaired estimate, and the measured flows. The scale ranges from zero to ten cfs, water level logger data end on September 21st.

DISCUSSION

Pacific lamprey are important ecologically and culturally, and are under many threats (Close, 2002; Simpson, 2019). The threats, or causes of population decline, include low streamflow, high water temperatures, poor water quality, and migration barriers. This research can help address these threats. The methods developed in determining how streamflow diversions impair lamprey ammocoete habitat quality can aid in water management to prevent the low flows detrimental to lamprey ammocoetes. The results showing slope is a significant predictor for ammocoete habitat can focus restoration priorities to address threats from high-water temperature, water quality, and migration barriers.

Study assessments and improvements

Objective #1: Predict ammocoete habitat distribution for coastal watersheds in Northern California based on channel morphology.

Slope was the best predictor for the location of ammocoete habitat prevalence and habitat density. Most ammocoete habitat deposits were in stream reaches with slopes less than 0.04.

Dams were a type of geomorphic control observed in statistically significantly higher slopes than 0.04, but these dams did not have a large habitat area. In the Hubbard Brook Experimental Forest in New Hampshire, researchers found that removing debris dams resulted in losing dissolved organic carbon and coarse particulate matter from the

stream reach and that debris dams contain three-quarters of the organic matter in first-order streams and half of the organic matter in second-order streams (Bilby & Likens, 1980). Debris removal from streams was once considered a restoration strategy in logged watersheds on the west coast, but is now recognized as detrimental to stream ecosystems (Bryant, 1983). Systematic removal of large woody debris may be why only few debris dams were encountered in our surveys. Log jams and beaver dam analogues can be built to retain fine sediment and store water (Burchsted et al., 2010; Burschsted, 2010; Pollock et al., 2014) benefiting larval lamprey habitat. In lower slopes, restoration techniques, such as geomorphic grade line design method, can encourage meanders and bankfull erosion (Cluer & Thorne, 2014; Powers et al., 2019). Many restoration techniques for creating slow water juvenile salmonid rearing habitat will also deposit fines that ammocoetes can occupy (Crandall & Wittenbac, 2015).

In my research, fines deposits associated with pool tail outs had significantly larger ammocoete habitat deposit areas (m^2) than other geomorphic control types. However, larger deposits are not necessarily more beneficial to ammocoetes. Pool tail outs full of fines are harmful to salmonids and lampreys because they may suffocate the eggs in redds (Stillwater Sciences, 2014).

The most common geomorphic control observed in conjunction with ammocoete habitat was obstruction, responsible for 53% of the ammocoete deposits measured. The second most common geomorphic control observed was sharp meander bend (at 24% of the ammocoete deposits). Large woody debris is a frequent type of obstruction that

formed ammocoete habitat deposits. Adding large woody debris is a common salmonid restoration technique (Flosi et al., 2002) that would also benefit Pacific lamprey.

Ammocoete habitat distribution aligns with models of ammocoete presence. Field-measured slope and radius of curvature were strong variables predicting the location of Sea Lamprey ammocoete habitat around the Great Lakes, but Neeson et al. (2007) could not rely on desktop-derived slopes. I observed higher densities of ammocoete habitat in low slope and large drainage areas closer to the coast. A spatial model of ammocoete presence in Portugal predicts ammocoetes in low altitude reaches with sandy substrate close to the coast (Ferreira et al., 2013).

The majority of measurements for this study was on reaches with small drainage areas because WY 2019 was a wet season that prevented measuring reaches in large basins. The protocol for measuring slope required surveying elevations between riffle crests. We were unable to measure riffle crest depth if the depth and velocity were too great to stand safely. Most research into lamprey has focused on wadable streams (Hume et al., 2020); methodologies must be improved to research broader areas that ammocoetes may be present such as in higher order rivers with larger upstream drainage areas, deeper water, and estuaries. This research could be improved by focusing on a single watershed where a more accurate channel slope is available for the whole watershed and data can be collected throughout the entirety of the watershed, especially the lower reaches.

I was unable to create a robust spatial model of ammocoete habitat distribution because slope could not be accurately predicted using available spatial layers and GIS tools. Other researchers also concluded the same, especially over short reach lengths

(Neeson et al., 2018). Some inventoried reaches measured were in confined valleys where channel widths were less than 10m, so it is unlikely that a 10m digital elevation model, DEM, would adequately calculate slope. Light detection and ranging (LiDar), though harder to come by and a larger, therefore more cumbersome, dataset than a 10m DEM offers finer resolution of headwater streams necessary to predict slope accurately (Passalacqua et al., 2010).

Slope was the best explanatory variable, but only explained 41% of the variability in ammocoete habitat distribution. What explains the other 59% of variability? Unlike what I hypothesized, bedrock hardness was not a significant predictor for ammocoete habitat presence or density distribution. The issue may be more complicated than using the Mohs hardness at the place of observation of ammocoete habitat. To predict the size distribution of sediment supplied from hillslopes may be a function of the bedrock lithology, the climate, biology, tectonics, and topography (Sklar et al., 2017). An erodibility index of the substrate or modeling human disturbances to the landscape may assist with modeling the supply of fine substrate (Moosdorf et al., 2018; Torgersen & Close, 2004). Unpaved roads, landslides, logging, and fires are a few examples of landscape disturbances generating fines upstream. I used bedrock hardness at the channel reach, but in the future model the upstream accumulation of fine sediment.

Objective #2: Explore the relationship between stream channel geomorphic features and risk of ammocoete habitat loss during the summer streamflow recession limb in a northern California watershed

I predicted the current flow and stage condition of Redwood Creek with the Elder Creek gage record (USGS gage # 11475560) and compared it to the WY 2019 correlation fit with a linear model. Unit discharge at Elder Creek and RC-4 gages was similar above 0.5 cfs/mi². The current condition correlation matched where points were measured, but there was an extreme dip in the prediction that could not be verified because the data logger was lost before the data for that time period could be downloaded. Because the past 30 years of May 1st flows have the same variability as the past 50 years, I streamlined my analysis without losing fidelity. I fit a two-part rating curve for RCT-Q, then created a binomial logit function for RCT to portion ammocoete habitat deposit inundated. From these three models, I estimated risk of poor water quality to ammocoete habitat deposits.

I used a novel approach to modeling diversion impacts. A total station survey generated 3D models of ammocoete deposit in Redwood Creek. Using the riffle crest thalweg depth as a reference stage, I modeled scenarios of the past 30 years of dry season hydrograph under (1) current (WY 2019 relationship with an unimpaired watershed), (2) unimpaired (using the watershed scaling model), and (3) impaired (fraction of flow diversions from the unimpaired) conditions based on a continuously running gage.

The difference in the modeled current condition and the unimpaired condition with 90% diversion rate was striking because the current condition dewatered almost

annually whereas the 90% diversion from the unimpaired did not. The 90% diversion from the unimpaired hydrograph, the hydrograph's duration, magnitude, frequency, timing, and intensity can continue to support many ecological processes. For example scouring flows would still shape ammocoete habitat deposits (Shields, 1936) and spring rain events would still promote adult Pacific lamprey upstream and macrophthalmia downstream migration (Goodman et al., 2015). Summer low flows can still grow ammocoetes by transporting detritus in the water column.(Finlay et al., 2002; Moore & Mallatt, 1980). In the current condition at RC-4, the low flow characteristics of the hydrograph were lost because the RC-4 deposit usually dewatered, stranding the ammocoetes in the hyporheic zone. In the lowest flow period of WY 2019, there was only 1% of the estimated unimpaired flow in Redwood Creek. I interpret the difference in the models of current and unimpaired flows two ways: 1) the Redwood Creek watershed is highly impaired by water diversions and land alterations, and/or 2) there are issues with modeling unimpaired flows between the two watersheds (Elder and Redwood).

Landowners typically do not divert a percentage of flow as the modeled scenario of taking a percentage of the unimpaired does. Typically, pumps run at a set diversion rate, for example 10 gallons per minute (gpm) (0.022 cfs). At flows above 0.5 cfs a single pump may not make a measurable difference, but as the flows naturally recede, a set diversion rate progressively takes a larger percentage of the ambient flow. Cumulatively, this can leave the channel dry. By taking a percentage of the flow, more water can be diverted when there is more flow in the channel, but a lower rate of diversion would be required later in the recession hydrograph to reduce the likelihood of a zero flow event.

At a lower diversion rate a longer period of diversion is required. For example, only 10 minutes are required to fill a 100 gallon tank at the 10 gpm rate, but when the stream flow drops to 20 gpm the diversion could decrease to one gpm, requiring just over an hour and a half to fill the same 100 gallon tank.

Redwood Creek is located within Humboldt County. Humboldt County sets performance standards for Cannabis Irrigation (Humboldt County, 2018). Growers are required to make a monthly water budget for irrigation demands, and the County recommends forbearing from diverting surface water during the low flow season. I believe the forbearance plan would have to address the cumulative effects of the water withdrawals. A 5% diversion from the riffle crest thalweg may not make an impact on certain stream processes, but landowners need to consider what their neighbors within the watershed are diverting as well, so the cumulative impact adds up to a maximum of 5%. My research showed that ammocoete habitat quality at Redwood Creek site RC-4 was not impacted until 20% of the unimpaired flow was diverted from the watershed. For the ammocoete habitat deposits at RC-4 to not reach section control in a scenario with 50 landowners, each landowner can take no more than an average of 0.4 % of the flow at any given time (also assuming no other impairments).

Baur et al. (2015) estimate that marijuana cultivation demand in Redwood Creek in the early 2000s was 34-165% of the low flow. My analysis of WY 2019 showed that Redwood Creek flow was 99% less than the estimated unimpaired flow for the lowest flow time period. Redwood Creek is impacted by more than water diversions. There is

also a history of landscape alterations that alter the surface flow. Culture and regulations have changed the water use practices since the commencement of the Bauer et al. (2015) study; many growers are either storing water for use during the low flow season or utilizing groundwater pumping instead (Dillis et al., 2020). A review of legal cannabis applications for California found that most irrigation comes from wells during the dry season (Dillis et al., 2019). Cannabis growers in Redwood Creek irrigating with groundwater, are preventing water from reaching the stream because the recession hydrograph comes from groundwater stored in Redwood Creek's weathered bedrock. In the Navarro watershed, groundwater pumping impacted the stream flows, but residential water use was four times greater than cannabis water use (Zipper et al., 2019)

Elder Creek (USGS gage # 11475560) may not be the ideal gage for comparison to Redwood Creek but was the best available. Elder Creek is far enough away from Redwood Creek that precipitation timing, magnitude, frequency, duration, and intensity are different. Elder Creek enters the South Fork of the Eel River on the east side whereas Redwood Creek enters the Eel on the west side. The geology of Elder Creek is slightly different from Redwood Creek; Elder Creek is completely in the Coastal Belt, whereas Redwood Creek is in the Coastal and Central Belts. This should sustain higher summer unit runoff in Elder Creek. WY 2019 was the only year that the Bull Creek Gage (USGS gage #11476600) has not been operating since 1960, operation restarted in WY 2020. Redwood Creek may be better suited to compare with Bull Creek (Cowen, 2018a; Klein, 2018). Bull Creek has a similar size drainage area, is nearby, has the same aspect, similar precipitation, similar geology, and joins the South Fork of the Eel River within miles of

Redwood Creek. The Bull Creek watershed has landscape alterations similar to Redwood Creek; such as logging, grazing, and roads. But unlike Redwood Creek, Bull Creek has very few known stream flow diversions. The mouth of Bull Creek is owned by the California Department of Parks and Recreation, but the headwaters are in private ownership (a majority of which is timberland). Sproul Creek is another option to use as an unimpaired stream. Sproul Creek is a bordering watershed with a similar drainage area, entering the South Fork Eel River just upstream of Redwood Creek. Sproul Creek has had a private gage to measure flow running on it for as long as the Redwood Creek gage, since 2013. Sproul Creek is majority-owned by a private timber company.

Modeled unimpaired Redwood Creek stream flow could be predicting that the stream dewatered most years because of the mathematics behind the model. I used a linear model to predict the current conditions of Elder Creek (USGS gage # 11475560) to Redwood Creek site RC-4 using a linear equation because it fit the observation points well. A power curve did not work because it would have never predicted that RC-4 went dry because power function cannot go to zero, but the linear equation may have predicted that the flow went too negative. There are different approaches to model watershed streamflow that take into account: 1) precipitation, 2) water infiltration capacity of the soil, and 3) evapotranspiration (Ward et al., 2016; Workman et al., 2000).

The current condition of the RC-4 habitat is that the deposits are under extreme risk annually of dewatering. The predicted unimpaired flow of Redwood Creek did not reach section control during the low flow season in WY 2019. Diverting water from the unimpaired flow lengthens the time the deposits are at high risk and decreases the portion

of the habitat inundated. On average, measured WY 2019 RC-4 flow was 24% of the modeled unimpaired WY 2019 flow; in late September, it was only 1% of the unimpaired flow. On August 10th, 2019 I measured a flow of 0.85 cfs at RC-4, while modeling an unimpaired flow of 6.4 cfs at RC-4. The difference in flow comes to 3.5 million gallons per day (11-acre feet). Second growth Douglas-fir plantations, as in Redwood Creek, can lower the summer streamflow by 50% (Perry & Jones, 2016). The remaining 50%, 1.25 million gallons, is less than the estimated demand for cannabis during the peak of the green rush (Bauer et al., 2015), but likely more than the actual water extraction in 2019. With legalization of cannabis farming, there are fewer farms all required to not divert water April through October but rely on stored water (Dillis et al., 2020).

The portion of habitat inundated at RC-4 in the unimpaired annual recession hydrograph scenario decreased to 50% as early as June or as late as September depending on the water year (Figure 36). Ammocoete habitat deposit area was <50% inundated for a duration of two weeks to six months in most years. The time when the deposit is 50% inundated happened a month earlier when the flow was diverted by 50%. At the 90% diversion rate, the deposits' area was likely to be <50% inundated all dry season (May-Oct). Once the deposits were under section control, there was only 25% of the deposit area inundated. The food supply and water quality are poor in those conditions, and there is only 25% of the substrate surface area at RC-4 to burrow into for the same number of ammocoetes.

Lovill et al. (2018) find that streams in the Coastal Belt geology will remain flowing even in dry years because of drainage from the weathered bedrock, except in areas with deep alluvial beds. Streams in the Central Belt geology (Dry and Hank Creek in the Eel River Critical Zone Observatory) dewatered in summer because there was not a thick layer of weathered bedrock, and subsurface water storage was limited (Lovill et al., 2018). My research aligned with theirs because Redwood Creek tributaries within the Coastal Belt (DC-1, CC-2, URC-1, MC-2, RC-1.5, and RC-1.8) had a higher unit runoff than the stream in the Central Belt (SC-1) and the stream with mixed geology (RC-3 and RC-4) (Figure 26).

These research methods can be a launch point for future research. The low flow analysis for RC-4 can be conducted for all ten sites I measured on Redwood Creek. Future research could compare how the sites react differently in the different geologic belts. It could explore the different channel types or different geologic controls (alcove, obstruction, etc.). Ammonoetes could be sampled throughout the dry season to see how they move through the watershed during recession hydrograph.

CONCLUSION

This research estimated quantity and quality of Pacific lamprey ammocoete habitat spatially and temporally. I looked at habitat presence and density throughout Coastal Northern California and focused my temporal analysis at a site on Redwood Creek, a tributary to the South Fork Eel River. The density and presence of Pacific lamprey ammocoete habitat depend on the channel slope; lower slope reaches support a higher density of ammocoete habitat. I have demonstrated how impacts from impairments, such as diversions and past land management, on a small stream using Redwood Creek as a case study. This research focused on the intersection of fluvial geomorphology and fisheries biology; lamprey ammocoetes live between the spawning gravels in upper stream reaches and off-channel habitat of lower reaches. This research joins the two.

I offered an analytical method for evaluating cumulative diversion impacts to the stream ecosystem. The research and methodologies applied to Redwood Creek habitat risk assessment can help guide future water allocations and streamflow enhancement in small drainages in Northern California to protect the ecosystem in impaired streams.

In Northern California, there are rural areas without municipal water. These streams are critical to many species that have their specific habitat requirements to complete their life cycle. Pacific lamprey ammocoetes rely on stream processes; if we restore and protect these processes, we protect healthy stream ecosystems on which they and many other species depend.

LITERATURE CITED

- Amoros, C., Roux, A. L., Reygrobellet, J. L., Bravard, J. P., & Pautou, G. (1987). A method for applied ecological studies of fluvial hydrosystems. *Regulated Rivers: Research & Management*, *1*(1), 17–36. <https://doi.org/10.1002/rrr.3450010104>
- Applegate, V. C. (1950). *Natural history of the Sea Lamprey (Petromyzon marinus) in Michigan* (Special Scientific Report: Fisheries No. 55; pp. 1–237). United States Department of the Interior Fish and Wildlife Service.
- Asarian, J. E., & Walker, J. D. (2016). Long-term trends in streamflow and precipitation in Northwest California and Southwest Oregon, 1953-2012. *JAWRA Journal of the American Water Resources Association*, *52*(1), 241–261. <https://doi.org/10.1111/1752-1688.12381>
- Bagnold, R. A. (1960). *Some aspects of the shape of river meanders*. US Government Printing Office.
- Bauer, S., Olson, J., Cockrill, A., van Hattem, M., Miller, L., Tauzer, M., & Leppig, G. (2015). Impacts of surface water diversions for marijuana cultivation on aquatic habitat in four northwestern California watersheds. *PLOS ONE*, *10*(3), e0120016. <https://doi.org/10.1371/journal.pone.0120016>
- Beamish, R. J., & Youson, J. H. (1987). Life history and abundance of young adult *Lampetra ayresi* in the Fraser River and their possible impact on salmon and herring stocks in the Strait of Georgia. *Canadian Journal of Fisheries and Aquatic Sciences*, *44*, 525–537.
- Best, J. L. (1987). Recent developments in fluvial sedimentology: Contributions from the Third International Fluvial Sedimentology Conference. *Society of the Economic Paleontologists and Mineralogists*, 389.
- Bettaso, J. B., & Goodman, D. H. (2010). A comparison of mercury contamination in mussel and ammocoete filter feeders. *Journal of Fish and Wildlife Management*, *1*(2), 142–145. <https://doi.org/10.3996/112009-JFWM-019>
- Bilby, R. E., & Likens, G. E. (1980). Importance of organic debris dams in the structure and function of stream ecosystems. *Ecology*, *61*(5), 1107–1113. <https://doi.org/10.2307/1936830>
- Brumo, A. (2006). *Spawning, Larval Recruitment, and Early Life Survival of Pacific Lampreys in the South Fork Coquille River, Oregon* [Master Thesis, Oregon State University]. <https://doi.org/10.13140/2.1.2789.6320>
- Brush, L. M. (1961). *Drainage Basins, Channels, and Flow Characteristics of Selected Streams in Central Pennsylvania*. U.S. Government Printing Office.
- Bryant, M. D. (1983). The role and management of woody debris in West Coast salmonid nursery streams. *North American Journal of Fisheries Management*, *3*(3), 322–330. [https://doi.org/10.1577/1548-8659\(1983\)3<322:TRAMOW>2.0.CO;2](https://doi.org/10.1577/1548-8659(1983)3<322:TRAMOW>2.0.CO;2)

- Burchsted, D., Daniels, M., Thorson, R., & Vokoun, J. (2010). The river discontinuum: Applying beaver modifications to baseline conditions for restoration of rorested headwaters. *BioScience*, 60(11), 908–922.
<https://doi.org/10.1525/bio.2010.60.11.7>
- Burschsted, D. (2010). Beaver dam impacts on sediment and water regime, and implications for river restoration. *2010 GSA Denver Annual Meeting*.
- Byrne, C. F., Pasternack, G. B., Guillon, H., Lane, B. A., & Sandoval-Solis, S. (2020). Reach-scale bankfull channel types can exist independently of catchment hydrology. *Earth Surface Processes and Landforms*, esp.4874.
<https://doi.org/10.1002/esp.4874>
- California Geological Survey. (2002). *California Geomorphic Provinces, Note 36*. California Department of Conservation.
- California Water Resources Control Board. (2014). *Policy for Maintaining Instream Flows in Northern California Coastal Streams* (p. 141). State Water Resources Control Board.
https://www.waterboards.ca.gov/waterrights/water_issues/programs/instream_flows/docs/adopted_policy.pdf
- Chanson, H. (1995). Air-water gas transfer at hydraulic jump with partially developed inflow. *Water Research*, 29(10), 2247–2254. [https://doi.org/10.1016/0043-1354\(95\)00056-Q](https://doi.org/10.1016/0043-1354(95)00056-Q)
- Chesterman, C. W. (1978). *The Audubon Society Field Guide to North American Rocks and Minerals* (A Chanticleer Press). Alfred A. Knopf, Inc.
- Clemens, B. J., Van De Wetering, S., Kaufman, J., Holt, R. A., & Schreck, C. B. (2009). Do summer temperatures trigger spring maturation in Pacific lamprey, *Entosphenus tridentatus*? *Ecology of Freshwater Fish*, 18(3), 418–426.
<https://doi.org/10.1111/j.1600-0633.2009.00358.x>
- Close, D. A. (2002). *Ecological and Cultural Importance of a Species at Risk of Extinction, Pacific Lamprey, 1964-2002 Technical Report*. (DOE/BP-00005455-4). Umatilla Confederated Tribes (CTUIR). <https://doi.org/10.2172/818645>
- Close, D. A., Fitzpatrick, M., Li, H., Parker, B., Hatch, D., & James, G. (1995). *Status Report of the Pacific Lamprey (Lampetra tridentata) in the Columbia River Basin*. Bonneville Power Administration.
- Cluer, B., & Thorne, C. (2014). A stream evolution model integrating habitat and ecosystem benefits. *River Research and Applications*, 30(2), 135–154.
<https://doi.org/10.1002/rra.2631>
- Cooper, E. J., London, M., O’Dowd, A., & Trush, B. (2017). *South Fork Eel River Geomorphic Field Data Collection Report*. HSU River Institute.
- Cowen, W. (2018a). *CDFW Flow Monitoring and Unimpaired Flow Redwood Creek, Humboldt County*. California Department of Fish and Wildlife.
- Cowen, W. (2018b). *Flow Monitoring and Unimpaired Flow estimation Report for Redwood Creek, Humboldt County*. (No. 18–1; Stream Evaluation Report, p. 33). California Department of Fish and Wildlife, Water Branch Instream flow Program.

- Crandall, J. D., & Wittenbac, E. (2015). *Pacific Lamprey Restoration Guide* (First edition; p. 54). Methow Salmon recovery Foudation.
- Data Basin. (2011). *Pacific Lamprey* (*Lampetra tridentata*) *Distribution and Status by HUC8* [Map]. Western Native Fishes Committee.
<https://databasin.org/datasets/6858961a72fa48959e8c769a7cfe1c9d>
- Dawson, H. A., Quintella, B. R., Almeida, P. R., Treble, A. J., & Jolley, J. C. (2015). The ecology of larval and metamorphosing lampreys. In M. F. Docker (Ed.), *Lampreys: Biology, Conservation and Control: Volume 1* (pp. 75–137). Springer Netherlands. https://doi.org/10.1007/978-94-017-9306-3_3
- Dillis, C., Grantham, T. E., McIntee, C., McFadin, B., & Grady, K. (2019). Watering the Emerald Triangle: Irrigation sources used by cannabis cultivators in Northern California. *California Agriculture*, 73(3), 146–153.
<https://doi.org/10.3733/ca.2019a0011>
- Dillis, C., McIntee, C., Butsic, V., Le, L., Grady, K., & Grantham, T. (2020). Water storage and irrigation practices for cannabis drive seasonal patterns of water extraction and use in Northern California. *Journal of Environmental Management*, 272, 110955. <https://doi.org/10.1016/j.jenvman.2020.110955>
- Docker, M. F. (Ed.). (2015). *Lampreys: Biology, Conservation and Control*. Springer Netherlands. <https://doi.org/10.1007/978-94-017-9306-3>
- Esselman, P. C., Infante, D. M., Lizhu Wang, Dayong Wu, Cooper, A. R., & Taylor, W. W. (2011). An index of cumulative disturbance to river fish habitats of the conterminous United States from landscape anthropogenic activities. *Ecological Restoration*, 29(1/2), 133–151. <https://doi.org/10.3368/er.29.1-2.133>
- Ferguson, R., Hoey, T., Wathen, S., & Werritty, A. (1996). Field evidence for rapid downstream fining of river gravels through selective transport. *Geology*, 24(2), 179. [https://doi.org/10.1130/0091-7613\(1996\)024<0179:FEFRDF>2.3.CO;2](https://doi.org/10.1130/0091-7613(1996)024<0179:FEFRDF>2.3.CO;2)
- Ferreira, A. F., Quintella, B. R., Maia, C., Mateus, C. S., Alexandre, C. M., Capinha, C., & Almeida, P. R. (2013). Influence of macrohabitat preferences on the distribution of European brook and river lampreys: Implications for conservation and management. *Biological Conservation*, 159, 175–186.
<https://doi.org/10.1016/j.biocon.2012.11.013>
- Finlay, J. C., Khandwala, S., & Power, M. E. (2002). Spatial Scales of Carbon Flow in a River Food Web. *Ecology*, 83(7), 15.
- Flosi, G., Downie, S., Bird, M., Coey, R., & Collins, B. (2002). *California Salmonid Stream Habitat Restoration Manual*.
https://scholarworks.umass.edu/fishpassage_unpublished_works/23
- Formosa, M. L., & Kelly, E. C. (2020). Socioeconomic benefits of a restoration economy in the Mattole River Watershed, USA. *Society & Natural Resources*.
<https://www.tandfonline.com/doi/abs/10.1080/08941920.2020.1718815>
- Gabrisch, G. (2013). *Multi-Volumes for ArcGIS 10*.
- Goertler, P. A. L., Shakya, A. W., Seesholtz, A. M., Schreier, B. M., Matica, S. Z., & Holley, K. S. (2019). Lamprey (*Entosphenus* sp. And *Lampetra* sp.) estuarine

- occupancy is regionally variable and constrained by temperature. *Journal of Fish Biology*, 0(ja). <https://doi.org/10.1111/jfb.14143>
- Goodman, D. H., Kinziger, A. P., Reid, S. B., & Docker, M. F. (2009). Morphological diagnosis of *Entosphenus* and *Lampetra* ammocoetes (Petromyzontidae) in Washington, Oregon, and California. *Biology, Management, and Conservation of Lampreys in North America. American Fisheries Society, Symposium*, 72, 223–232.
- Goodman, D. H., & Reid, S. B. (2012). *Pacific Lamprey (Entosphenus tridentatus) Assessment and Template for Conservation Measures in California. Region 8 U.S. fish and Wildlife Service Sacramento, California.*
- Goodman, D. H., & Reid, S. B. (2017). Climbing above the competition: Innovative approaches and recommendations for improving Pacific Lamprey passage at fishways. *Ecological Engineering*, 107, 224–232. <https://doi.org/10.1016/j.ecoleng.2017.07.041>
- Goodman, D. H., Reid, S. B., Som, N. A., & Poytress, W. R. (2015). The punctuated seaward migration of Pacific lamprey (*Entosphenus tridentatus*): Environmental cues and implications for streamflow management. *Canadian Journal of Fisheries and Aquatic Sciences*, 72(12), 1817–1828. <https://doi.org/10.1139/cjfas-2015-0063>
- Guillon, H., Byrne, C. F., Lane, B. A., Sandoval Solis, S., & Pasternack, G. B. (2020). Machine learning predicts reach-scale channel types from coarse-scale geospatial data in a large river basin. *Water Resources Research*. <https://doi.org/10.1029/2019WR026691>
- Gunther, S. (1960). Die Neunaugen (Petromyzonidae). In *Hanbuch Der Binnenfischerei Mitteleuropas: Vol. III B.* Stuttgart, E. Schweizerbart'sche verlagsbuchhandlung Erwin Nägele g.m.b.h.
- Higgins, P. (2013). *Eel River Recovery Project 2013 Citizen Assisted Water Temperature and Flow Monitoring.* Eel River Recovery Project.
- Holmes, J. A. (1990). Sea lamprey as an early responder to climate change in the Great Lakes basin. *Transactions of the American Fisheries Society*, 119(2), 292–300. [https://doi.org/10.1577/1548-8659\(1990\)119\[0292:SLAAER\]2.3.CO;2](https://doi.org/10.1577/1548-8659(1990)119[0292:SLAAER]2.3.CO;2)
- Humboldt Ordinance Amending Provisions of Title III of the Humboldt county Code Relating to the Commercial Cultivation, Processing, Manufacturing, Distribution, Testing, and Sale of Cannabis for Medicinal or Adult Use for the Areas Outside the Coastal Zone, 2559 Ordinance (2018).
- Hume, J. B., Bracken, F. S. A., Mateus, C. S., & Brant, C. O. (2020). Synergizing basic and applied scientific approaches to help understand lamprey biology and support management actions. *Journal of Great Lakes Research*. <https://doi.org/10.1016/j.jglr.2020.07.002>
- Kastl, B., Winklerprins, L., Leathers, K., Dinh, Z., & Witherby, S. (2019). *Geomorphic and Hydraulic Controls on coho Salmon Outmigration in the Russian River Watershed, California.* UC Berkely graduate student research papers. <https://escholarship.org/uc/item/6hh170jm>

- Keller, E. A., & Swanson, F. J. (1979). Effects of large organic material on channel form and fluvial processes. *Earth Surface Processes*, 4(4), 361–380.
<https://doi.org/10.1002/esp.3290040406>
- Klein, R. D. (2018). *Low Flow Stream Discharge Monitoring Report for the Redwood Creek Watershed, 2015-16*. Salmonid Restoration Federation.
- Klein, R. D., McKee, T., & Nystrom, K. (2016). Shrinking Streamflows in the Redwood Region. *Proceedings of the Coast Redwood Science Symposium*.
- Kline, M., Alexander, C., Pytlik, S., & Pomeroy, S. (2009). *Stream Geomorphic Assessment Handbook*. <https://dec.vermont.gov/watershed/rivers/river-corridor-and-floodplain-protection/geomorphic-assessment>
- Kubicek, P. F. (1977). *Summer Water Temperature Conditions in the Eel River System, with Reference to Trout and Salmon* [Thesis, Humboldt State University].
<http://scholarworks.calstate.edu/handle/2148/1011>
- Lane, B. A., Sandoval-Solis, S., Dahlke, H. E., & Pasternack, G. B. (2016). *Geomorphic Classification of Natural Flow Classes for the State of California* (No. 2; p. 25). University California Davis for State Water Resources Control Board.
- Leach, W. J. (1940). Occurrence and life history of the Northern Brook Lamprey, *Ichthyomyzon fossor*, in Indiana. *Copeia*, 1940(1), 21.
<https://doi.org/10.2307/1439019>
- Legleiter, C. J. (2014). A geostatistical framework for quantifying the reach-scale spatial structure of river morphology: 1. Variogram models, related metrics, and relation to channel form. *Geomorphology*, 205, 65–84.
<https://doi.org/10.1016/j.geomorph.2012.01.016>
- Leopold, L. B., & Maddock, T. (1953). *The Hydraulic Geometry of Stream Channels and Some Physiographic Implications*. United States Government Printing Office.
- Leopold, L. B., Wolman, M. G., & Miller, J. P. (1964). *Fluvial Processes in Geomorphology*. Dover Publications.
- Liedtke, T. L., Weiland, L. K., & Mesa, M. G. (2015). *Vulnerability of Larval Lamprey to Columbia River Hydropower System Operations—Effects of Dewatering on Larval Lamprey Movements and Survival* (USGS Numbered Series No. 2015–1157; Open-File Report, p. 36). U.S. Geological Survey.
<http://pubs.er.usgs.gov/publication/ofr20151157>
- Lisle, T. (1987). *Using “Residual Depths” to Monitor Pool Depths Independently of Discharge* (Research Note PSW-394).
- Lisle, T. (1988). Channel-dynamic control on the establishment of riparian trees after large floods in Northwestern California. *Protection, Management, and Restoration for the 1990s*. California Riparian Systems Conference, Davis, California.
- Lisle, T. E., Woman, M. G., & Riggs, H. C. (1990). *The Eel River, Northwestern California: High Sediment Yields from a Dynamic Landscape.: Vol. Volume 0-1: the geology of North America*. Geological Society of North America.

- Lisle, Thomas E., & Hilton, S. (1999). Fine bed material in pools of natural gravel bed channels. *Water Resources Research*, 35(4), 1291–1304. <https://doi.org/10.1029/1998WR900088>
- Lovill, S. M., Hahm, W. J., & Dietrich, W. E. (2018). Drainage from the critical zone: Lithologic controls on the persistence and spatial extent of wetted channels during the summer dry season. *Water Resources Research*, 54(8), 5702–5726. <https://doi.org/10.1029/2017WR021903>
- Ludington, S., Moring, B. C., Miller, R. J., Flynn, K. S., Stone, P. A., & Dedford, D. R. (2005). *Preliminary Integrated Geologic Map Databases for the United States-Western States: California, Nevada, Arizona, and Washington* [Map]. U.S. Geological Survey. <https://mrdata.usgs.gov/geology/state/state.php?state=CA>
- Mazgareanu, I., Biron, P. M., & Buffin-Bélanger, T. (2020). A fuzzy GIS model to determine confluence morphological sensitivity to tributary inputs at the watershed scale. *Geomorphology*, 357, 107095. <https://doi.org/10.1016/j.geomorph.2020.107095>
- McGree, M., Whitesel, T. A., & Stone, J. (2008). Larval metamorphosis of individual Pacific Lampreys reared in captivity. *Transactions of the American Fisheries Society*, 137(6), 1866–1878. <https://doi.org/10.1577/T07-206.1>
- McLaughlin, R. J., Ellen, S. D., Blake, M. C., Jr., Jayko, A. S., Irwin, W. P., Aalto, K. R., Carver, G. A., & Clarke, S. H. Jr. (2000). *Geology of the Cape Mendocino, Eureka, Garberville, and Southwestern Part of the Hayfork 30 x 60 Minute Quadrangles and adjacent offshore Area, Northern California* [Map]. <https://pubs.usgs.gov/mf/2000/2336/gamap.pdf>
- Mierau, D. W., Trush, W. J., Rossi, G. J., Carah, J. K., Clifford, M. O., & Howard, J. K. (2018). Managing diversions in unregulated streams using a modified percent-of-flow approach. *Freshwater Biology*, 63(8), 752–768. <https://doi.org/10.1111/fwb.12985>
- Miller, M. C., McCave, I. N., & Komar, P. D. (1977). Threshold of sediment motion under unidirectional currents. *Sedimentology*, 24(4), 507–527. <https://doi.org/10.1111/j.1365-3091.1977.tb00136.x>
- Moore, J. W., & Mallatt, J. M. (1980). Feeding of Larval Lamprey. *Canadian Journal of Fisheries and Aquatic Sciences*, 37(11), 1658–1664. <https://doi.org/10.1139/f80-213>
- Moosdorf, N., Cohen, S., & von Hagke, C. (2018). A global erodibility index to represent sediment production potential of different rock types. *Applied Geography*, 101, 36–44. <https://doi.org/10.1016/j.apgeog.2018.10.010>
- Morman, R. H. (1987). Relationship of density to growth and metamorphosis of caged larval sea lampreys, *Petromyzon marinus* Linnaeus, in Michigan streams. *Journal of Fish Biology*, 30(2), 173–181. <https://doi.org/10.1111/j.1095-8649.1987.tb05743.x>
- Moser, M. L., Jackson, A. D., Lucas, M. C., & Mueller, R. P. (2015). Behavior and potential threats to survival of migrating lamprey ammocoetes and

- macrophthalmia. *Reviews in Fish Biology and Fisheries*, 25(1), 103–116.
<https://doi.org/10.1007/s11160-014-9372-8>
- Moyle, P. B. (2002). *Inland Fishes of California* (Rev. and expanded). University of California Press.
- Neeson, T. M., Doran, P. J., Ferris, M. C., Fitzpatrick, K. B., Herbert, M., Khoury, M., Moody, A. T., Ross, J., Yacobson, E., & McIntyre, P. B. (2018). Conserving rare species can have high opportunity costs for common species. *Global Change Biology*. <https://doi.org/10.1111/gcb.14162>
- Neeson, T. M., Koonce, J. F., & Whiting, P. J. (2007). Predicting Sea Lamprey (*Petromyzon marinus*) Ammocoete Habitat Using Geographic Information Systems. *Journal of Great Lakes Research*, 33(3), 546–553.
[https://doi.org/10.3394/0380-1330\(2007\)33\[546:PSLPMA\]2.0.CO;2](https://doi.org/10.3394/0380-1330(2007)33[546:PSLPMA]2.0.CO;2)
- Nilsen, E. B., Hapke, W. B., McIlraith, B., & Markovchick, D. (2015). Reconnaissance of contaminants in larval Pacific lamprey (*Entosphenus tridentatus*) tissues and habitats in the Columbia River Basin, Oregon and Washington, USA. *Environmental Pollution*, 201, 121–130.
<https://doi.org/10.1016/j.envpol.2015.03.003>
- Parker, K. A. (2018). *Evidence for the Genetic Basis and Inheritance of Ocean and River-Maturing Ecotypes of Pacific lamprey (Entosphenus tridentatus) in the Klamath River, California*. Humboldt State University.
- Passalacqua, P., Trung, T. D., Foufoula-Georgiou, E., Sapiro, G., & Dietrich, W. E. (2010). A geometric framework for channel network extraction from lidar: Nonlinear diffusion and geodesic paths. *Journal of Geophysical Research: Earth Surface*, 115(F1). <https://doi.org/10.1029/2009JF001254>
- Perry, T., & Jones, J. (2016). Summer streamflow deficits from regenerating Douglas-fir forest in the Pacific Northwest, USA. *Ecohydrology*, 10(2), e1790.
<https://doi.org/10.1002/eco.1790>
- Petersen, R. S. (2006). *The role of traditional ecological knowledge in understanding a species and river system at risk: Pacific lamprey in the lower Klamath Basin* [Master Thesis]. Oregon State University, Department of Anthropology.
- Pollock, M., Beechie, T. J., Wheaton, J. M., Jordan, C. E., Bouwes, N., Weber, N., & Volk, C. (2014). Using beaver dams to restore incised stream ecosystems. *BioScience*, 64(4), 279–290.
- Powers, P. D., Helstab, M., & Niezgodna, S. L. (2019). A process-based approach to restoring depositional river valleys to Stage 0, an anastomosing channel network. *River Research and Applications*, 35(1), 3–13. <https://doi.org/10.1002/rra.3378>
- PRISM Climate Group, & Oregon State University. (2004, February 4). *PRISM Time Series Data*. prism.oregonstate.edu
- Rantz, S. E. (1982). Measurement and computation of streamflow: Volume 1. Measurement of stage and discharge. In *Measurement and computation of streamflow* (USGS Numbered Series No. 2175; Water Supply Paper, Vol. 2175). U.S. G.P.O. <https://doi.org/10.3133/wsp2175>

- Reid, S. B., & Goodman, D. H. (2015). Detectability of Pacific Lamprey occupancy in western drainages: Implications for distribution surveys. *Transactions of the American Fisheries Society*, *144*(2), 315–322.
<https://doi.org/10.1080/00028487.2014.991448>
- Reid, S. B., & Goodman, D. H. (2016). Pacific Lamprey in coastal drainages of California: Occupancy patterns and contraction of the southern range. *Transactions of the American Fisheries Society*, *145*(4), 703–711.
<https://doi.org/10.1080/00028487.2016.1159615>
- Reid, S. B., & Goodman, D. H. (2020). Natural recolonization by Pacific Lampreys in a Southern California Coastal Drainage: Implications for their biology and conservation. *North American Journal of Fisheries Management*.
<https://doi.org/10.1002/nafm.10412>
- Renaud, C. B. (2011). *Lampreys of the World: An Annotated and Illustrated Catalogue of Lamprey Species Known to Date*. Food and Agriculture Organization of the United Nations.
- Richards, K. S. (1976). The morphology of riffle-pool sequences. *Earth Surface Processes*, *1*(1), 71–88. <https://doi.org/10.1002/esp.3290010108>
- Rodríguez-Lozano, P., Leidy, R. A., & Carlson, S. M. (2019). Brook lamprey survival in the dry riverbed of an intermittent stream. *Journal of Arid Environments*.
<https://doi.org/10.1016/j.jaridenv.2019.04.016>
- Schultz, L. D., Mayfield, M. P., Sheoships, G. T., Wyss, L. A., Clemens, B. J., Whitlock, S. L., & Schreck, C. B. (2014). Role of large- and fine-scale variables in predicting catch rates of larval Pacific lamprey in the Willamette Basin, Oregon. *Ecology of Freshwater Fish*, *25*(2), 261–271.
<https://doi.org/10.1111/eff.12207>
- Shields, Dr. Ing. A. (1936). *Application of Similarity Principles and Turbulence Research to Bed-Load Movement* (W. P. Ott & J. C. van Uchelen, Trans.; No. 167). Mitteilungen der Preussischen Versuchsanstalt für Wasserbau und Schiffbau.
- Shirakawa, H., Yanai, S., & Goto, A. (2013). Lamprey larvae as ecosystem engineers: Physical and geochemical impact on the streambed by their burrowing behavior. *Hydrobiologia*, *701*(1), 313–322. <https://doi.org/10.1007/s10750-012-1293-8>
- Simpson, K. L. (2019). *Overlooked Fisheries of Baduwa't: An Oral History Study Exploring the Environmental and Cultural Histories of Eulachon and Pacific Lamprey in the Mad River Basin, a Wiyot Watershed* [Master of Arts in Social Science: Environment and Community]. Humboldt State University.
- Sklar, L. S., Riebe, C. S., Marshall, J. A., Genetti, J., Leclere, S., Lukens, C. L., & Mercus, V. (2017). The problem of predicting the size distribution of sediment supplied by hillslopes to rivers. *Geomorphology*, *277*, 31–49.
<https://doi.org/10.1016/j.geomorph.2016.05.005>
- Stillwater Sciences. (2010). *Pacific Lamprey in the Eel River Basin: A Summary of Current Information and Identification of Research Needs*. Stillwater Sciences, Arcata, California for Wiyot Tribe, Loleta, California.
<https://doi.org/10.13140/RG.2.1.2557.3609>

- Stillwater Sciences. (2013). *Pacific and Western Brook Lamprey Spawning and Rearing Habitat in Newly Accessible Reaches of the North Umpqua River Watershed, Oregon*. USDA Forest Service Umpqua National Forest 2900 NW Stewart Parkway Resebur, OR 97471.
http://www.stillwatersci.com/resources/2013umpqualampreyhabitat_finalLR.pdf
- Stillwater Sciences. (2014). *A conceptual framework for understanding factors limiting Pacific lamprey production in the Eel River basin*. Stillwater Sciences, Arcata, California for Wiyot Tribe, Loleta, California.
<https://doi.org/10.13140/RG.2.1.3081.6487>
- Stolzman, D., Schremmer, S., Klein, R., & Eastwood, B. (2015). *Quality Assurance Project Plan (QAPP) for the Redwood Creek, South Fork Eel River, Water Conservation, Monitoring, Planning and Assessment, and Education Project. 1*, 35.
- Stone, J., & Barndt, S. (2005). Spatial distribution and habitat use of Pacific Lamprey (*Lampetra tridentata*) ammocoetes in a Western Washington stream. *Journal of Freshwater Ecology*, 20(1), 171–185.
<https://doi.org/10.1080/02705060.2005.9664950>
- Streif, B. (2008). *Fact Sheet Pacific Lamprey (Lapetra tridentata)*. USFSW Portland OR.
- Stubblefield, A., Kaufman, M., & Blomstrom, G. (2012). *Summer Water Use by Mixed-Age and Young Forest Stands, Mattole River, Northern California, U.S.A.* (General Technical Report PSW-GTR-238; p. 11). Forest Service.
- Sugiyama, H., & Goto, A. (2002). Habitat selection by larvae of a fluvial lamprey, *Lethenteron reissneri*, in a small stream and an experimental aquarium. *Ichthyological Research*, 49(1), 62–68. <https://doi.org/10.1007/s102280200006>
- Torgersen, C. E., & Close, D. A. (2004). Influence of habitat heterogeneity on the distribution of larval Pacific lamprey (*Lampetra tridentata*) at two spatial scales. *Freshwater Biology*, 49(5), 614–630.
- Trush, W., Connor, E. C., & Knight, A. W. (1988). Alder Establishment and Channel Dynamics in a Tributary of the South Fork Eel River, Mendocino County, California. *Protection, Management, and Restoration for the 1990s*. California Riparian Systems Conference, Davis, California.
- Trush, W. J. (1989). *Salmonid Geomorphology*. 7.
- Unrein, J. R., Morris, J. M., Chitwood, R. S., Lipton, J., Peers, J., van de Wetering, S., & Schreck, C. B. (2016). Pacific lamprey (*Entosphenus tridentatus*) ammocoetes exposed to contaminated Portland Harbor sediments: Method development and effects on survival, growth, and behavior. *Environmental Toxicology & Chemistry*, 35(8), 2092–2102. <https://doi.org/10.1002/etc.3367>
- USGS. (2019). *StreamStats*. <https://streamstats.usgs.gov/ss/>
- Vaile, J. E., Nawa, R. K., Lind, P., Nadananda, McKay, T., Elkins, C., Bakke, B., Miller, J., Wood, W., Beardslee, K., & Wales, D. (2003). *A Petition for Rules to List: Pacific Lamprey (Lampetra tridentata); River Lamprey (Lampetra ayresi); Western Brook Lamprey (Lampetra richardsoni); and Kern Brook Lamprey*

(*Lampetra hubbsi*) as *Threatened or Endangered Under the Endangered Species Act*.

- Wang, C., & Schaller, H. (2015). Conserving Pacific Lamprey through collaborative efforts. *Fisheries*, 40(2), 72–79. <https://doi.org/10.1080/03632415.2014.996871>
- Ward, A. D., Trimble, S. W., Burkhard, S. R., & Lyon, J. G. (2016). *Environmental Hydrology, Third Edition*. CRC Press.
- White, J. L., & Harvey, B. C. (2003). Basin-scale patterns in the drift of embryonic and larval fishes and lamprey ammocoetes in two coastal rivers. *Environmental Biology of Fishes*, 67(4), 369–378. <https://doi.org/10.1023/A:1025891216345>
- Willoughby, L. G. (1974). Decomposition of litter in fresh water. In C. H. Dickinson & G. J. F. Pugh (Eds.), *Biology of Plant Litter Decomposition V2*. Academic Press.
- Workman, S. R., Spruill, C. A., & Taraba, J. L. (2000). Simulation of daily and monthly stream discharge from small watersheds using the SWAT model. *Transactions of the ASAE*, 43(6), 1431–1439. <https://doi.org/10.13031/2013.3041>
- Yager, E. M., Dietrich, W. E., Kirchner, J. W., & McArdell, B. W. (2012). Patch dynamics and stability in steep, rough streams. *Journal of Geophysical Research: Earth Surface*, 117(F2), n/a-n/a. <https://doi.org/10.1029/2011JF002253>
- Zipper, S. C., Carah, J. K., Dillis, C., Gleeson, T., Kerr, B., Rohde, M. M., Howard, J. K., & Zimmerman, J. K. H. (2019). Cannabis and residential groundwater pumping impacts on streamflow and ecosystems in Northern California. *Environmental Research Communications*, 1(12), 125005. <https://doi.org/10.1088/2515-7620/ab534d>